Bioactivity Screening of Natural Compounds for Pharma and Nutri-cosmetic applications

Ida Paolillo

Dottorato in Biotecnologie – XXXVIII ciclo Università di Napoli Federico II

Dottorato in Biotecnologie – XXXVIII ciclo Università di Napoli Federico II

Bioactivity Screening of Natural Compounds for Pharma and Nutri-cosmetic applications

Ida Paolillo

Dottorando: Ida Paolillo

Relatore: Prof.ssa Viola Calabrò

Correlatore: Prof. Marco Masi

Coordinatore: Prof. Marco Moracci

Settore Scientifico Disciplinare BIOS-14/A Genetica

INDEX

Riassunto

I prodotti naturali sono composti o sostanze prodotte da organismi viventi quali piante, funghi, organismi marini e microrganismi. Negli ultimi decenni, sia la ricerca biomedica sia quella nutri-cosmetica si sono molto interessate a queste molecole bioattive, in virtù dei loro potenziali benefici terapeutici per la salute umana e della loro quasi assente tossicità. Grazie alla loro diversa struttura chimica, tali composti sono in grado di interagire con i sistemi biologici, contrastando o mitigando il processo di invecchiamento e riducendo l'incidenza di cancro, diabete, obesità, malattie cardiovascolari e processi neurodegenerativi (Narayanankutty et al., 2024). È bene osservare che la maggior parte delle malattie umane è associata a infiammazione sistemica, squilibrio dei ROS e stress ossidativo (Lugrin et al., 2014). I ROS sono specie dell'ossigeno con strutture chimiche altamente instabili e per questo motivo hanno una forte reattività. Queste molecole sono prodotte anche in uno stato fisiologico e sono importanti per la funzione cellulare. I ROS possono regolare meccanismi fisiologici rilevanti come la proliferazione cellulare, la differenziazione, la pluripotenza delle cellule staminali e l'auto-rinnovamento (Davalli et al., 2016). Tuttavia, un aumento anomalo della concentrazione intracellulare di ROS, dovuto a uno squilibrio tra antiossidanti e specie reattive, provoca stress ossidativo. Questo è il precursore del danno ossidativo subìto dalle cellule e dai tessuti quando esse non sono in grado di controbilanciare la produzione di radicali liberi.

La mia tesi di dottorato verte sull'analizzare le proprietà biologiche di sostanze naturali per il loro impiego in applicazioni farmaceutiche e nutri-cosmetiche.

In primo luogo, grazie a una collaborazione con la Prof.ssa Carmen Arena del Dipartimento di Biologia dell'Università degli Studi di Napoli Federico II, ho studiato come la modulazione dell'intensità e la selezione di specifiche lunghezze d'onda della luce possano migliorare la produttività di alcune colture, utilizzando la tecnologia dei diodi a emissione luminosa (LED).
Infatti, variando lo spettro luminoso — in particolare le componenti rossa e blu — e l'intensità della luce, è possibile controllare con precisione la crescita delle piante, aumentare la biomassa, favorire la produzione di molecole bioattive (come gli antiossidanti) e migliorare l'efficienza fotosintetica.

Questa tecnologia è stata impiegata per irraggiare i germogli della specie *Brassica rapa* L. durante la fase di crescita. Brassica è un genere di piante appartenente alla famiglia delle Brassicaceae, ampiamente coltivata nel mondo e in particolare nel bacino del Mediterraneo. Questa è ricca di numerosi composti bioattivi come composti fenolici e isoflavonoidi che le conferiscono innumerevoli benefici sulla salute umana. Infatti, sono noti i suoi effetti nel contrastare l'obesità, gli alti livelli di colesterolo nel sangue e prevenire il cancro (Jahangir et al., 2009). Nei test *in vitro*, l'estratto ottenuto da germogli di *B. rapa L*. coltivati sotto luce rossa e blu (RB) ha evidenziato una maggiore attività antiossidante rispetto a quello ottenuto da germogli esposti all'intero spettro luminoso (luce bianca, W). In particolare, il pretrattamento dei cheratinociti spontaneamente immortalizzati con l'estratto RB ha mostrato una notevole capacità di contrastare la produzione di ROS intracellulari anche a basse concentrazioni, mentre l'estratto W richiedeva dosaggi più elevati per ottenere un effetto analogo. Inoltre, l'estratto RB ha esercitato un effetto protettivo contro i danni al DNA indotti dallo stress ossidativo, riducendo la formazione di foci γH2AX e modulando la distribuzione subcellulare della proteina YB-1, un noto sensore di stress. Le analisi di Western blot hanno mostrato che entrambi gli estratti aumentano l'espressione del fattore di trascrizione NRF2, principale regolatore della risposta antiossidante; tuttavia, solo l'estratto RB ha determinato una riduzione significativa dell'espressione dell'inibitore delle chinasi ciclina-dipendenti p21WAF in condizioni di stress ossidativo, suggerendo un ripristino più efficiente del normale ciclo cellulare. Nel complesso, questi risultati indicano che le cellule trattate con l'estratto RB presentano una migliore capacità di neutralizzare i ROS intracellulari, di prevenire i danni ossidativi e preservare la stabilità genomica, caratteristiche di particolare interesse per potenziali applicazioni nutraceutiche e cosmeceutiche.

La seconda pianta su cui ho lavorato è stata *Staphylea pinnata*. Conosciuta come "falso pistacchio", questa è una specie sporadica, endemica italiana e alquanto rara, appartenente alla famiglia delle Staphyleaceae. Nella medicina tradizionale viene comunemente utilizzata per problemi della pelle e per disturbi respiratori. Delle proprietà di *S.pinnata* si conosce davvero molto poco anche se alcune ricerche stanno facendo luce sulla presenza di metaboliti secondari, come polifenoli, flavonoidi e derivati idrossicinnamici, con proprietà

antibatteriche, antiproliferative e antiossidanti (Andreas, 2014). Al fine di valutare le proprietà benefiche di estratti o/e di composti bioattivi presenti nelle foglie di questa pianta abbiamo confrontato due metodi estrattivi, la estrazione in fase liquida (LLE) e l'estrazione in fase solida (SPE). Questa parte del progetto si è svolta nel Dipartimento di Scienze Chimiche dell'Università Federico II sotto la supervisione del Prof Marco Masi. L'estrazione in fase solida ha garantito un risultato migliore per procedere all'isolamento dei metaboliti, risultando anche più eco-sostenibile rispetto al metodo di estrazione classico. Dalla SPE, ho ottenuto la frazione C che ha mostrato una forte attività antimicrobica, in particolare contro *Staphylococcus aureus* e un'attività antifungina moderata contro *Candida albicans*, probabilmente grazie a effetti sinergici tra i suoi componenti. Ho poi proceduto all'identificazione di sei metaboliti puri da questa frazione, facenti parte della classe dei glicosidi flavonolici. In particolare, la loro struttura di base è costituita da un flavonolo, chiamato anche aglicone, a cui è legata una parte zuccherina. I flavonoli, appartenenti alla classe dei flavonoidi, sono presenti in piante, frutti e vegetali e posseggono innumerevoli effetti benefici sulla salute umana, tra cui attività antinfiammatoria, antivirale, antiossidante e preventiva per malattie come il cancro (Ullah et al., 2020). Dei sei composti puri che ho isolato, in tre di essi l'aglicone corrispondeva alla quercitina mentre negli altri tre era rappresentato dall'isoramnetina. Dai test microbiologici i flavonoidi puri hanno mostrato una buona attività contro *Pseudomonas aeruginosa*. Sui cheratinociti immortalizzati, i metaboliti puri hanno evidenziato proprietà antiossidanti, effetti positivi sul *wound healing* e sul riparo dei danni al DNA suggerendo una loro possibile applicazione in prodotti cosmeceutici per la protezione della pelle.

La terza pianta studiata è stata *Lavandula angustifolia* Mill. Questa parte della tesi è stata svolta in collaborazione con la Dr.ssa Federica Carraturo del laboratorio di Igiene del Dipartimento di Biologia, Università Federico II, e con la start up HoloBiotics Srl UNINA Spinoff. *L. angustifolia* è una pianta appartenente alla famiglia delle Lamiaceae. È originaria del Mediterraneo occidentale e cresce spontaneamente in Spagna nord-orientale, Francia e Italia. È inoltre nota per avere effetti benefici contro lo stress ossidativo, l'infiammazione e le infezioni batteriche (Betlej et al., 2023). *L. angustifolia* è una pianta aromatica medicinale che viene coltivata su vasta scala proprio per scopi

industriali. Il prodotto più utilizzato è l'olio essenziale di lavanda. Tuttavia, per ottenere questo prezioso olio vengono prodotte tonnellate di scarti che risultano ancora ricchi di sostanze benefiche. Per tale motivo è necessario adottare nuove strategie in un'ottica volta all'ecosostenibilità. Recentemente, allo scopo di ottimizzare la produzione di olio essenziale di lavanda è stata introdotta la tecnologia delle colture cellulari vegetali *in-vitro* per ottenere un'elevata biomassa vegetale indipendentemente da fattori ambientali. Tale tecnologia innovativa consente la crescita di cellule vegetali in condizioni ambientali controllate. A tale scopo, mi sono occupata di confrontare le proprietà di tre diversi estratti di *L. angustifolia* su linee cellulari di cheratinociti e fibroblasti. Il primo estratto è stato ottenuto da cellule staminali vegetali, derivate dai calli della pianta (estratto stem); il secondo da macerazione di foglie e fiori della pianta (estratto totale) e infine l'ultimo ottenuto utilizzando lo scarto del processo di distillazione per produrre l'olio essenziale di lavanda (estratto distillato). Ho condotto test su cellule HaCaT (cheratinociti immortalizzati) e BJ5ta (fibroblasti immortalizzati), dato che rappresentano le principali componenti della pelle umana. I risultati hanno evidenziato che gli estratti non sono citotossici, se non a dosi elevate, e mostrano una marcata attività antiossidante, associata a una riduzione dell'espressione del fattore NRF2, indicatore di un migliore equilibrio redox intracellulare. Tale effetto potrebbe essere mediato da flavonoidi o molecole affini. L'estratto ottenuto da cellule staminali vegetali ha inoltre incrementato l'espressione della proteina Mytho, implicata nei processi di autofagia e mantenimento della longevità cellulare, suggerendo un potenziale effetto anti-aging. L'estratto stem e quello derivante da processi di distillazione, dist, hanno mostrato un'azione antinfiammatoria, riducendo l'espressione di IL-6. L'estratto distillato ha inoltre mostrato la capacità di aumentare la metilazione del DNA nelle cellule HaCaT, un fenomeno che merita approfondimenti per comprenderne i meccanismi molecolari. Questi primi risultati ottenuti con gli estratti di *L.angustifolia,* sembrano promettenti per una loro possibile applicazione nel settore della cosmeceutica. Inoltre, l'utilizzo dell'estratto distillato, derivante dallo scarto della produzione di olio essenziale, rappresenta un esempio virtuoso di economia circolare e innovazione sostenibile.

Parte della mia tesi di dottorato si è concentrata nello sviluppare delle formulazioni nutraceutiche valorizzando un prodotto di scarto delle aziende vinicole, ovvero le vinacce. Queste non sono altro che le bucce e i semi degli acini d'uva e i vinaccioli che si ottengono dopo la pressatura e spremitura dell'uva durante il processo produttivo del vino. Normalmente vengono utilizzate in agricoltura come ammendante, come foraggio per gli animali, per la stagionatura dei formaggi e nelle aziende di distillazione, per la produzione della grappa. Purtroppo, nonostante abbiano innumerevoli utilizzi, una grande parte rimane alle aziende vitivinicole, diventando un serio problema economico, dato l'enorme costo relativo al loro smaltimento. Le vinacce sono ricchissime in polifenoli e composti bioattivi, per tale motivo la ricerca scientifica si sta impegnando a trovare loro un nuovo ed ecosostenibile utilizzo. Con questo obiettivo sotto la supervisione del Prof Marco Masi e con la collaborazione del Dr. Giovanni Dal Poggetto e della Dr.ssa Gabriella Santagata (CNR-IPCB), ho preparato un estratto dalle vinacce, utilizzando etanolo, un solvente poco tossico ed ecosostenibile. Da test *in-vitro* condotti su cheratinociti immortalizzati, l'estratto è risultato non citotossico e con una spiccata attività antiossidante. Per migliorarne la stabilità e permettere un lento rilascio, l'estratto è stato incapsulato in perle idrogel a base di alginato e/o pectina, reticolate con ioni Ca^{2+} o Fe^{2+}. Tra le formulazioni testate, il rilascio ottenuto dalla formulazione T ha mostrato la maggior efficacia antiossidante, riducendo i ROS intracellulari del 77,5%, grazie alla struttura porosa del reticolo Ca^{2+}-dipendente che ne facilita il rilascio. Le perle formate da pectina e reticolate con Ca^{2+} rappresentano un sistema promettente per applicazioni nutraceutiche, con potenziale impatto nel campo della cosmeceutica e della sostenibilità, valorizzando un sottoprodotto dell'industria vinicola.

Abstract

My PhD research focused on the biological properties of natural compounds for use in pharmaceuticals and nutricosmetics. Natural products are bioactive molecules found in plants, fungi and microorganisms. They exhibit beneficial effects due to their antioxidant, anti-inflammatory and anti-ageing properties. In collaboration with Professor Carmen Arena of the Department of Biology at the University of Naples Federico II, I studied *Brassica rapa* L. sprouts grown under different LED light spectra. Red-blue (RB) light was found to significantly enhance the production of antioxidant compounds compared to white (W) light. Extracts from red-blue light conditions exhibited enhanced antioxidant and DNA-protective activity in HaCaT cells compared to extracts from white light conditions. The second part of my research focused on *Staphylea pinnata*, a rare Mediterranean species that has traditionally been used to treat skin and respiratory disorders. Using the innovative, eco-friendly technique of solid-phase extraction (SPE), I isolated flavonol glycosides (quercetin and isorhamnetin derivatives), which have antioxidant, antimicrobial and DNA-repair properties, suggesting potential applications in cosmeceuticals. A third study, conducted with Dr Federica Carraturo and the startup HoloBiotics Srl (a UNINA spin-off), investigated *Lavandula angustifolia* Mill. extracts: one derived from plant stem cells; one from leaf and flower maceration; and one from distillation by-products. Tests on an *in vitro* skin cells revealed antioxidant and anti-inflammatory properties, particularly in the stem cell extract, which increased the expression of the Mytho protein associated with autophagy and cellular longevity. The distilled extract enhanced the methylation of DNA in the cell genome, suggesting possible anti-ageing and epigenetic-modulating effects. Using distillation waste also represents an example of the circular economy and sustainable innovation. Finally, thanks a collaboration with Dr. Giovanni Dal Poggetto and Gabriella Santagata (CNR-IPCB), I developed sustainable nutraceutical formulations using grape pomace extract, which is rich in antioxidant molecules. This extract was encapsulated in Ca^{2+}-pectin hydrogels to achieve strong antioxidant efficacy and controlled release. Overall, my work showcases eco-friendly strategies for the valorisation of natural bioactives in health and skincare innovations.

Aim

My PhD project focused on analysing the biological properties of natural substances for use in pharmaceutical and nutricosmetic applications. My research was based on an interdisciplinary approach, combining organic chemistry analyses, molecular biology techniques, and edible beads formulations. My work went through four different phases.

Identification of beneficial extracts, fractions or bioactive compounds from natural sources. I carried out this part of my PhD project in collaboration with Professor Carmen Arena and Dr Federica Carraturo from the Department of Biology at the University of Naples Federico II and at the Department of Chemical Sciences of the University of Naples Federico II, under the supervision of my co-tutor, Prof. Marco Masi. Together, we developed the protocols for extracting grape pomace and *Staphylea pinnata*, which were then purified in order to identify metabolites.

Biological characterization of extracts, fractions or purified metabolites. At the Department of Biology at the University of Naples Federico II, I performed in vitro assays to determine the cytotoxic and antioxidant activity of extracts, fractions or purified metabolites. To understand the potential molecular mechanisms or signalling pathways involved, I performed gene expression analyses on an *in-vitro* skin cells, as well as immunoblots and immunofluorescence analyses to monitor the expression levels of well-known markers of the cell cycle, oxidative stress, autophagy, inflammation, apoptosis and DNA damage, including cyclin D1, p21WAF, NRF2, Mytho and IL-6. I also tested the effect of isolated metabolites or natural extracts on wound repair and their possible role in cell migration.

The sustainable use of grape pomace extract in the circular economy. With a view to promoting the circular economy and ensuring potential nutraceutical applications, I have sought to reuse wine industry waste products, namely grape pomace. After demonstrating that grape pomace extract was rich in beneficial antioxidants, a collaboration with Dr. Giovanni Dal Poggetto and Dr. Gabriella Santagata (CNR-IPCB) made it possible to study the best formulation of beads that would ensure slow release of the extract without altering it in any way.

Foreign experience. During my PhD, I spent six months at the Epigenomics Unit of the Instituto de Investigación Sanitaria de Santiago (IDIS) in Santiago de Compostela, Spain. Under the supervision of my external supervisor, Dr Ángel Díaz Lagares, I learnt innovative approaches to investigating the methylation status of cells based on epigenetic analysis. In particular, I conducted experiments to determine whether treating HaCaT cells with distilled *Lavandula angustifolia* extract could alter their global methylation levels compared with control samples.

CHAPTER I

1. Introduction

1.1 Natural compounds

The term natural metabolites refer to a heterogeneous group of chemical compounds produced by living organisms, such as plants, microorganisms and animals. These compounds are biosynthesized by the producer organism through secondary metabolic pathways. Unlike primary metabolites, which are essential for cell growth and survival, secondary metabolites play key roles for the life of the organisms. For the plants these compounds are involved in plant-environment interactions: they contribute to defence against pathogens and predators, mediate intra- and interspecific communication, attract pollinators, and facilitate adaptation to adverse environmental conditions. These functions represent a fundamental evolutionary strategy for plant survival in complex and often hostile ecosystems.

Secondary metabolites are commonly classified based on their chemical structures and biological functions (Dewick, 2002). The main categories include phenolic compounds, terpenoids, and alkaloids, all characterized by a wide spectrum of biological activities. These substances are defined as bioactive due to their ability to modulate physiological processes in living organisms and they are of particular interest for the prevention and treatment of several diseases, including diabetes, cardiovascular disorders, Alzheimer's disease, Parkinson's disease and cancer (Pant et al., 2021).

The three principal classes of secondary metabolite are **alkaloids**, **terpenes**, and **phenolic compounds**.

Alkaloids are nitrogen-containing heterocyclic rings (N). They are usually derived from basic amino acids, which serve as the starting point for their biosynthetic pathways. Produced by plants, bacteria, fungi, and some animals. In plants many of them are biosynthesized as defence compounds against herbivores, due to their bitter taste and toxic or addictive effects, even at low concentrations. Well-known examples include morphine, caffeine and nicotine.

Terpenes are compounds consisting of one or more isoprene units (five-carbon structure); While terpenes are simple hydrocarbons, terpenoids include heteroatoms such as oxygen and may exhibit

structural rearrangement. They are synthesized by animals, plants, bacteria, and fungi. Many terpenes are volatile and contribute to the characteristic aroma of flowers and fruits, thereby attracting pollinators and acting as chemical messengers between plants and insects (Boncan et al., 2020). Some plant-derived terpenes, such as taxol, are widely used as anticancer agents, inhibiting cancer cell proliferation; for instance, ursolic acid, a tetracyclic triterpenoid, exerts potent anti-tumour activity by inhibiting STAT3/PD-L1 signalling in non-small cell lung cancer (Drašar et al., 2022). Others possess significant antibacterial properties (Parveen et al., 2018).

Among secondary metabolites, phenolic compounds represent a particularly interesting and diverse class. Derived from phenol, they are broadly divided into: *simple phenols* (with a single aromatic ring) and *polyphenols* (with multiple aromatic rings). Unlike alkaloids and terpenoids, polyphenols are produced exclusively by plants, fungi, and microorganisms; animals are unable to synthesize them. Plants are the major natural source of polyphenols, which serve multiple protective functions: they deter herbivorous with their bitter taste, shield tissue from UV radiation, attract pollinators, and contribute to the coloration of flowers and fruits. Some polyphenols polymers, such as lignin, are structural component of the plant cell wall and play a crucial role in plant growth and morphogenesis, and mechanical resistance as well as in the regulation of stress response to biotic and abiotic and factors (e.g., pathogens) (Naczk et al., 2004).

Flavonoids, a prominent subgroup of polyphenols, exhibit a wide range of biological activity including anti-inflammatory, antiallergic, antithrombotic, vasoprotective, anti-tumour, anti-viral and antioxidant effects. They protect the gastric mucosa and inhibit the oxidation of low-density lipoproteins, thereby contributing cardiovascular protection (Kaur et al., 2021). The current scientific interest in polyphenols largely stems from their well-established antioxidant capacity, which counteracts oxidative stress and neutralizes reactive oxygen species (ROS) generated by cells.

1.2 Importance of natural compounds in biotechnological industries

Herbal medicine, historically referred to as herbalism and now known as phytotherapy, is among the oldest healing practices known to

humankind. The development of herbal medicine in ancient Mesopotamia, Egypt, China, and India shows that treating diseases with herbs is inextricably linked to human history. Today, epidemiological studies demonstrate that diets rich in bioactive compounds exert beneficial effects on human health, slowing the aging process and reducing the incidence of chronic diseases such as cancer, diabetes, obesity, cardiovascular disorders, and neurodegenerative conditions. Natural molecules offer distinct advantages to consumers, being generally free from harsh synthetic chemicals and well tolerated. In addition, organic beauty products not only support skin health and overall well- e but also have a lower environmental impact.

These properties have fuelled growing interest in the pharmaceutical and nutricosmetic industries while the scientific community has become increasingly aware of the potential risks linked to synthetic chemicals in cosmetics, food and dietary supplements (Liu et al., 2022).

Within this context, natural compounds represent a valuable resource for multidisciplinary research. Their broad spectrum of biological activities and cross-sectoral applications, make them promising candidates for the development of novel therapeutic strategies, developing new therapeutic approaches and understanding the the elucidation of molecular mechanisms underlying physiological and pathological processes, and the design of innovative, sustainable materials.

1.3 Oxidative stress and antioxidant molecules

Oxidative stress, also known as redox imbalance, occurs when there is an imbalance between the production of oxidizing agents and their neutralization by antioxidant defence systems. Under physiological conditions, cells produce a certain level of reactive species necessary for the key biological processes, such as cell cycle regulation and immune defence. However, excessive generation of reactive species, coupled with insufficient antioxidant defences triggers damaging reactions that impair cellular and tissue integrity.

The main actors in these processes are free radicals, atoms or molecules with unpaired electrons, and more broadly reactive oxygen species (ROS) and reactive nitrogen species (RNS). Among these, the superoxide anion, hydrogen peroxide, and the hydroxyl radical are among the best characterized and most reactive. Their high chemical

reactivity enables them to attack lipids, proteins, and DNA, leading to structural and functional damage. In particular, ROS can oxidize DNA bases, such as guanine, inducing mutations associated with neurodegenerative, inflammatory, and neoplastic diseases.

The sources of reactive oxygen species (ROS) can be both endogenous and exogenous. Endogenous ROS are generated during normal metabolic processes, particularly through oxidative phosphorylation in mitochondria, as well as by the activity of the endoplasmic reticulum and peroxisomes. Exogenous sources, on the other hand, include environmental factors such as cigarette smoke, ionizing radiation, and air pollution. In all these contexts, an excessive accumulation of reactive species can overwhelm the cellular antioxidant capacity, resulting in severe biological consequences.

To counteract this, cells are equipped with multiple antioxidant defence systems, both enzymatic and non-enzymatic, that maintain redox homeostasis. Among the key enzymatic antioxidants are superoxide dismutase (SOD), which catalyzes the conversion of superoxide radicals into hydrogen peroxide, and catalase, which further decomposes hydrogen peroxide into water and oxygen. These enzymatic defences are complemented by small molecules such as glutathione and coenzyme Q10, which scavenge free radicals and protect cellular structures from oxidative injury. Metal-binding proteins such as ferritin and transferrin also plays an essential role by sequestering free iron and thereby preventing the formation of highly reactive hydroxyl radicals.

In addition to endogenous antioxidants, the body benefits from exogenous antioxidants obtained through diet. Among these, vitamins C and E are particularly important: vitamin C, a water-soluble compound, protects cells from oxidative damage and enhances iron absorption, whereas vitamin E, which is lipid-soluble, shields cellular membranes from lipid peroxidation. Other dietary antioxidants, including carotenoids, polyphenols, and lipoic acid, contribute to neutralizing ROS and preventing the onset of inflammatory and degenerative processes. Polyphenols, in particular, exhibit strong metal-chelating activity, they chelate metals and inhibit enzymes involved in the propagation of oxidative reactions.

In summary, oxidative stress is not merely a chemical imbalance but a central process in both physiological and pathological conditions. When

pro-oxidant activity exceeds antioxidant defences, molecular and cellular mechanisms are triggered that lead oxidative damage, premature aging, and the development of chronic diseases such as diabetes, atherosclerosis, neurodegenerative disorders, and cancer. Nevertheless, the role of oxidative stress remains complex: it can act both as a cause and a consequence of disease, establishing a self-perpetuating cycle that is difficult to interrupt. Understanding these mechanisms together with the importance of an antioxidant-rich diet, is therefore crucial for maintaining redox equilibrium and promoting long-term health.

CHAPTER II

2. *Brassica rapa L.*

Brassica rapa L. is a Mediterranean medium-sized economically valuable plant belonging to the family of Brassicaceae, and it is considered one of the world's oldest cultivated vegetables. Extract of *B. rapa* have been traditionally used against different types of cancer. The various subspecies of *B. rapa* including Pak choi, Chinese cabbage, *sylvestris*, *rapa*, and other vegetable types exhibit both anticancer and antioxidant properties. Different plant parts, such roots, leaves, fruit, and seeds are rich in important anticancer and antioxidant compounds including glucosinolates, carotenoids, flavonoids, ketones, aldehydes, vitamin C, etc.

Despite numerous studies on the chemical constituents and biological activities of Brassica, only a few have identified the specific active ingredients responsible for its diverse bioactivities. Flavonoids and phenolics compounds with strong free radical scavenging activity have been to account for its antioxidant effects while arvelexin, an indole derivative found in Brassica, has demonstrated anti-inflammatory, antihypertensive, and hypolipidemic potential (Paul et al., 2019).

However, the antioxidant and anticancer activities of *B. rapa* vary according to genotype, dose concentration and exposure time, solvent and extraction methods, plant part used, and other biotic or abiotic factors. Therefore, further research is required to fully identify and characterize the bioactive compounds present in the diverse *B. rapa* subspecies.

2.1 *In-vitro* antioxidant activity of extracts from white (W) or red & blue (RB) light exposed *Brassica rapa*

In recent years, the adjustment of light quality in Controlled Environment Agriculture (CEA) using Light-Emitting Diodes (LED) technology has been widely adopted to increase crop yield. Several studies have shown that modifying light intensity or selecting specific wavelength enhance the productivity of certain crops, improving both yield and food quality. Indeed, this technology has been demonstrated to alter various aspects of plant structure, anatomy, and physiology (Arena et al., 2019). Moreover, light manipulation can be applied to boost the accumulation of antioxidant compounds, such as

polyphenols, anthocyanins, and flavonoids (Lee et al.,2008; Soufi et al., 2023).

In collaboration with Prof. Carmen Arena's laboratory, I began investigating how different light regimes may influence the production of antioxidant compounds in *B. rapa* L. This section of the project builds on previous observations showing that light regimes can modulate the concentration of antioxidant metabolites in Citrus (Costanzo et al. 2023).

One hundred seeds of *B. rapa* L. subsp. *rapa* were sown in two 0.5 L containers filled with Vigorplant© universal potting soil, consisting of 21% Baltic peat (0–10 mm), 37% Irish peat (0–20 mm), slow-release fertilizer, 13% volcanic pumice (3–8 mm), and 29% superfine peat (0–3 mm). The containers were placed in a growth chamber under controlled environmental conditions: Photosynthetic Photon Flux Density (PPFD) of 270 ± 10 μmol(photon) m^{-2} s^{-1}, temperature of 25/15 °C (day/night), relative humidity of 50/70% (day/night), and a 12-hour photoperiod. Two light quality treatments were applied in the chamber: broad-spectrum white (W) and red–blue (RB) light in a 60:40 ratio, with emission peaks at 630 nm (red) and 460 nm (blue), respectively (Fig.1). Temperature and relative humidity (RH%) were monitored using a digital thermo-hygrometer (HC520 Digital Thermo-Hygrometer, Cheerman, Shenzhen, China), while PPFD was measured with a quantum sensor (Li-Cor, Lincoln, NE, USA). Microgreens were maintained in the growth chamber for fifteen days and regularly irrigated to compensate for water loss due to evapotranspiration.

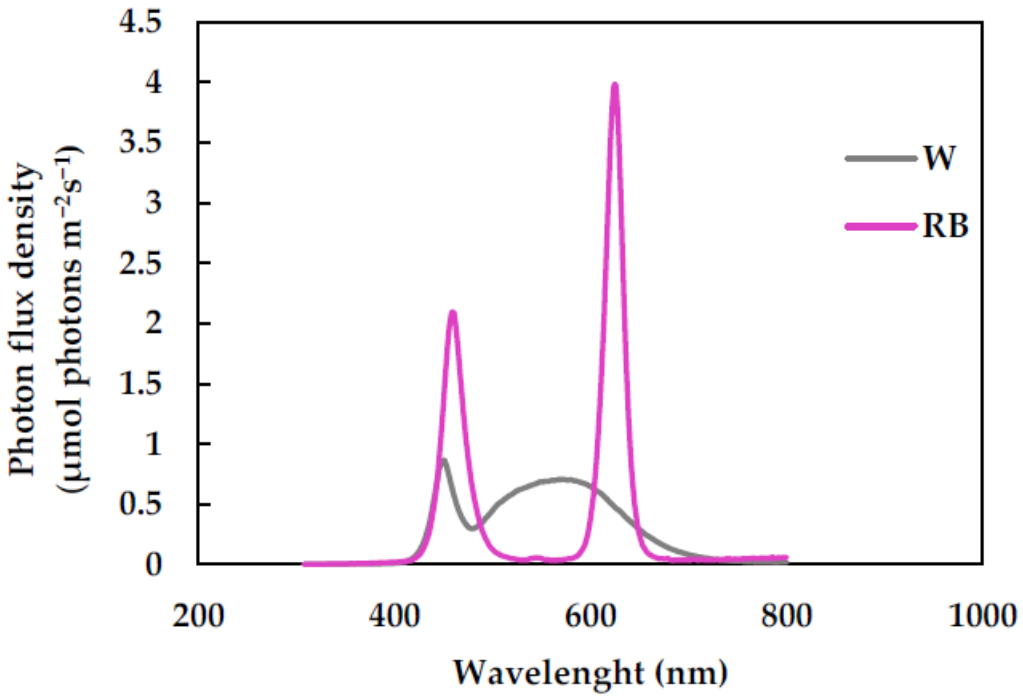

Fig. 1. Light quality treatments applied to plants in containers: white (W) and red-blue (RB), with a red emission peak at 630 nm, and a blue emission peak at 460

After fifteen days, 0.20g of microgreens, finely powered with liquid nitrogen using mortar and pestle, were extracted in 2 mL of 80% methanol, centrifugated at 11.000 rpm and ready for analysis.

The content of polyphenols and flavonoids, as well as the total antioxidant potential, in W and RB extracts were assessed using several colorimetric assays, including the Folin-Ciocolteu and FRAP assays.

The Folin-Ciocolteu assay has long been used ever since to evaluate the total polyphenols content of various samples, including natural extracts, food and plant products. The principle behind it is that, under alkaline condition, the Folin-Ciocolteu reagent is reduced by phenolic compounds to form a blue complex that can be measured at approximately 760 nm (Martins and at., 2021). In our case, an aliquot of the W and RB methanolic extracts, was mixed with 10% Folin-Ciocalteu solution and 700 mM Na_2CO_3 (in a volume ratio of 1:1 and 1:5, respectively), and the mixture was incubated in the dark for 2 hours.

The absorbance was then recorded at 765 nm using a spectrophotometer (UV-VIS Cary 100, Agilent Technologies, Palo Alto, CA, USA). The total polyphenol content was calculated using a gallic acid standard curve and expressed as milligrams of gallic acid equivalents (GAE) per gram of free water (FW). To quantify the flavonoids, a small amount of the supernatant was added to 75 µL of 5% sodium nitrite (NaNO2). Then, 150 µL of 10% $AlCl_3$ (aluminium chloride) and 500 µL of 1 M NaOH (sodium hydroxide) were added to the mixture, bringing the final volume to 1.525 mL. The absorbance was quantified spectrophotometrically (UV-VIS spectrophotometer Cary 100, Agilent Technologies, Palo Alto, CA, USA) at 510 nm. Flavonoid concentration was estimated using a catechin standard curve, expressed as milligrams of catechin equivalents per gram of fresh weight (mg CE g^{-1} FW).

The FRAP assay was performed to evaluate the antioxidant capacity of the W and Rb extracts, by determining their ability to reduce Fe^{3+} to Fe^{2+} ions. When this reduction occurs, a blue product is formed between Fe^{2+} and a chromogenic ligand, which can be measured at around 593 nm. Briefly, the extraction of 0.25 g of powdered sample (W and RB) was conducted with 5 mL of a methanol/water solution (60:40 v/v). The extracts were kept on ice for one hour and then centrifuged at 14,000 rpm for 15 minutes at 4°C. Subsequently, 150 µL of the sample was added to the FRAP reagents (2.5 mL of 300 mM acetate buffer at pH 3.6, 250 µL of 10 mM triperidoltriazine (TPTZ) and 250 µL of 12 mM $FeCl_3$). The mixture was incubated in the dark for one hour. Absorbance was recorded at 593 nm using a spectrophotometer and a Trolox standard curve was used to calculate the antioxidant capacity of the W and RB extracts,expressed as µmol Trolox equivalents (µmol TE g^{-1} FW)

All assays consistently showed that total antioxidant content was significantly higher ($p<0.05$ in microgreens extracts exposed to red and blue (RB) light compared to those grown under white (W) light confirming that RB light exposure enhances the accumulation of antioxidant metabolites in plant extracts (see Table1).

	W Light Regime	RB Light Regime
Antioxidant capacity *(µmol TE g^{-1} FW)*	9.46 ± 0.11 b	13.56 ± 0.16 a
Total polyphenols *(mg GAE g^{-1} FW)*	2.96 ± 0.07 b	4.45 ± 0.07 a
Total flavonoids *(mg CE g^{-1} FW)*	3.86 ± 0.06 b	4.40 ± 0.09 a

Table 1. Antioxidant capacity, total polyphenols, and total flavonoids measured in extracts from microgreens of *Brassica rapa* L. grown for 15 days under W light (full spectrum) and RB light (60% R:40% B) regimes. Data are means ± standard error (n=8). Different letters in the same line represent significant differences between conditions ($P<0.05$).

2.2 Biological properties of LED irradiated *Brassica rapa* L. extracts

Since the LED spectrum was found to markedly increase the antioxidant content *in vitro*, I proceeded to test whether this translated into a biological effect in human cells. To investigate the cytotoxicity of W and RB extracts. I performed MTT cell viability assays on HeLa cells after 24 and 48h of treatment of W and RB extracts. This assay is based on reduction of 3-(4,5-methylthiazol-2)-2,5-diphenyltetrazolium bromide (MTT) to formazan salt by the mitochondrial enzyme named succinate dehydrogenase. Cells were treated with W or RB extracts at concentrations of 1, 10, 100 and 1000 µg/mL. Lycorine, a well characterized cytotoxic metabolite, was used as positive control.

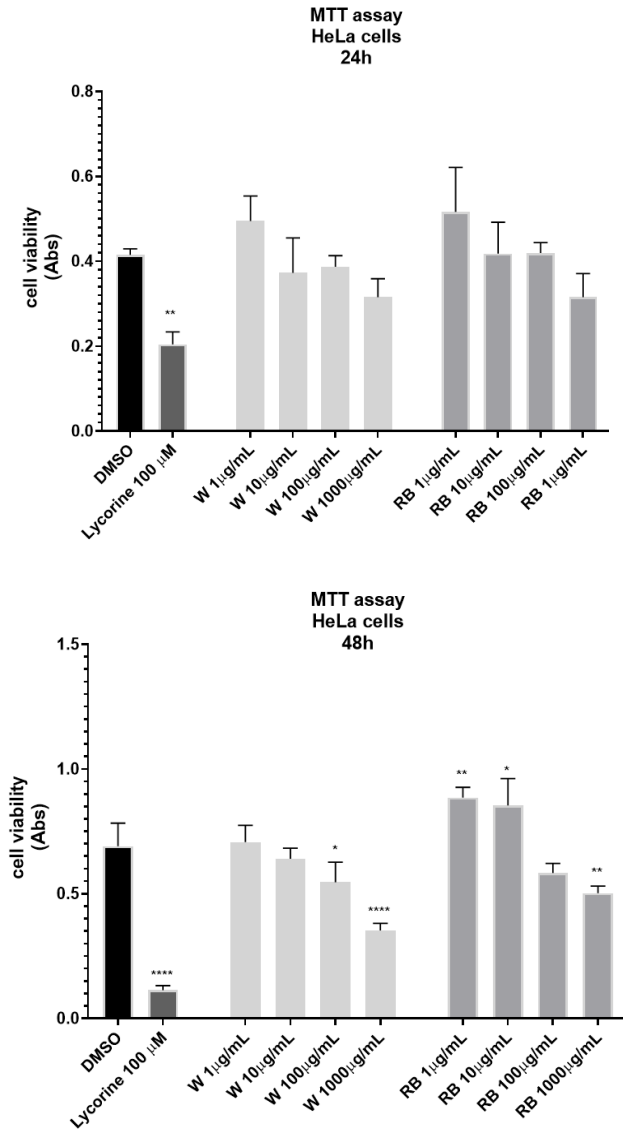

Fig. **2.** MTT assay. The cells were treated with the indicated doses of both extracts for 24h and 48h. In all the samples there was 0,1% DMSO. The values were the mean's six values for each experimental point of three independent biological replicates. Each mean was compared using a Dunnett's multiple comparisons test of ANOVA one-way (p-value *< 0.01, ** < 0.05, ****p < 0.0001).

As shown in Figure 2, W and RB extracts exhibited no or very low toxicity between 1 and 10 µg/mL the showed both after 24 and 48h of

treatment. Remarkably, RB extract at the lowest concentrations,1 and 10 µg/mL, significantly enhanced cell viability after 48h of treatment. Both W and RB extracts were toxic at the highest concentration tested, 1000 µg/mL.

To evaluate the antioxidant activities of W and RB extracts, I performed a DCFDA assay on HeLa cells. This assay relies on 2′-7′ dichlorofluorescein diacetate (DCFDA), a non-fluorescent compound that, that is converted into a fluorescent form upon oxidation by reactive oxygen species (ROS). Oxidative stress was induced by 4 mM H_2O_2; I treated HeLa cells for 4h with W or RB extracts at non-toxic concentrations (1, 10, 100 µg/mL). The oxidative stress was induced by treatment with H_2O_2 4 mM; 3%. Trolox, a permeable analogue of vitamin E, was used as positive control and DMSO as negative control. My results showed that the RB extract has strong antioxidant activity reaching a plateau already at 1µg/mL compared to control sample (DMSO); whereas W extract displayed significant antioxidant capacity only at 100 µg/mL (Fig. 3).

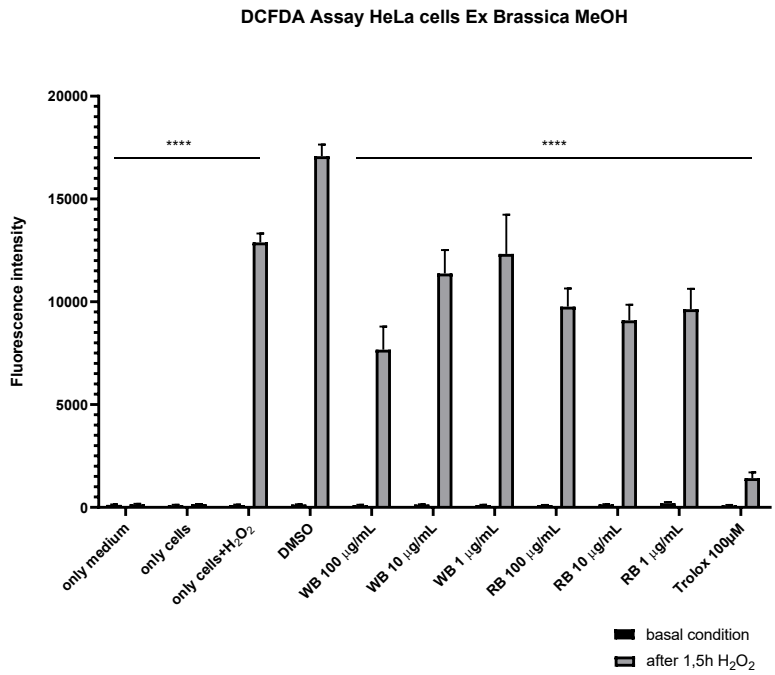

Fig. 3. DCFDA antioxidant assay. HeLa cells were seeded and pretreated with the indicated amount of W and RB organic extract for 4 h. Trolox was used as a positive control and DMSO as negative control. The fluorescence intensity of DCFDA was read in the basal condition (NT) or samples treated with H_2O_2 (4 mM; 3%) for 1.5 h. The values are the mean's six values for

each experimental point of three independent biological replicates. Statistical analysis was performed with two-way ANOVA, using Tukey's multiple comparison test, compared to the negative control (DMSO) Levels of significance between points of expression are shown (p-value ****$p < 0.0001$).

Because HeLa cells are transformed, the experiments were repeated in HaCaT cells, which are immortalized but not transformed keratinocytes derived from human adult skin.

I performed the MTT assay using the same protocol used for HeLa cells. HaCaT cells were treated with W and RB extracts at the concentrations of 1, 10, 100 and 1000 µg/mL (Fig. 4). As shown in Figure 4, unlike the W extract, the RB extracts increased HaCaT cell viability at both 24 and 48h of incubation. Consistent with HeLa results, both extracts induced a substantial reduction in cell viability at the highest concentration tested, 1000µg/mL.

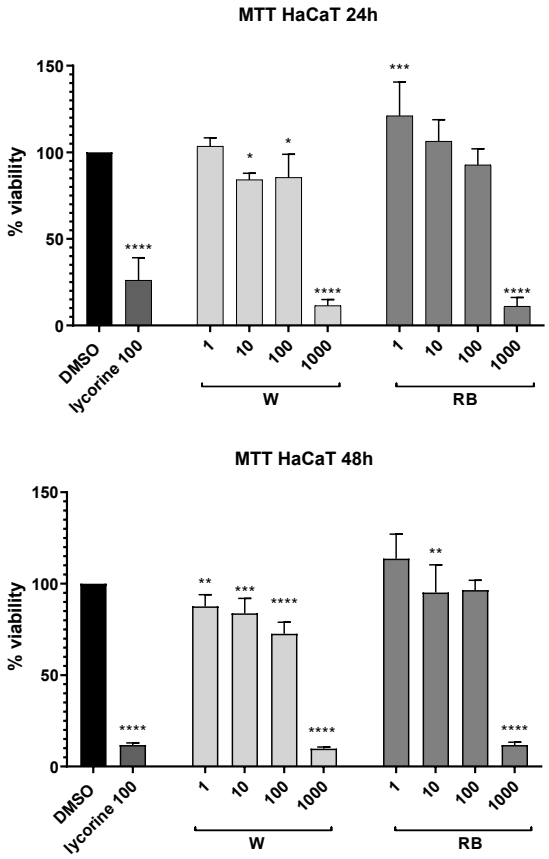

Fig. 4. MTT assay. HaCaT cells were treated with the indicated doses of both extracts for 24h and 48h. In all the samples there was 0,1% DMSO. The values were the mean's six values for each experimental point of three independent biological replicates. Each mean was compared using a Dunnett's multiple comparisons test of ANOVA one-way (p-value *< 0.01, ** < 0.05, ***p < 0.001; ****p < 0.0001).

Next, I performed the DCFDA assay on the previously mentioned HaCaT cells. The results indicate that both RB and W extracts exhibited significant antioxidant activity, although the RB extract was more effective than the W extract at low concentrations. However, increasing the concentration of the extract from 1 to 100 µg/mL did not result in a substantial additional improvement in antioxidant activity (Fig. 5).

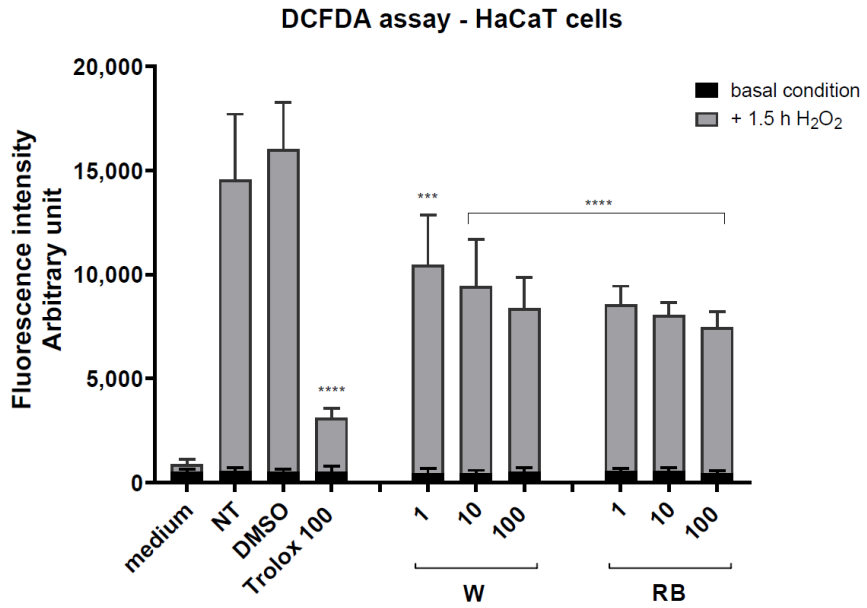

Fig. 5. DCFDA antioxidant assay. HaCaT cells were seeded and pretreated with the indicated amount of W and RB organic extract for 4 h. Trolox 100µm was used as a positive control. The fluorescence intensity of DCFDA was read in the basal condition (NT) or samples treated with H_2O_2 (4 mM; 3%) for 1.5 h. The values are the mean's six values for each experimental point of three independent biological replicates. Statistical analysis was performed with two-way ANOVA, using Tukey's multiple comparison test. Levels of significance between points of expression are shown (p-value ***p < 0.001; ****p < 0.0001).

Cell subjected to oxidative stress responds by forming protective cytoplasm structures known as stress granules (SGs). SGs safeguard messenger RNAs and allow their translation only once the stress stimulus ceased. Their assembly involves the protein YB-1, a cold shock protein that regulates multiple cellular processes, including transcription and translation, DNA repair, and cell cycle progression. However, upon DNA damage, SGs disassemble and YB-1 translocate to the nucleus, where it cooperates, with DNA repair machinery (Guarino et al.,2019).

One of the earliest cellular responses to DNA damage is the phosphorylation of histone H2AX on Ser-139, generating γH2AX by ATM and other DNA damage-activated kinases, (Savic et al., 2009; Mah et al., 2010). For this reason, γH2AX is widely considered a marker of DNA damage. I performed immunofluorescence experiments in HaCaT cells using antibodies against γH2AX to assess whether W and RB extracts counteract ROS-induced DNA damage (Fig. 6). HaCaT

cells, pretreated or not with W or RB microgreen extracts, were stimulated with 300 μM H_2O_2 to induce oxidative stress. As negative control, we used unstimulated cells with DMSO vehicle alone, while H_2O_2-stimulated cells were the positive control. Treatment with 100 μM Trolox was used as positive control. Hydrogen peroxide treatment promoted the formation of YB-1–positive SGs, detectable as green cytoplasmic puncta, and γH2AX foci, indicating the occurrence of DNA damage (Fig. 6A, lower panel). As expected, in cells treated with the antioxidant Trolox, SGs were undetectable, YB-1 was uniformly distributed into the cytoplasm (Fig. 6B, lower panel), and γH2AX foci were reduced.

In unstimulated cells treated with the W extract, γH2AX foci increased in a dose-dependent manner, indicating the occurrence of DNA damage (Fig 6C upper panel, E). Upon oxidative stress induction, W-pretreated cells did not show a significant reduction of γH2AX foci compared to the control. After the treatment with 10 and 100μg/mL of RB extract we observed a significant reduction of γH2AX foci (Fig. 6D, F).

Consistently, YB-1 accumulated in the perinuclear region (Fig. 6 C) at 100 μg/mL with the W extract. Conversely, in cells pretreated with 10 μg/mL and 100 μg/mL of RB extract YB-1 was detected within aggregates distributed between the nucleus and cytoplasm (Fig. 6D).

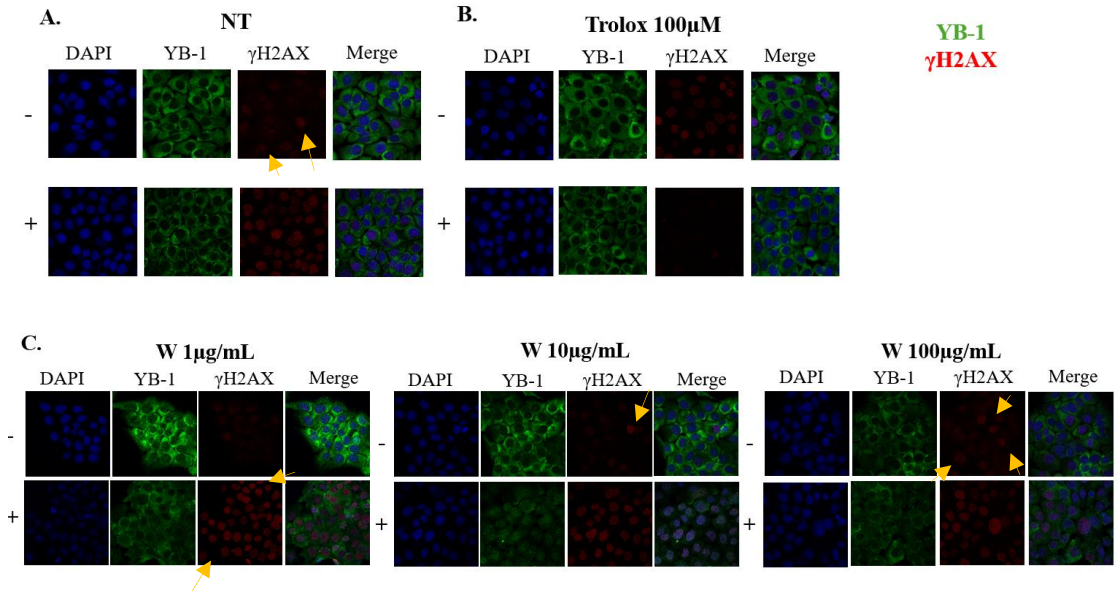

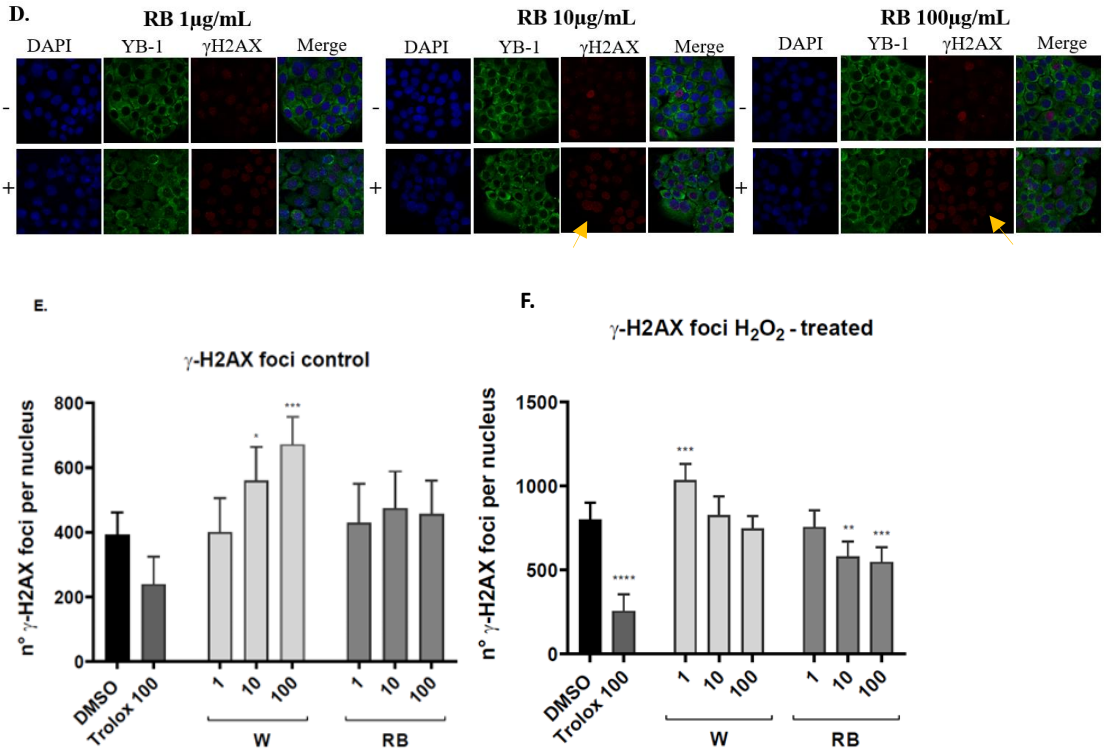

Fig. 6. Confocal immunofluorescence to detect YB-1 subcellular localization and γ-H2AX foci in basal and oxidative stress conditions. (**A**) Control cells untreated (upper panel) or treated with hydrogen peroxide (lower panel). Cells were stained with α-YB1 (green) and α-γ-H2AX (red) antibodies. Nuclei were stained with DAPI. (**B**) Trolox treated cells, untreated (upper panel) or treated with hydrogen peroxide (lower panel). (**C**) W extract-treated cells (1-100 µg/mL) untreated (upper panel) or treated with hydrogen peroxide (lower panel). (**D**) RB extract-treated cells (1-100 µg/mL) untreated (upper panel) or treated with hydrogen peroxide (lower panel). (**E-F**) Quantification of γ-H2AX foci of hydrogen peroxide untreated and treated cells performed by Fiji ImageJ software. Values were compared to the baseline/physiologic number of foci of the DMSO (cells in 0.1% DMSO, negative control) and Trolox 100 µg/mL (positive control). Data are the means ± standard error (n = 6) of three independent biological replicates. Statistical analysis was carried out by two-way ANOVA followed by Sidak's multiple comparison tests (*p*-value * < 0.01, ** < 0.05, *** *p* < 0.001; **** *p* < 0.0001).

Finally, I performed the Western Blot analysis to evaluate the effect of W and RB extracts on the level of redox-sensitive NRF2 transcription factor and the cell cycle checkpoint regulator p21 WAF. P21WAF is a well-characterized inhibitor of CDK-cyclin complexes. NRF2 and p21WAF proteins are known to be upregulated in response to oxidative stress, contributing to cellular protection against oxidative damage. In mammals, the NRF2 transcription factor regulates the expression of ROS-detoxifying enzymes to preserve cellular homeostasis (Bellezza et al.,2018) while the p21WAF protein promotes cell survival in response to oxidative stress (O'Reilly, 2005). In control cells, low doses

of the W extract (1 and 10 µg/mL) increased NRF2 and p21WAF protein levels, representing an early defensive response typically activated under mild oxidative stress. However, at the highest concentration (100 µg/mL) of W extract, both NRF2 and p21WAF levels dramatically decreased confirming the previously observed cytotoxic effect. (Fig. 7A-C). Under oxidative stress conditions, both W and RB extracts decreased NRF2 expression, indicating that both extracts can trigger a protective response against oxidative stress. However, their effects on the cell cycle regulator p21WAF were markedly different. Specifically, only the RB extract was efficiently reduced p21WAF levels, suggesting that RB-treated cells displayed signs of recovery from oxidative stress thereby facilitating cell cycle progression. In contrast, the W extract did not significantly reduce p21WAF levels, indicating a lower efficiency in promoting recovery from stress (Fig. 7D-F).

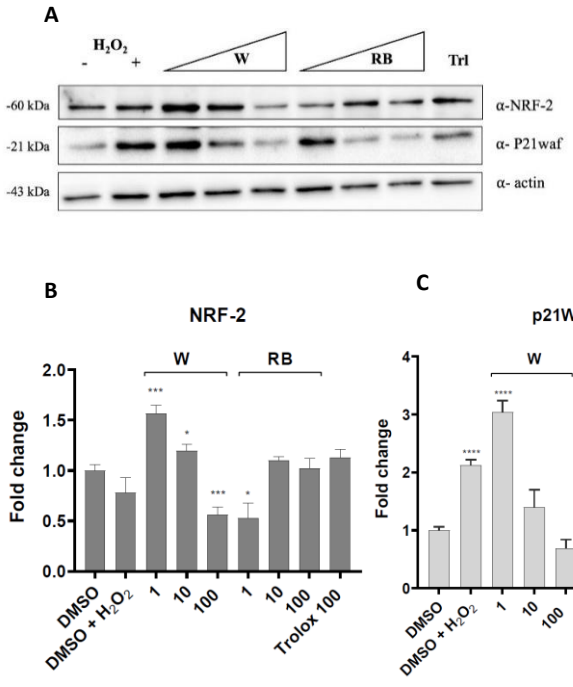

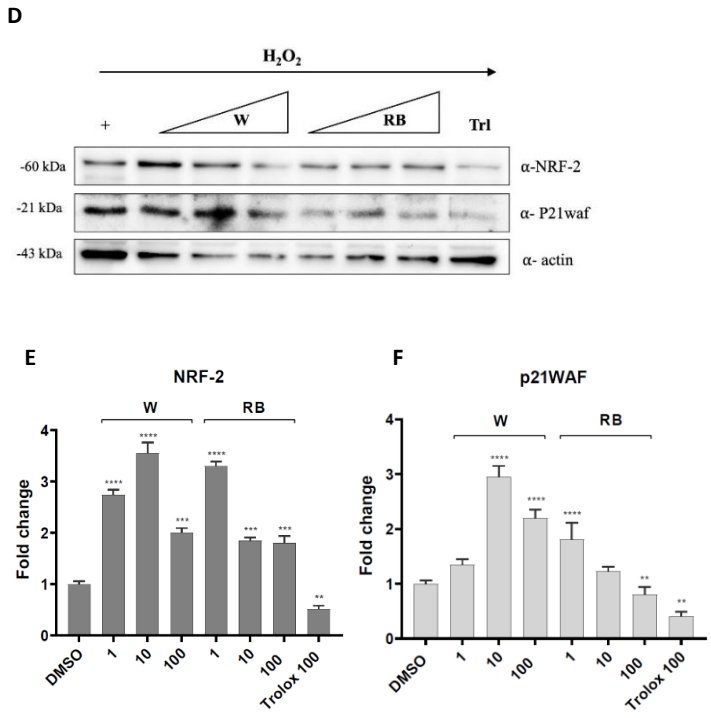

Fig. 7. Western blot analysis of total extracts from HaCaT keratinocytes treated for 4 h with 1, 10 and 100 µg/mL of W (white light) and RB (red–blue light) extracts stimulated with H_2O_2 (D-F) and without H_2O_2 (A-C). DMSO (cells in 0.1% DMSO, negative control); DMSO + H_2O_2 (cells in 0.1% DMSO, negative control plus H_2O_2) and Trolox 100 µg/mL (positive control). Immunoblots were probed with NRF2 and p21WAF antibodies. β-actin was used as a loading control. The protein bands were quantified by ImageLab software version 4.1 (Bio-Rad, Hercules, CA, USA). Statistical analyses were carried out by two-way ANOVA followed by Sidak's or Dunnett's multiple comparison test (**** $p < 0.0001$,*** $p < 0.001$, ** $p < 0.01$, * $p < 0.05$)

2.3 Discussion and conclusion

This study provides new insights into the influence of light quality on the phytochemical composition and bioactivity of *B. rapa* L. microgreens. My findings confirm that both white (W) and red-blue (RB) LED light regimes enhance the accumulation of antioxidant metabolites, including polyphenol and flavonoids, but RB light was consistently more effective in promoting antioxidant capacity. This finding is consistent with previous reports in *Citrus* and other crops, where RB light enhanced the biosynthesis of secondary metabolites with strong antioxidant potential (Arena et al., 2019; Soufi et al., 2023). *In vitro* assays demonstrated that the RB extract not only exhibited stronger antioxidant activity in cell-free systems (Folin–Ciocalteu, FRAP) but also provided superior biological protection in human cells compared to the W extract.

Specifically, the RB extract reduced ROS accumulation at very low concentrations (1–10 µg/mL), whereas the W extract required higher doses to achieve comparable effects. This suggests that RB-induced metabolites may be more potent antioxidants or act through synergistic mechanisms. Importantly, the RB extract exerted protective effects against DNA damage induced by oxidative stress, as shown by a significant reduction in γH2AX foci and by modulation of YB-1 subcellular localization. These results indicate that RB-treated cells were better able to counteract genotoxic stress and maintain genomic stability, a property of high relevance for nutraceutical and cosmeceutical applications. Consistently, Western blot data revealed that both extracts activated NRF2, the master regulator of antioxidant responses, but only the RB extract significantly reduced p21WAF expression under oxidative stress, suggesting a more efficient recovery of normal cell cycle progression. Together, these findings highlight that RB exposure drives the production of phytochemicals that not only enhance the antioxidant pool but also translate into tangible biological effects in mammalian cells. This dual activity—antioxidant and genoprotective—suggests a promising role of RB-exposed *B. rapa* microgreens as functional ingredients in health-promoting formulations. Nonetheless, several aspects warrant further investigation. First, the precise metabolites responsible for the observed effects remain to be identified. While polyphenols and flavonoids are likely candidates, other phytochemicals such as glucosinolates and their hydrolysis products may also contribute. Second, the bioavailability and metabolic fate of these compounds *in vivo* should be assessed, as in vitro activity does not always translate into systemic efficacy. Finally, scaling up LED-based cultivation in controlled environments requires an evaluation of cost–benefit ratios and life-cycle sustainability to fully support industrial application.

In conclusion LED mediated light manipulation represents a sustainable and non-invasive strategy to enrich crops with high value bioactive. *B. rapa* microgreens grown under RB light could therefore serve as an innovative source of natural antioxidants for nutraceutical, cosmeceutical, and potentially therapeutic applications. Future research should focus on metabolite profiling, in vivo validation, and formulation studies to translate these results into practical products, while also addressing the scalability and environmental impact of LED-based controlled agriculture.

CHAPTER III

3. *Staphylea pinnata L.*

Staphylea is a genus of plants belonging to the family Staphyleaceae, distributed across tropical and temperate regions of America, Europe, and the Far East. The name of the genus derives from the Greek *staphyle*, meaning “cluster,” referring to the characteristic inflorescences arranged in a cluster These plants are mainly cultivated for ornamental purposes, appreciated for their white flowers and bright green leaves. In traditional Chinese medicine, a decoction made from Staphylea fruits has been used as a remedy for coughs. Native Americans employed an infusion of *Staphylea trifolia* for its anti-rheumatic, dermatological, sedative, and gynecological properties (Lacikova et al., 2009). *S. pinnata* is a deciduous shrub that can reach of 6 meter in height. The species name refers to the appearance of its leaves. It grows at altitudes between 0 and 900 meters in most Italian regions, except for Valle d'Aosta, Liguria, Sardinia, and Sicily. The plant flowers between May and June and is hermaphroditic. It produces edible seeds in a capsule containing 2 or 3 lobes that ripen from September to November. The fruits assume a distinctive bladder-like shape, which explains the common name: “European bladdernut.” In reference to this morphology, the plant is also colloquially known as ‘bossolo’ or ‘false pistachio’. *S. pinnata* is a species that prefers temperate climates and humid habitats, and it is commonly found along watercourses and forest edges. Its natural distribution extends across central-southern and southeastern Europe, as well as in Asia Minor. It is the only representative of the genus Staphylea occurring in Europe. Within the continent, it is particularly widespread from Moldova, Bulgaria, and Romania to the northern Alpine border and Italy. Its northern distribution reaches the Czech Republic and southern Poland, while the southernmost records are reported in Calabria. Previous studies have shown that this species of plant produces bioactive metabolites with antioxidant properties, including polyphenols, although their precise nature has not been fully characterized (Lacikova et al., 2009). One study reported the isolation of six flavonoids from *Staphylea bumalda*, but did not assess their bioactivity (Sohn et al., 2004). More recently Šircelj et al. (2019) investigated the bioactive components of *S. pinnata* seeds however, to date no data are available on the chemical composition of bioactive constituents in the leaves.

Current research on the biotechnological potential of bladdernut focuses on secondary metabolites particularly polyphenols, flavonoids,

and hydroxycinnamic derivatives – due to their possible antibacterial, antiproliferative, and antioxidant activities.

3.1 Natural Flavonol Glycosides derived from *S. pinnata*

3.1.1 Chemical analysis of *S. pinnata* extracts and isolation of specialized metabolites

The chemical characterization of metabolites from *S. pinnata* was carried out under the supervision of Prof. Marco Masi at the Department of Chemical Sciences, University of Naples, Federico II, Italy. The plant material was collected in Campania, Italy by Dr. Michele Innangi of the University of Molise and the specimen has been deposited in the herbarium collection of the same Institution.

Fresh leaves of *S. pinnata* were dried at room temperature and subsequently finely powdered. Ten grams of resulting powder were extracted overnight at room temperature (25°C) with 400 mL MeOH/H_2O 1:1. The suspension was filtered, yielding 300 mL of extract, which was further processed using two different extraction approaches. Specifically, 150 mL of the hydroalcoholic solution were subjected to a liquid-liquid extraction (LLE) using solvents of increasing polarity (i.e. *n*-hexane, dichloromethane (CH_2Cl_2) and ethyl acetate (EtOAc)), whereas the remaining 150 mL were processed by solid-phase extraction (SPE) as illustrated in Figure 8.

SPE is an extractive technique applied to separate analytes from complex matrix. In this process, the liquid sample is passed through adsorbent particles. These particles exhibit a higher affinity for the target analytes than for the surrounding liquid. Consequently, the analytes are selectively retained on the solid material and subsequently eluted with an appropriate solvent. This technique enables both separation and pre-concentration of specific compounds from the crude extract. Moreover, SPE is considered environmentally friendly, as it requires only minimal volumes of solvents (Badawy et al., 2022).

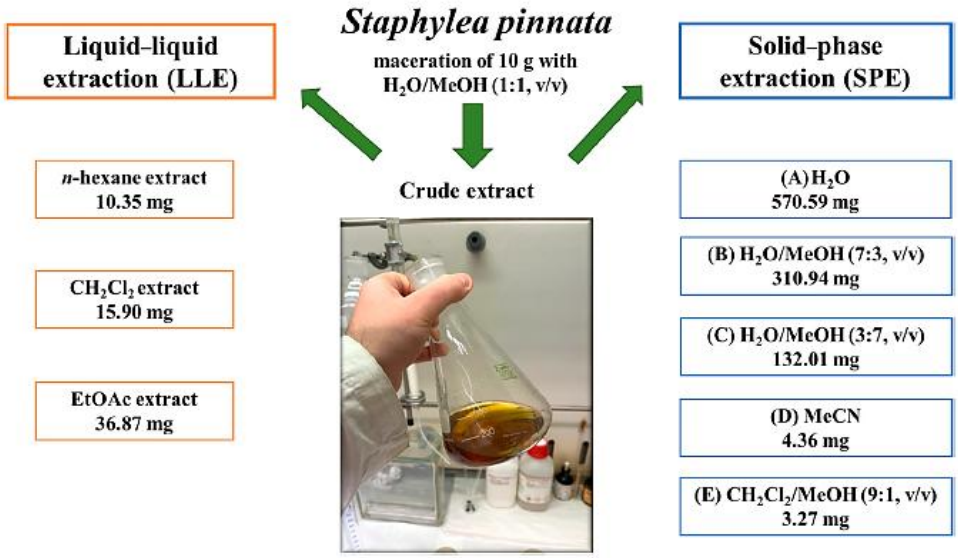

Fig. 8. Flow chart showing the fractions obtained using the two procedures (LLE e SPE)

The SPE procedure was performed through stepwise elution with different solvent mixtures. The extraction yield obtained by SPE was higher than that of LLE. Analysis of the fractions revealed differences in metabolite content, with some major compounds being detected in both the EtOAc extract from LLE and the C fraction from SPE. Fraction C from SPE was further purified through two successive steps of TLC, using both direct and reverse phase systems. This process resulted in an enriched metabolite profile comprising six flavonol glycosides.

Flavonol glycosides are flavonoids bound to one or more sugar moieties, such as glucose, glucorhamnose, arabinose, galactose and rhamnose. They represent one of the most abundant classes of polyphenols in the human diet, as fruit and vegetables are particularly rich in these compounds. These natural products are reported to exert multiple beneficial effects on human health including the modulation of anti-inflammatory and immunomodulatory responses. (Godinho et al, 2021).

The isolated metabolites (Fig. 9) were identified by comparison of their spectroscopic data (essentially the 1H NMR) with those reported in the literature and were identified as isoquercetin (**1**) (He et al., 2017), rutin (**2**) (Kazuma et al., 2003), isorhamnetin glucoside (**3**) (He et al., 2017), narcissoside (**4**) (Eskalieva et al., 2004), quercetin malonyl glucoside (**5**) (Wald et al.,1989), and isorhamnetin malonyl glucoside (**6**) (Wald et

al.,1989). The identifications were further supported by ESIMS data recorded in the negative ion mode, which showed the deprotonated pseudomolecular ion [M-H]- peaks at *m*/*z* 463, 609, 477, 623, 549, and 563 (**1**–**6**). Finally, the stereochemical configuration was confirmed by comparison of the specific optical rotation values with those reported in the literature (He et al., 2017; Kazuma et al., 2003; Eskalieva et al., 2004; Wald et al.,1989).

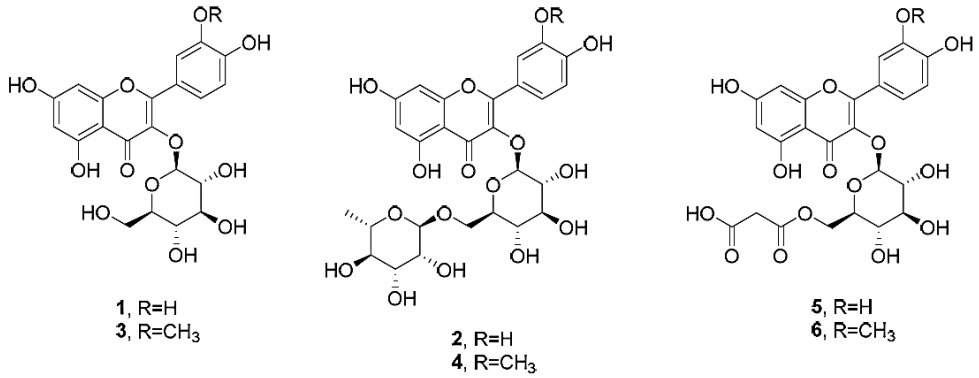

Fig. 9. Chemical structures of six pure metabolites isolated from *S. pinnata*: isoquercetin (**1**), rutin (**2**), isorhamnetin glucoside (**3**), narcissoside (**4**), quercetin malonyl glucoside (**5**), and isorhamnetin malonyl glucoside (**6**).

3.1.2 *In-vitro* testing of the effects of *S. pinnata* fractions and their pure metabolites

First, I performed MTT assays (a cytotoxicity assay) on the non-transformed keratinocyte cell line, HaCaT, and the transformed cervical cancer cell line, HeLa, to evaluate the potential effect of the crude extract from *S. pinnata*. Cells were treated with increasing concentrations of the extract (from 1 to 500 µg/mL) and 5% of DMSO as positive control. As shown in Figure 10A, the crude extract did not exhibit cytotoxicity in either HaCaT or HeLa cells.

Subsequently, I carried out an in vitro antioxidant assay (DCFDA) using the same concentration range previously tested in the MTT assay, in order to assess the extract's ability to counteract intracellular ROS accumulation. As reported in Figure 10B the crude extract displayed significant antioxidant activity in both cell lines.

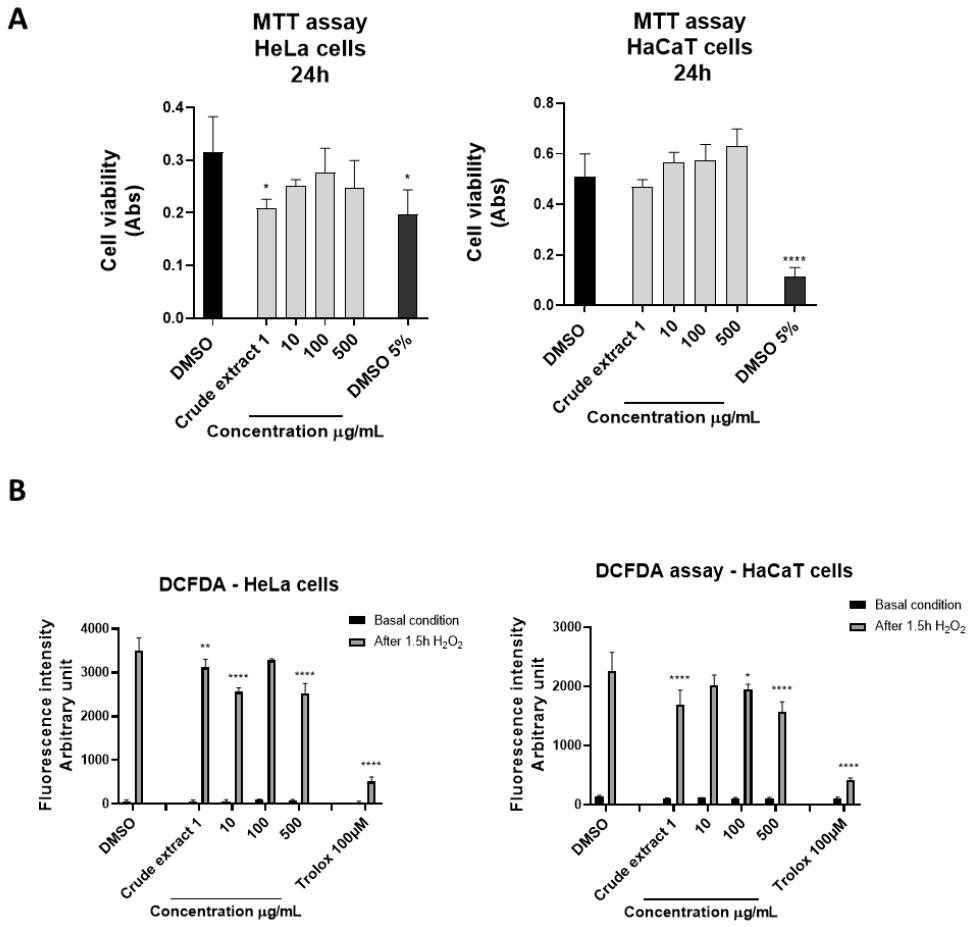

Fig. 10. (**A**) MTT viability test. HeLa and HaCaT cells were treated with the indicated amount of crude hydroalcoholic for 24 h and 5% of DMSO as positive control. The values were the mean's six values for each experimental point of two independent biological replicates. Each mean was compared using a Dunnett's multiple comparisons test of a one-way ANOVA (*p*-value * $p < 0.01$, **** $p < 0.0001$). (**B**) DCFDA assay. HeLa and HaCaT cells were seeded and pre-treated for 4 h with 1, 10, 100, and 500 µg/mL of crude hydroalcoholic extract. H2O2 (4mM; 3%) was added to the medium for 1.5 h. The fluorescence intensity of DCFDA was read after 45 min of incubation. Trolox was used as a positive control, and 0.5% DMSO, in which the metabolites were dissolved, was used as a negative control. The values are the mean's six values for each experimental point of two independent biological replicates. The statistical analysis was performed with a two-way ANOVA using Tukey's multiple comparison test. The levels of significance between the points of expression are indicated (**** $p < 0.001$, ** $p < 0.05$, * $p < 0.01$).

Considering the initial promising results, I evaluated the LLE and SPE fractions by performing the MTT assay to assess their cytotoxicity on HaCaT cells at the concentrations reported in Figure 11A. At 500 µg/mL all the LLE extracts and SPE fractions A, B and C exhibited toxicity in HaCaT cells. Therefore, the antioxidant activity was subsequently assessed using the DCFDA assay at concentrations associated with minimal or no cytotoxicity. As shown in Figure 11B, all three LLE fractions at 100 µg/mL reduced intracellular ROS levels by approximately 30% in HaCaT cells. Amon the SPE fractions, both B and C demonstrated significant antioxidant activity with fraction C exhibiting the strongest effect at 100 mg/mL.

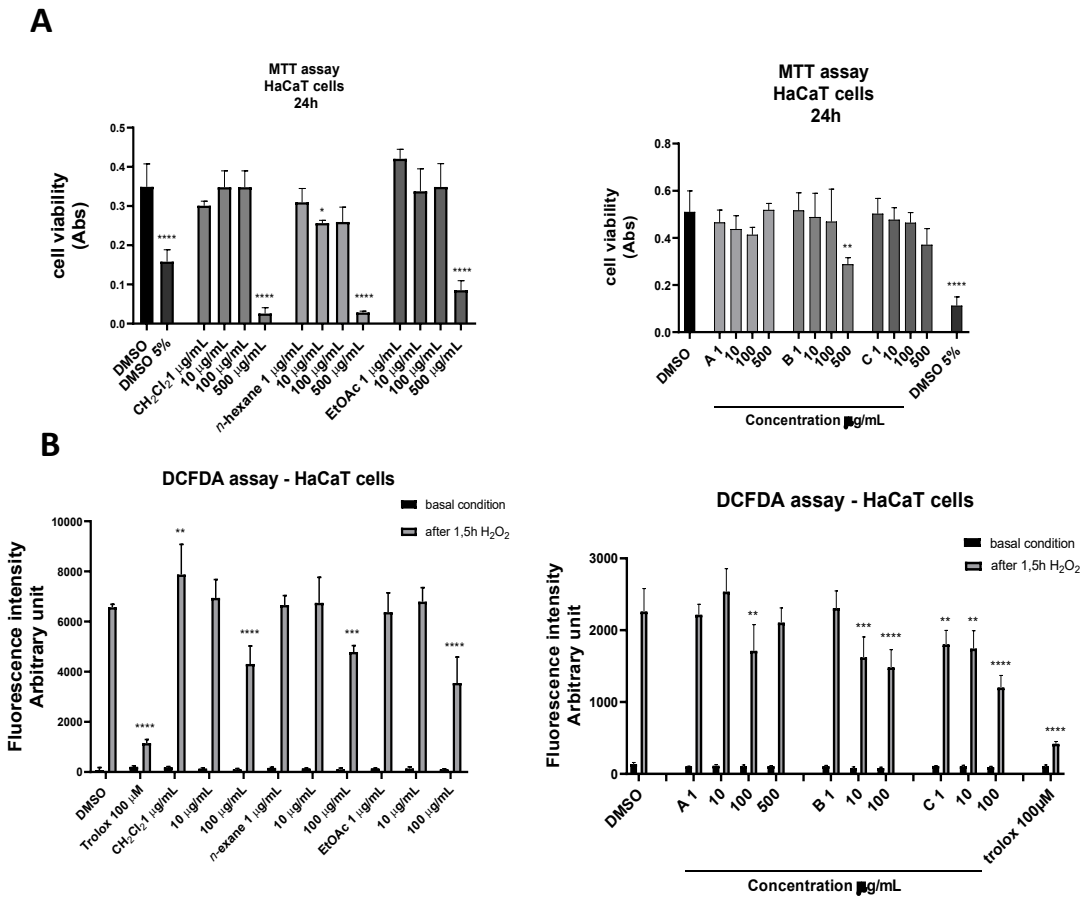

Fig. 11. (A) MTT assays at 24 h of the CH_2Cl_2, *n*-hexane, and EtOAc fractions obtained through the LLE procedure on HaCaT cells at concentrations of 1, 10, 100, and 500 µg/mL. 5% DMSO was used as a positive control. MTT viability test. HaCaT cells were incubated with the indicated amount of the A, B, and C fractions obtained through the SPE technique for 24 h.The values were the mean's six values for each experimental point of two independent biological replicates.

Each mean was compared using a Dunnett's multiple comparisons test of a one-way ANOVA (p-value * $p < 0.01$, ** $p < 0.05$,; **** $p < 0.0001$) (**B)** DCFDA assay of the CH_2Cl_2, *n*-hexane, and EtOAc fractions on HaCaT cells. Trolox was used as a positive control. DCFDA assay. HaCaT cells were seeded and pre-treated for 4 h with no toxic concentrations of the A, B, and C fractions obtained through the SPE technique. H_2O_2 (4 mM; 3%) was added to the medium for 1.5 h. The fluorescence intensity of DCFDA was read after 45 min of incubation. Trolox was used as a positive control, and DMSO, in which the extracts or fractions were dissolved, was used as a negative control. The values are the mean's six values for each experimental point of two independent biological replicates. The statistical analysis was performed with a two-way ANOVA using Tukey's multiple comparison test. The levels of significance between the points of expression are indicated (**** $p < 0.001$, *** $p < 0.01$, ** $p < 0.05$).

At this stage, since SPE fraction C exhibited the most promising biological activities, it was further purified to yield six pure flavonol glycosides: isoquercetin (**1**), rutin (**2**), isorhamnetin glucoside (**3**), narcissoside (**4**), quercetin malonyl glucoside (**5**), and isorhamnetin malonyl glucoside (**6**) (Fig. 4). Isoquercetin (**1**), rutin (**2**) and quercetin malonyl glucoside (**5**) were quercetin glycoside, while **3**, **4**, and **6** were isorhamnetin glycosides.

To investigate the effect of the six isolated metabolites on cell viability, HaCaT cells were treated for 24h with increasing concentrations of each compound, from 25 to 100µM followed by MTT assay. None of the metabolites (1-6) exhibited significant cytotoxicity or affected cell growth rate (Fig. 12A, C, D). Furthermore, their antioxidant potential was assessed using the DCFDA assay at the same concentrations tested in the MTT assay. As shown in Figure 12B isoquercetin (**1**) and quercetin malonyl glucoside (**5**) provide strong protection against oxidative stress in HaCaT cells highlighting their potential relevance for cosmeceutical applications such as anti-aging moisturisers or serums.

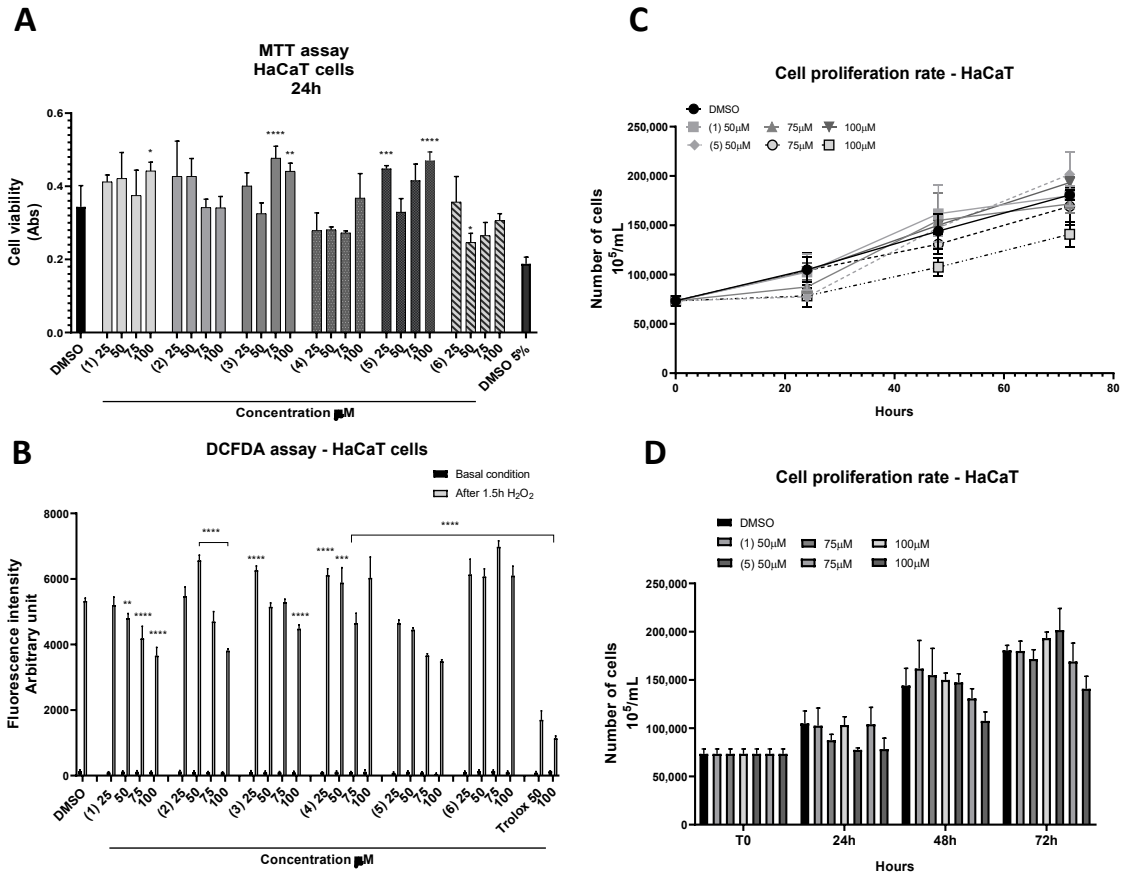

Fig. 12. (A) MTT viability test. HaCaT cells were incubated with the indicated amount of pure metabolites (1–6) obtained from fraction C of *S. pinnata* for 24 h. The values were the mean's six values for each experimental point of two independent biological replicates. Each mean was compared using a Dunnett's multiple comparisons test of a one-way ANOVA (p-value * $p < 0.01$, ** $p < 0.05$, *** $p < 0.001$; **** $p < 0.0001$). (**B)** DCFDA assay. HaCaT cells were seeded and pre-treated for 4 h with no toxic concentrations of the pure metabolites (1–6) obtained from fraction C of S. pinnata. H2O2 (4mM; 3%) was added to the medium for 1.5 h. The fluorescence intensity of DCFDA was read after 45 min of incubation. Trolox was used as a positive control, and DMSO, in which the metabolites were dissolved, was used as a negative control. The values are the mean's six values for each experimental point of two independent biological replicates. The statistical analysis was performed with a two-way ANOVA using Tukey's multiple comparison test. The levels of significance between the points of expression are indicated (**** $p < 0.001$, *** $p < 0.01$, ** $p < 0.05$). (**C**,**D**) Cell growth profile. HaCaT cells were seeded and treated with isoquercitin (**1**) and quercetin malonyl glucoside (**5**) at the indicated concentrations. The cells were counted at T0, 24, 48, and 72 h of treatments, and the number was compared to the untreated cells. The results are the mean ± SEM of three independent biological replicates relative to the experimental control (DMSO). The statistical analysis was performed with a one-way ANOVA using Dunnett's multiple comparison test.

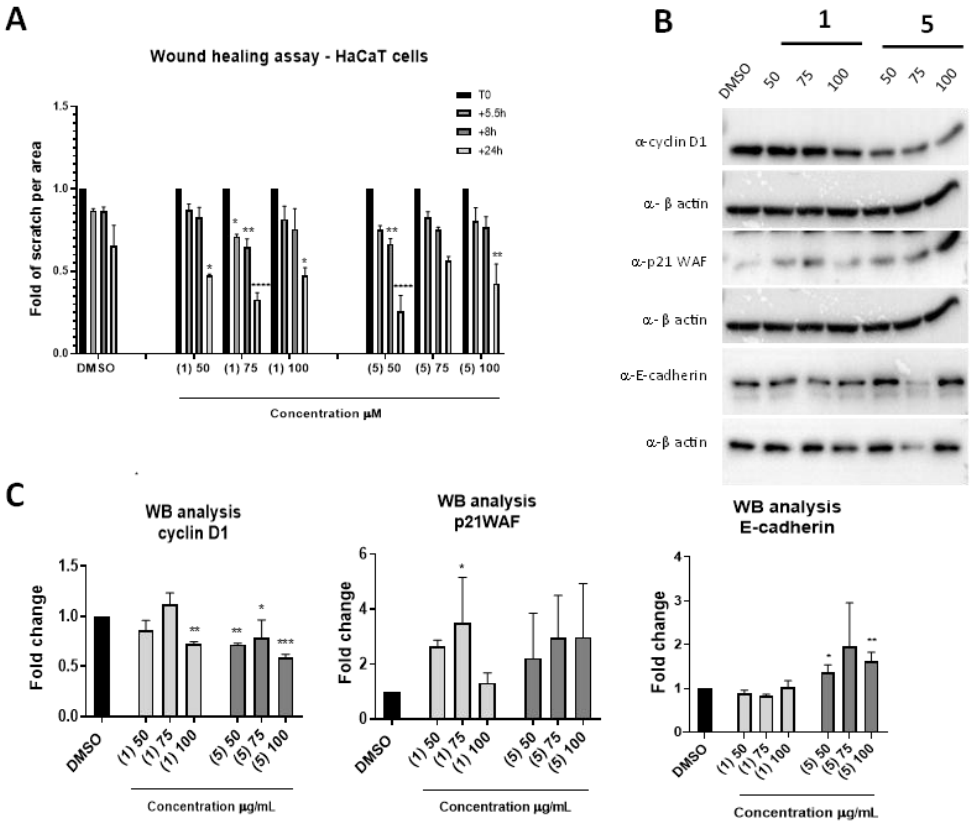

Fig. 13. Wound healing assay. (**A**) The HaCaT cell monolayer was scratched in the center with asterile tip and treated with isoquercetin (**1**) or quercetin malonyl glucoside (**5**) at 50 µM, 75 µM, and 100 µM. The statistical analysis was performed with a two-way ANOVA using Dunnett's multiple comparison test (p-value * $p < 0.01$, ** $p < 0.05$, **** $p < 0.0001$). The results are the mean ± SEM of three independent biological experiments relative to the experimental control (DMSO). (**B**) Representative image of the Western blot analysis of the extracts from HaCaT keratinocytes treated for 24 h with 50, 75, and 100 µg/mL of (**1**) and (**5**). DMSO (cells in 0.1% DMSO, negative control). The immunoblots were probed with p21WAF, cyclin D1, and E-cadherin antibodies. β-actin was used as a loading control. (**C**) The protein bands were quantified using ImageLab software version 4.1 (Bio-Rad, Hercules, CA, USA). The statistical analyses were carried out using an ordinary one-way ANOVA followed by Dunnett's multiple comparison test (*** $p < 0.001$, ** $p < 0.01$, * $p < 0.05$) and Student's t-test (** $p < 0.01$, * $p < 0.05$) for E-cadherin analysis. The results are the mean ± SEM of three independent biological experiments relative to the experimental control (DMSO).

To assess the effects of isoquercetin (**1**) and quercetin malonyl glucoside (**5**) on wound repair, I performed a wound healing assay in HaCaT cells, using the metabolites concentrations that had previously shown the greatest antioxidant activity. Both compounds enhanced the rate of wound closure, with quercetin malonyl glucoside (**5**) being the

most effective. Wound repair involves both keratinocyte proliferation and migration. Since no significant changes in proliferation rate were observed, the enhanced wound closure is likely attributable to an increase of keratinocyte migration. These findings were further confirmed by Western Blot (WB) analysis of cell proliferation markers including p21WAF and cyclin D1. Notably, treatment with quercetin malonyl glucoside (**5**) resulted in an increased expression of E-cadherin, a key cell adhesion molecule. This suggests that the compound may promote the formation of adherent junctions between neighboring epithelial cells, thereby facilitating more efficient wound closure. (Fig. 13)

Considering the interesting and promising results obtained in human cells, particularly regarding wound closure, and considering the potential application of these natural molecules in cosmeceutical products, as well as their possible antimicrobial activity on the skin, we initiated a collaboration with Dr Federica Carraturo's laboratory in the Department of Hygiene at University of Naples Federico II. The effect of fraction C (from SPE), together with isoquercetin (**1**) and quercetin malonyl glucoside (**5**), were investigated on the survival and die-off rates of selected bacteria and fungi.

The skin is our first line of defence against external factors such as microbial infections, UV radiation, and mechanical or chemical insults. It also harbours a diverse microbiome composed of bacteria, fungi and viruses that contribute to the integrity of this natural barrier (Byrd et al., 2018). Maintaining the balance between beneficial and pathogenic microorganisms is crucial, as factors as factors such as stress, pollution, or alterations in skin pH can disrupt this equilibrium. Such imbalances may compromise the skin's natural defenses, increasing susceptibility to inflammatory and infectious conditions. Pathogens such as *Staphylococcus aureus*, *Pseudomonas aeruginosa* and *Candida albicans*, which can interact synergistically, can cause skin infections that are very difficult to manage pharmacologically (Fasha et al., 2023; Lindsay et al., 2014). *Staphylococcus aureus* is a Gram-positive bacterium belonging to the *Staphylococcaceae* family and it is a common commensal of the skin and mucosal surfaces (Gherardi, 2023). *Pseudomonas aeruginosa* is a Gram-negative opportunistic pathogen often associated with severe human infections (Mielko et al., 2019). Finally, *Candida albicans* is a commensal fungus that colonises the skin, as well as the oral, gastrointestinal and genital mucosa (Lopes et al., 2022).

Sample	**Die-Off Concentration (Mean ± SE) [CFU/mL]**	**Log CFU Reduction**	**Die-Off Rate [%]**	**p-Value**
Negative control [50 µL DMSO]	1,750,000 ± 50	2×10^5	7.89	-
Positive control [100 µg/mLchloramphenicol]	5500 ± 15	2×10^6	99.71	≤0.0001
Fraction C [150µg/mL]	57,525 ± 4	2×10^6	96.97	≤0.0001 **
Fraction C [100µg/mL]	172,267 ± 15	2×10^6	90.93	≤0.0001 **
*Isoquercetin (**1**) [100µM]*	1,708,000 ± 125	2×10^5	10.11	>0.05 *
*Quercetin malonyl glucoside (**5**) [100 µM]*	1,742,333 ± 89	2×10^5	8.30	>0.05 *

Table 2. Antibacterial/bactericidal susceptibility assays performed on Staphylococcus aureus ATCCR6538 [10^6 CFU/mL][1]. [1]Die-off concentration (3 replicates mean ± SE, expressed in CFU/mL = colony forming units/mL), log CFU reduction and die-off rate (percentage) of S. aureus ATCCR6538 following contact with fraction C at two different concentrations: isoquercetin (**1**) and quercetin malonyl glucoside (**5**) at 100 µM. Negative control = 50 µL of DMSO; positive control = 100 µg/mL chloramphenicol; * $p < 0.05$, ** $p \leq 0.0001$ compared to the negative control (a one-way ANOVA followed by Turkey's and Dunnett's post hoc tests).

Sample	**Die-Off Concentration (Mean ± SE) [CFU/mL]**	**Log CFU Reduction**	**Die-Off Rate [%]**	**p-Value**
Negative control [50 µL DMSO]	1,636,667 ± 79	4×10^4	2.58	-
Positive control [100 µg/mLchloramphenicol]	5083 ± 13	2×10^6	99.70	≤0.0001
Fraction C [150µg/mL]	1,013,283 ± 101	7×10^5	39.69	≤0.0001 **

Fraction C [100µg/mL]	1,586,000 ± 225	9×10^4	5.60	>0.05 *
*Isoquercetin (**1**) [100µM]*	239,000 ± 107	1×10^6	85.77	≤0.0001 **
*Quercetin malonyl glucoside (**5**) [100 µM]*	455,700 ± 68	1×10^6	72.88	≤0.0001 **

Table 3. Antibacterial/bactericidal susceptibility assays performed on Pseudomonas aeruginosa ATCCR9027 [10^6 CFU/mL][1]. [1]Die-off concentration (mean ± SE of 3 replicates, expressed in CFU/mL = colony forming units/mL), log CFU reduction and die-off rate (percentage) of P. aeruginosa ATCCR9027 after exposure to fraction C at two different concentrations, as well as isoquercetin (**1**) and quercetin malonyl glucoside (**5**) at 100 µM. Negative control = 50 µL of DMSO; positive control = 100 µg/mL chloramphenicol; * $p < 0.05$, ** $p \leq 0.0001$ compared to the negative control (a one-way ANOVA followed by Turkey's and Dunnett's post hoc tests).

Sample	**Die-Off Concentration (Mean ± SE) [CFU/mL]**	**Log CFU Reduction**	**Die-Off Rate [%]**	**p-Value**
Negative control [50 µL DMSO]	1,400,000 ± 71	8×10^4	5.41	-
Positive control [100 µg/mLchloramphenicol]	46,913 ± 9	1×10^6	96.83	≤0.0001
Fraction C [150µg/mL]	700,333 ± 72	8×10^5	52.68	≤0.0001 **
Fraction C [100µg/mL]	1,168,867 ± 220	3×10^5	21.02	<0.05 *
*Isoquercetin (**1**) [100µM]*	1,391,500 ± 122	9×10^4	5.98	>0.05 *
*Quercetin malonyl glucoside (**5**) [100 µM]*	1,359,667 ± 73	1×10^5	8.13	>0.05 *

Table 4. Antibacterial/bactericidal susceptibility assays performed on Candida albicans ATCCR14053 [10^6 CFU/mL][1]. [1]Die-off concentration (3 replicates mean ± SE, expressed in CFU/mL = colony forming units/mL), log CFU reduction and die-off rate (percentage) of C. albicans ATCCR14053 following contact with fraction C at two different concentrations: isoquercetin (**1**) and quercetin malonyl glucoside (**5**) at 100 µM. Negative control = 50 µL of DMSO; positive control = 100 µg/mL chloramphenicol; * $p < 0.05$, ** $p \leq 0.0001$ compared to the negative control (a one-way ANOVA followed by Turkey's and Dunnett's post hoc tests).

Staphylococcus aureus ATCC®6538 (Table 2), *Pseudomonas aeruginosa* ATCC®9027 (Table 3) and *Candida albicans* ATCC®14053 (Table 4) were exposed to fraction C at concentrations of 150 µg/mL and 100 µg/mL, as well as to isoquercetin (**1**) and quercetin malonyl glucoside (**5**) at 100 µM. Fraction C at 150 µg/mL reduced the survival rate of *S. aureus* ATCC®6538 by 96.97% after 30 minutes of exposure, whereas the lower concentration (100 µM) achieved a 90.93% reduction. By contrast, isoquercetin (**1**) and quercetin malonyl glucoside (**5**), both tested at 100 µM, displayed only modest activity, with die-off rates ranging between 8% and 10% (see Table 2). For *P. aeruginosa* ATCC®9027, fraction C induced reductions of 39.64% and 5.60%at 150 µg/mL and 100 µg/mL, respectively Interestingly, isoquercetin (**1**) and quercetin malonyl glucoside (**5**), exhibited stronger activity, reducing bacterial loads by 85.77% and 72.88% respectively (Table 3). Antifungal assays against *C. albicans* ATCC® 14053 revealed statistically significant reductions in viable cells ($p < 0.05$ to $p \leq 0.0001$), with die-off rates ranging from 21.02% at 100 µg/mL to 52.68% at 150 µg/mL for fraction C (see Table 4). At 100 µM, isoquercetin (**1**) and quercetin malonyl glucoside (**5**) did not induce a statistically significant reduction in fungal survival.

Overall, considering the concentration tested, fraction C demonstrated strong bactericidal efficacy against *S. aureus* ATCCR6538 (91-97% reduction) and moderate activity against *C. albicans* ATCCR14053 while, isoquercetin (**1**) and quercetin malonyl glucoside (**5**) showed pronounced antibacterial effects against *P. aeruginosa* ATCCR9027 (73% 86% reduction).

3.2 Discussion and conclusion

These findings indicate that fraction C possesses a marked anti-staphylococcal effect, suggesting either a synergistic interaction among its components or the presence of compounds with higher potency compared to the isolated flavonoids. The inversion of efficacy between fraction C and the pure compound against *P. aeruginosa* may reflect different mechanisms of action: while the complex matrix of fraction C seems more effective against Gram-positive bacteria, the individual flavonoids appear to target Gram-negative bacteria more efficiently. Such behavior could be linked to differences in cell wall structure and permeability, particularly the outer membrane of *P. aeruginosa*, which often limits the penetration of complex mixtures. Antifungal assays against *C. albicans* ATCC®14053 suggest that fraction C unlike the

pure compounds retains moderate antifungal activity, possibly due to the combined presence of secondary metabolites that my interfere with fungal cell membrane integrity or oxidative stress pathways, whereas the individual flavonoids are insufficient to achieve a comparable effect. Such findings may guide future studies aimed at elucidating the mechanisms of action of these compounds, as well as their possible synergistic or antagonistic interactions when present in complex mixtures. From the perspective of a circular economy, these results demonstrate that SPE extraction represent an eco-sustainable and efficient strategy for isolating bioactive natural compounds. *S. pinnata* has emerged as a valuable reservoir of antioxidant molecules, particularly quercetin derivatives, which are known to exert multiple beneficial effects.

In our in vitro experiments, the pure metabolites displayed strong antioxidant and antimicrobial properties, as well as the ability to promote DNA repair and wound healing. These findings suggest that such compounds could be incorporated into formulations of moisturizing and cosmeceutical products aimed at strengthening the skin barrier, protecting against biotic and abiotic stressors, and preventing premature skin aging. Beyond their immediate applications, these results open further lines of investigation. The clear antimicrobial potential observed highlights the possibility of developing natural alternatives or adjuvants to conventional antibiotics, which is particularly relevant in the context of increasing antimicrobial resistance. Moreover, DNA repair and wound-healing activities suggest potential uses in dermatological therapies, for example in chronic wounds, post-surgical recovery, or conditions characterized by impaired barrier function such as atopic dermatitis. Future studies should also explore the synergistic or antagonistic interactions between the different metabolites within the extract, as such interactions may either enhance or limit the overall bioactivity compared to individual compounds.

Finally, the eco-sustainability of the extraction process aligns with the principles of green chemistry and supports the valorization of underutilized plant species, integrating biotechnological innovation with environmental responsibility. This dual perspective—scientific and ecological—reinforces the potential of *S. pinnata* extracts as a sustainable source of bioactive molecules for both pharmaceutical and cosmeceutical applications.

CHAPTER IV

4. *Lavandula angustifolia*

The genus Lavandula belongs to the Lamiaceae family and includes approximately 39 species of aromatic plant, as well as 79 intraspecific taxa and hybrids. These botanical entities are divided into three main subgenera — Lavandula, Fabricia and Sabaudia — based on morphological, phytogeographical and biochemical characteristics. This classification system emphasises the genus's remarkable genetic diversity, resulting from evolutionary processes and environmental influences. Lavandula species are primarily found in the Mediterranean basin, particularly in Italy (especially in alpine regions), Spain, and France. They also grow in the Middle East (Iran and Saudi Arabia), Southeast Asia (China and India), and some regions of Africa. These herbaceous plants prefer sunny, arid environments and can adapt to calcareous or siliceous soils depending on the species. The most notable species include *Lavandula angustifolia*, *Lavandula latifolia*, *Lavandula stoechas*, and the sterile hybrid *Lavandula* × *intermedia*. The beneficial properties of *Lavandula angustifolia* are well-documented in the literature. The dominant components of lavender extract include linalool, linalyl acetate, terpinene-4-ol, lavandulyl acetate, *o*-cimene, and cineole. Various studies have revealed special properties of lavender essential oils, such as anxiolytic effects during surgery, anti-inflammatory, antimicrobial, antioxidant, and carminative (smooth muscle-relaxing) activities (Cardia et al., 2018).

The most valuable product obtained from this crop is essential oil, which is used in a wide variety of cosmetic, pharmaceutical and nutraceutical formulations. Traditionally, production follows a simple, linear process. It begins with the manual harvesting of the inflorescences from the second year of planting, during full bloom (between June and July). The flowers are then left to wilt briefly in the field to reduce their moisture content, before being subjected to steam distillation within 24 hours of harvesting, while still fresh. Only the inflorescences are used for essential oil extraction, as they guarantee a higher yield of both quality and quantity than the leaves and shoots, being richer in linalool and linalyl acetate. While this approach is effective and profitable, it is now considered limiting as it relies on a single raw material to produce a single main product: essential oil. In an increasingly sustainable and multifunctional modern market, it is necessary to adopt innovative strategies that fully exploit the plant's economic and ecological potential. Currently, the residual biomass from lavender distillation is

mainly used for mulching or energy recovery through combustion, despite still containing beneficial substances such as polyphenols. Therefore, the valorisation of these residues represents a strategic opportunity to increase the economic value of lavender crops.

One of the innovative practices that enables us to offer a production system capable of overcoming the environmental limitations of wild plant cultivation and, above all, of providing consistent quality and high yields on a continuous basis is the in vitro production of plant callus. In response to stress, such as wounding, plants increase cell growth and accumulation, forming a disorganised structure known as callus tissue. These masses are formed from undifferentiated cells that have the potential to regenerate the entire plant. (Ikeuchi et al., 2013). Around 1900, the study and production of in vitro callus generation began. The balance between auxin and cytokines in the culture medium was found to allow different states of differentiation and dedifferentiation to be produced. Furthermore, this technique can be used to extract high levels of secondary metabolites from any plant, even rare ones (Babich et al., 2020).

4.1 Bioactivity testing of different types of extracts from *L. angustifolia*

In collaboration with Dr Federica Carraturo from the Hygiene lab at the University of Naples Federico II, and with the innovative startup HoloBiotics Srl UNINA Spinoff, we obtained three interesting and different extracts from *L. angustifolia*. These formulations were patented: one was obtained from plant stem cells (Stem), another derived from the plant's apical flowers (Tot), and the third was an aqueous by-product resulting from the distillation process used to obtain essential oils (Dist).

To discover a new potential beneficial role for these extracts in cosmeceutical applications with an eco-sustainable approach, I used a spontaneously immortalised human keratinocytes (HaCaT cells) and immortalised human hTERT fibroblasts (BJ5ta cells), which are the main cells responsible for producing collagen, elastin and the extracellular matrix in the dermal stroma.

To evaluate possible toxicity, I performed an MTT viability assay. HaCaT and BJ5ta cells were treated with increasing concentrations of the three

extracts (1, 50, 100, 250, 500 and 1000 µg/mL), with 5% DMSO acting as a positive control.

As shown in Figure 14A, the stem extract was not toxic after 24 and 48 hours of treatment. The total and distilled extracts showed no cytotoxicity at lower concentrations but significantly reduced cell viability at concentrations of 100 µg/mL and 250 µg/mL, respectively. Given these results on HaCaT cells, I performed the same experiment on BJ5ta cells using the concentrations that were non-toxic on HaCaT cells. The stem extract was non-toxic on these cells, while the distilled extract was toxic at 50 µg/mL and above. To determine whether this result was due to a change in metabolism or proliferation rate, I assessed the cell proliferation rate in HaCaT and BJ5ta cells. As shown in Figure 14C, treatment with distilled extract (1, 25 and 50 µg/mL) did not affect the proliferation rate, suggesting increased metabolism.

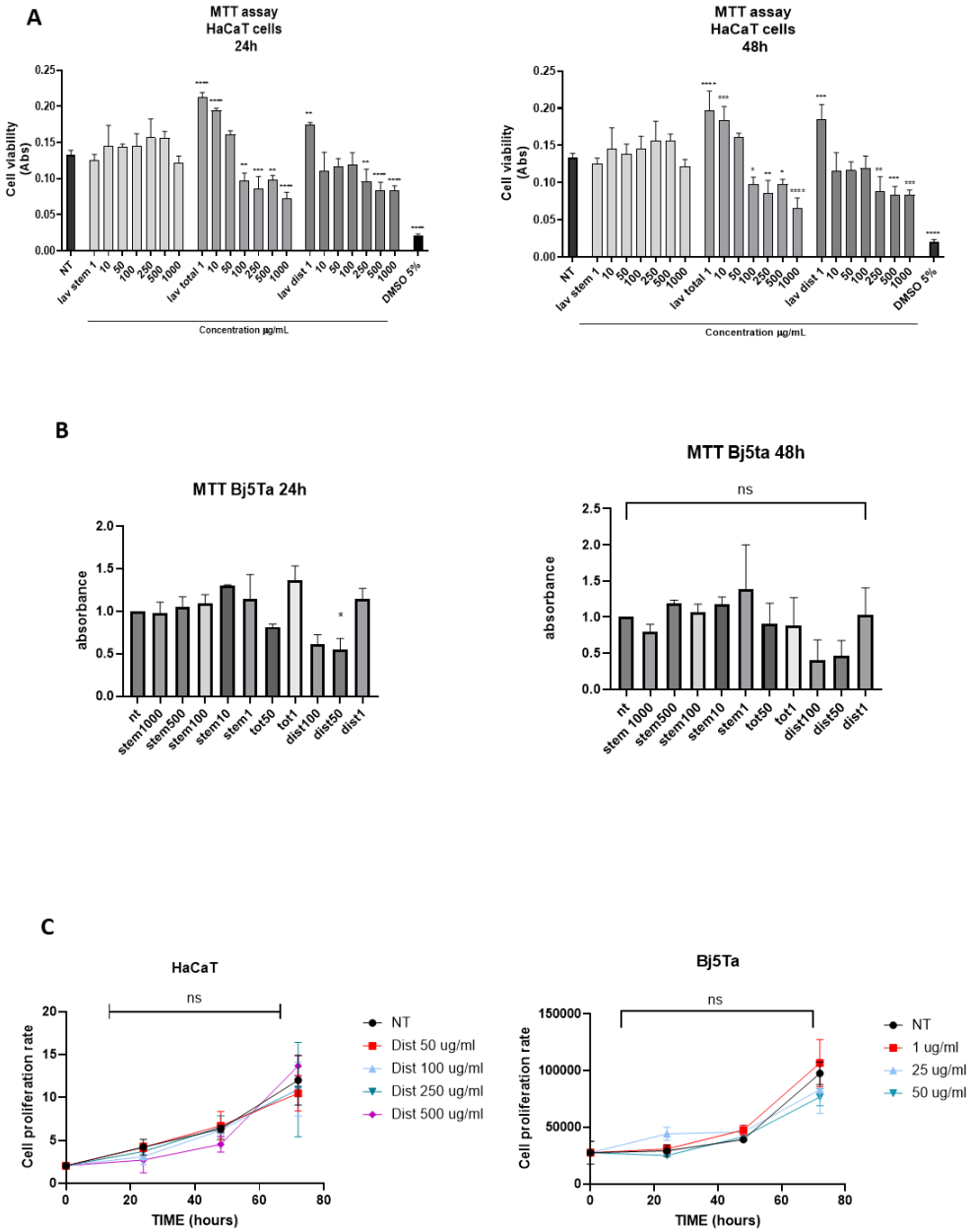

Fig. 14. MTT viability test. **(A)** HaCaT and **(B)** BJ5ta cells were incubated with the indicated amount of stem, total and distilled extracts from *Lavandula angustifolia* for 24 h and 48h. The values were the mean's six values for each experimental point of two independent biological replicates. Each mean was compared using a Dunnett's multiple comparisons test of a one-way ANOVA (p-value * $p < 0.01$, ** $p < 0.05$, *** $p < 0.001$; **** $p < 0.0001$). **(C)** Cell growth profile. HaCaT and BJ5ta cells were seeded and treated with distilled extract at the indicated concentrations. The cells were counted at T0, 24, 48, and 72 h of treatments, and the number was compared to the untreated cells. The results are the mean ± SEM of three independent biological replicates relative to the experimental control (DMSO). The statistical analysis was performed with a one-way ANOVA using Dunnett's multiple comparison test.

The capacity of these three to decrease the intracellular ROS was evaluated by an antioxidant assay (DCFDA). As shown in Figure 15A on HaCaT cells the stem extract has an antioxidant power starting to 250 µg/mL, the distilled one, exhibited a powerful antioxidant capacity at lower concentrations (10,50 and 100 µg/mL), while the total extract didn't exhibit any effect. Interestingly on BJ5ta all the extracts have an effect as scavengers of intracellular ROS (Fig. 15B).

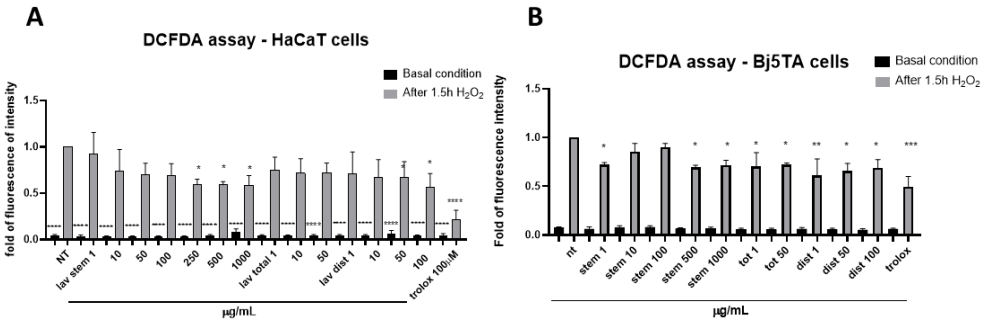

Fig. 15. DCFDA assay. **(A)** HaCaT and **(B)** BJ5ta cells were seeded and pre-treated for 4 h with no toxic concentrations of stem, total and distilled extracts from Lavandula angustifolia. H_2O_2 (4mM; 3%) was added to the medium for 1.5 h. The fluorescence intensity of DCFDA was read after 45 min of incubation. Trolox was used as a positive control, and NT was used as a negative control. The values are the mean's six values for each experimental point of two independent biological replicates. The statistical analysis was performed with a One-way ANOVA using Dunnett's multiple comparison test. The levels of significance between the points of expression are indicated (**** $p < 0.001$, *** $p < 0.01$, ** $p < 0.05$, * $p < 0.01$).

To investigate the role of these three natural extracts in oxidative stress, inflammation, and cellular regeneration processes in more depth, I performed a Western blot analysis on HaCaT and BJ5ta cells. I studied the expression levels of NRF2 (nuclear factor erythroid 2-related factor 2), which plays a key role in defence against oxidative stress by increasing the expression of antioxidant enzymes; IL-6 (interleukin-6), which regulates the immune response; and Mytho (macroautophagy and YouTH optimizer), which is involved in regulating autophagy and regeneration processes. HaCaT and BJ5ta cells were treated with stem extract at 1000 µg/mL and 500 µg/mL, respectively. Both cell lines were treated with a dose of 50 µg/ml of total and distilled extract. As shown in Figure 16A,B, all the extracts decreased the expression level of NRF2 (except the total extract on HaCaT cells), which confirms the results of the antioxidant assay. All the extracts decreased the

intracellular level of IL-6 except the total extract on BJ5ta cells. Finally, Mytho protein levels increased significantly in HaCaT cells stimulated with stem extract.

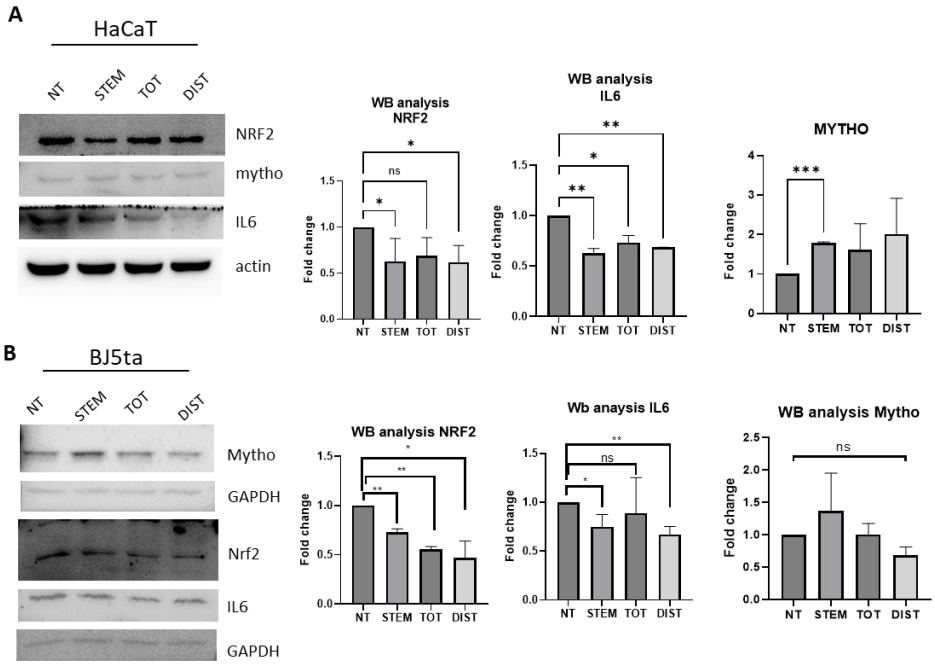

Fig. 16. Representative image of the Western blot analysis of the extracts from **(A)** HaCaT and **(B)** BJ5ta cells treated for 24 h with 1000 µg/mL and 500 µg/mL of stem extracts, respectively, 50 µg/mL of total and distilled extracts for both cell lines (NT, not treated cells as negative control). The immunoblots were probed with NRF2, IL-6 and Mytho antibodies. β-actin or GAPDH were used as a loading control. The protein bands were quantified using ImageLab software version 4.1 (Bio-Rad, Hercules, CA, USA). The statistical analyses were carried out using an ordinary one-way ANOVA followed by Dunnett's multiple comparison test (*** $p < 0.001$, ** $p < 0.01$, * $p < 0.05$). The results are the mean ± SEM of three independent biological experiments relative to the experimental control, NT.

To determine whether these three natural extracts could modulate the migration of HaCaT and BJ5ta cells, I conducted wound healing and Boyden chamber assays. The cells were treated with the same concentrations of extract used previously in WB analysis. As shown in Figures 17A and B, the rate of wound closure after treatment with the three extracts was comparable to the control sample in both cell lines, except after treatment with the stem extract, when wound closure decreased. These results were supported by the trend obtained from the Boyden chamber assay (Fig. 17C and D), suggesting that none of these three extracts increased cell migration.

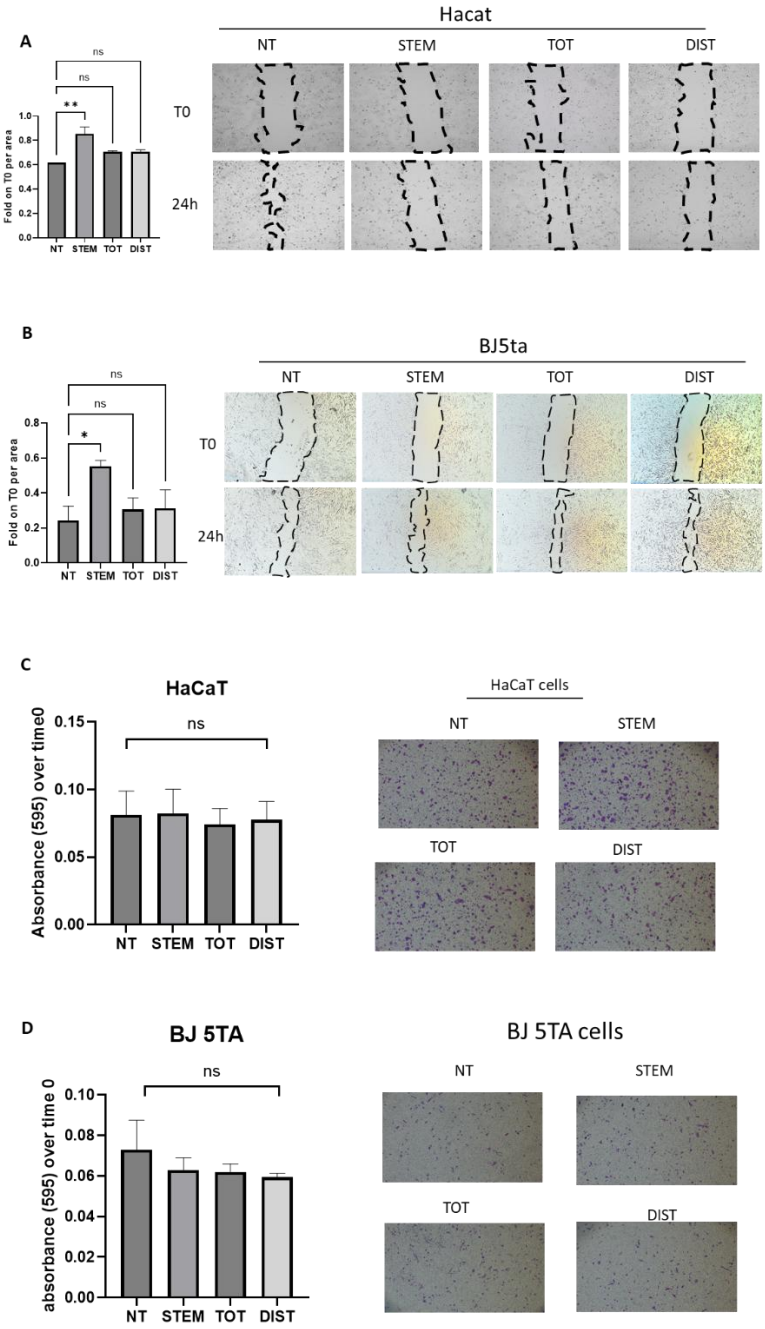

Fig. 17. Wound healing assay. (**A**) The HaCaT and **(B)** BJ5ta cell monolayer was scratched in the center with asterile tip and treated for 24 h with 1000 µg/mL and 500 µg/mL of stem extracts, respectively, 50 µg/mL of total and distilled extracts for both cell lines The statistical analysis was performed with a One-way ANOVA using Dunnett's multiple comparison test (p-value * p < 0.01). The results are the mean ± SEM of three independent biological experiments relative to the experimental control, NT. Boyden chamber assay **(C)** The HaCaT and **(D)** BJ5ta cells

were seeded above the transwells support containing polycarbonate membrane. The lower chamber was added medium supplemented with 1000 µg/mL and 500 µg/mL of stem extracts, respectively, 50 µg/mL of total and distilled extracts for both cell lines. After 24h, the transwells were removed and stained 0.1% Crystal Violet in 25% methanol. The percentage of migrated cells was determined by eluting the Crystal Violet stain with 1% SDS and measuring the absorbance at 570 nm. The statistical analysis was performed with a two-way ANOVA using Dunnett's multiple comparison test. The results are the mean ± SEM of three independent biological experiments relative to the experimental control, NT.

Considering these results, the distilled extract was of particular interest, as it was effective at a low concentration (50 µg/mL) in counteracting intracellular reactive oxygen species (ROS) and the inflammatory process, and in decreasing the pro-inflammatory cytokine IL-6. While on my placement at the Epigenomics Unit at the Instituto de Investigación Sanitaria de Santiago (IDIS) in Santiago de Compostela, Spain, under the supervision of my external supervisor, Dr Ángel Díaz Lagares, I investigated the potential of the distilled extract to alter the methylation status of HaCaT cells. The cells were treated with 50 µg/mL of the extract for 24 and 48 hours, and for five days. After this, the DNA genome was extracted, and DNA methylation profiling was conducted. As shown in Figure 18A and B, considerable alterations in DNA methylation were observed across all 22 somatic chromosomes, with 12,242 CpGs showing a difference after five days of treatment with the distilled extract compared with untreated cells. Analysis of CpG methylation β-values demonstrated an 18% increase in hypermethylated sites in the keratinocyte genome after five days of distilled extract treatment, compared to treatment for 24 hours.

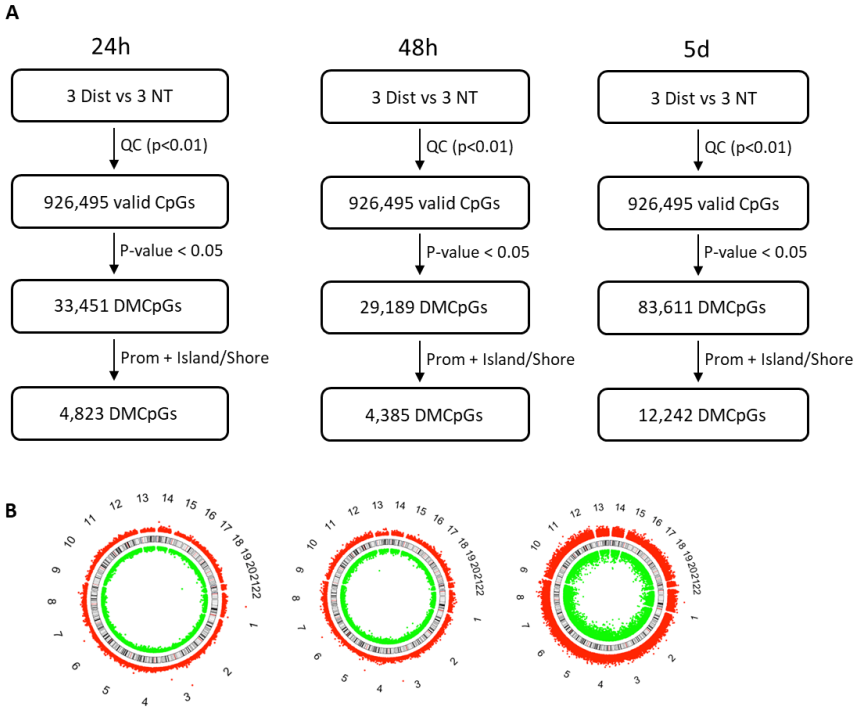

Fig. 18. (A) Schematic flowchart used to identify significant differentially methylated CpGs in HaCaT cells during 24, 48 hours and 5 days of treatment with distilled extract. **(B)** Chromosome's location of methylation status. In green were the hypomethylated CpGs and in red the hypermethylated CpGs

Among the differentially methylated CpG sites, 3% of CpG islands were hypermethylated and 7% were hypomethylated. Furthermore, a significant proportion of these differentially methylated CpG sites (16%) were located within promoter regions, where both hypermethylation and hypomethylation were observed (see Figure 19A and B).

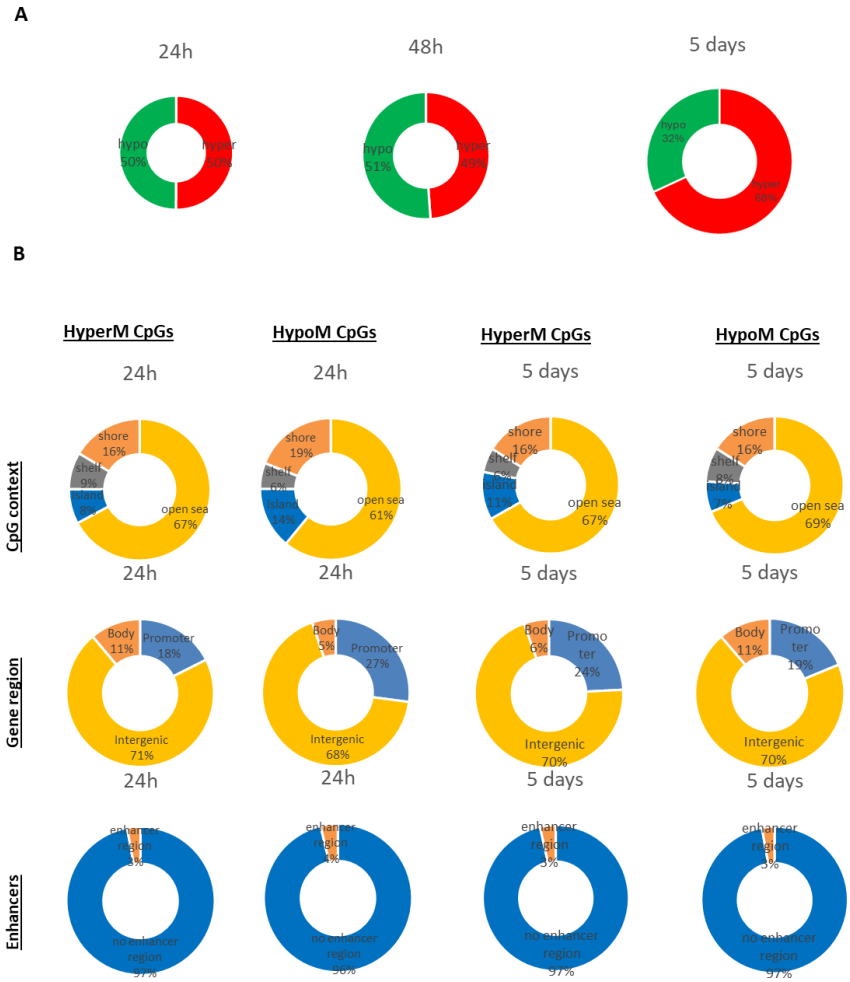

Fig. 19. (A) Global genome methylation status, **(B)** CpG context, gene region and enhancers of HaCaT cells genome after the treatment for 24, 48 hours and 5 days of distilled extract.

4.2 Discussion and conclusion

The aim of the study was to evaluate the antioxidant, anti-inflammatory and regenerative properties of three *L. angustifolia* extracts on skin cells. The first extract was obtained from plant stem cells, the second was produced by macerating the leaves and flowers, and the third was obtained from the waste product of the distillation process used to extract lavender essential oils. To this end, HaCaT (human spontaneously immortalised keratinocytes) and BJ5ta (human immortalised fibroblasts) were employed. These cells were adopted because keratinocytes and fibroblasts account for nearly all skin cells.

These cells play a fundamental role in the inflammatory response, tissue repair processes and the structure and protection of the skin. Fibroblast cells are the main cells of the dermal stroma. They produce collagen, elastin and the extracellular matrix.

The results showed that these extracts were not toxic, except at higher doses of total and distilled extracts on HaCaT cells, and that they also had antioxidant properties. These observations were supported by the analysis of NRF2, a key transcription factor in the antioxidant response. Its expression was significantly reduced, indicating maintenance of a more balanced intracellular redox state. Since NRF2 activation involves the induction of antioxidant enzymes such as SOD1, CAT and GSSG, it is plausible that the activity of the extracts is mediated by flavonoids or similar compounds that support these defence mechanisms. A particularly significant result was the increased expression of the Mytho protein only after treatment with the stem extract. Since Mytho regulates autophagy, an essential process for removing damaged organelles and protecting against cellular senescence, it can be hypothesised that this extract promotes cellular longevity and maintains skin homeostasis, highlighting its potential anti-ageing properties. Regarding anti-inflammatory activity, both cell lines demonstrated that the stem and distilled extracts reduced intracellular IL-6 expression, thereby decreasing inflammation. Furthermore, migration assays, wound healing and Boyden chamber tests showed that the extracts had no effect on wound closure rate, suggesting that future experiments are needed to establish whether this phenomenon could be due to stimulation of cell differentiation. Finally, the results obtained during my period abroad showed that the distilled extract could generally increase the methylation status of the HaCaT cell genome, but further analysis is necessary to investigate this result in more detail, for example by performing an enrichment analysis to understand which genes and pathways are involved.

In conclusion, the data obtained demonstrate that *L. angustifolia* extracts exhibit antioxidant and anti-inflammatory properties and may activate autophagy. These results open prospects for their use in cosmetic and cosmeceutical formulations with potential anti-ageing, soothing and protective applications. Furthermore, using the distillate, a by-product of essential oil production, enhances the circular economy by combining environmental sustainability and biotechnological innovation.

CHAPTER V

5. Grape pomace: from waste to innovative and sustainable nutraceutical product

Grapes are among the most extensively cultivated crops worldwide, with most of the production dedicated to winemaking. Grape pomace, the major by-product of the winemaking process, consists of skins, seeds and residual pulp remaining after grape pressing. Italy is recognized as one of the global leaders in wine production, and the management of grape pomace waste represents both an environmental and economic challenge. This issue must be addressed within the framework of the circular economy, as established by the European Parliament's Waste Framework Directive (Directive 2008/98/EC).

Considering the large quantities of grapes processed annually in Italy and the high potential of pomace as source of antioxidant compounds, this section of my PhD project focuses on its valorization as a value-added material, exploring its potential applications in the nutraceutical sector.

A major limitation to the commercialization of natural products lies in the challenge of preserving the active molecular form of bioactive compounds until the moment of consumption, as well as their limited residence time in the gastrointestinal tract (Bartosz et al.,2016). Encapsulation represents a promising technological strategy in which active substances, or their combinations, are enclosed within a polymeric coating that protects them from adverse environmental conditions and enables controlled release in specific target sites. Controlled release is a key feature to enhance the bioavailability of phenolic compounds in the human body (Grgić et al., 2020).

Among the most promising delivering approaches in the nutraceuticals and cosmeceuticals industries are colloidal particulate systems. In this context, hydrogels are three-dimensional polymeric network either physically or chemically linked capable of retaining large amount of water or biological fluids. Hydrogels exhibit advantageous properties such as high biocompatibility, tunable chemical and physical characteristic, non-toxicity, and ease of fabrication. Specific biopolymers can be selected to entrap bioactive compounds according to the desired release profile within the gastrointestinal tract. These polymers are often combined in binary or ternary mixtures to optimize functionality. Commonly used biopolymers for the fabrication of hydrogel beads include agar, pectin, alginate, chitosan, cellulose,

carrageenan, and protein-based materials such as collagen, gelatin, and egg white. These materials play a crucial role in encapsulating and delivering bioactive compounds (Saqib et al., 2022).

5.1 Grape pomace extraction procedure and formulation of edible beads

Grape pomace was supplied by Mastroberardino, a leading winery located in the Campania region. The extraction of extract enriches in antioxidant compounds was selected as the primary goal. In literature, it is reported that ethanol can be used to extract phenolic and flavonoid compounds from natural sources (Do et al., 2014). For this reason, we decided to use it, as a solvent to extract grape pomace. The extraction procedure began with freeze-drying, which was carried out to remove water from the samples and preserve the stability of phenolic constituents. Subsequently, the dried pomace was subjected to maceration in pure ethanol for 24 hours at room temperature, to prevent the degradation of thermolabile polyphenols. The ethanol phase enriched in antioxidant compounds was then collected, and the solvent was removed by rotary evaporation under reduced pressure, yielding the crude extract (Fig. 20).

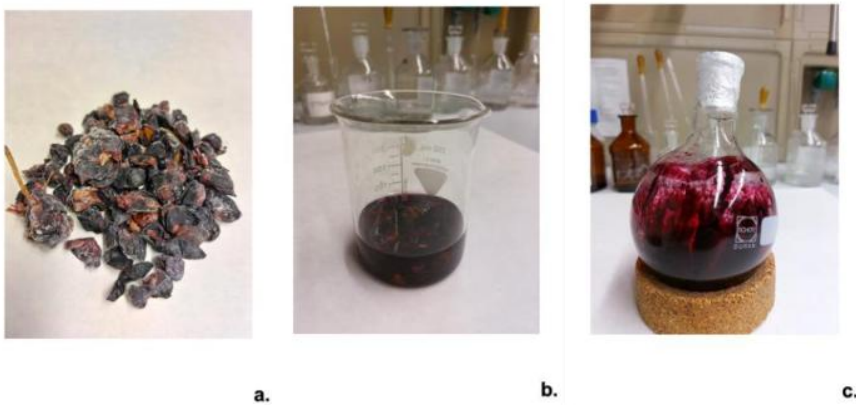

Fig. 20. Schematic representation of the pomace extraction process. (a) freeze-dried pomace; (b) maceration in ethanol; (c)recovery of the organic extract obtained after filtration and solvent evaporation.

With the aim of identifying antioxidant and anti-inflammatory extracts from natural sources for potential nutraceutical applications, a collaboration was established with Dr. Giovanni Dal Poggetto and Dr. Gabriella Santagata (CNR-IPCB), whose research group has extensive

expertise in the formulation of edible hydrogel beads. Leveraging this collaboration, different formulations were explored to optimize the release of antioxidant metabolites, comparing beads based on alginate, pectin, and a binary mixture containing 80% pectin and 20% alginate.

Alginate is natural polysaccharide extracted from brown algae and composed of D-mannuronic and L-guluronic acids (Hu et al., 2021). This polymer is widely used for encapsulation due to its ability to form stable and thermo-irreversible gels through cross-linking with divalent cations (Saqib et al., 2022). Such characteristics make alginate particularly attractive in the food, pharmaceutical and biotechnological industries, as an encapsulation matrix for bioactive compounds.

Pectin is a natural, non-toxic heteropolysaccharide abundantly found in the cell walls of higher plants, particularly in citrus fruits and apples. Its backbone consists primarily of main galacturonic acid units. Pectin is valued for its gelling and emulsifying properties as well as for its recognized health benefits, including the modulation of glucose absorption and the prevention of hypertension, atherosclerosis, glucose intolerance, and intestinal disorders (Roman-Benn et al., 2023).

For the preparation of hydrogel beads, 4% (w/v) aqueous solutions of alginate, pectin, or their mixture were prepared, to which different concentrations of grape pomace extract (50% or 75%) were added under magnetic stirring. To induce gelation and entrap the extract within the polymeric matrix, divalent metal ions (Fe^{2+} or Ca^{2+}) were employed as cross-linking agents. The polymer–extract mixtures were added dropwise into aqueous solutions of $CaCl_2$ or $FeSO_4 \cdot 7H_2O$ at two different concentrations, 4% (w/v) (1×) and 8% (w/v) (2×), resulting in the formation of hydrogel beads (Fig. 21).

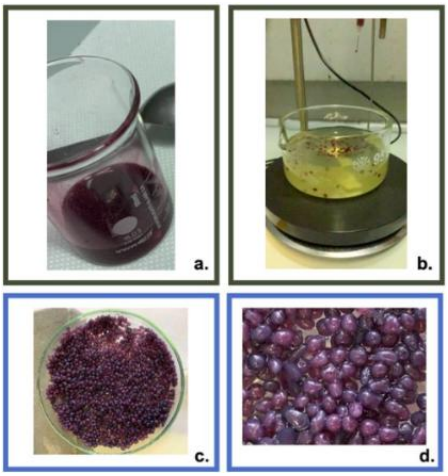

Fig. 21. *Schematic representation of the bead formulation process.*
(a) Preparation of alginate, pectin, and mixed polymer solutions containing grape pomace extract;
(b) Dropwise addition into Ca^{2+} or Fe^{2+} solutions to induce ionic cross-linking;
(c) Formation and collection of hydrogel beads.

All the different formulations obtained are summarized in Table 5. The resulting hydrogel beads were subsequently subjected to spectroscopic (UV–Vis), thermogravimetric (TGA), and morphological (SEM) analyses to evaluate their physicochemical properties and structural characteristics.

SAMPLES	POLYSACCHARIDE	EXTRACT	FE^{+2} /CA^{+2}
A	Alginate	50%	Ca 1X
B	Alginate	50%	Fe 1X
C	Alginate	50%	Ca 2X
D	Alginate	50%	Fe 2X
E	Alginate	75%	Fe 1X
F	Alginate	75%	Fe 2X
G	Pectin	50%	Fe 1X
H	Pectin	50%	Ca 1X
I	Pectin	50%	Fe 2X
L	Pectin	50%	Ca 2X

M	Pectin	75%	Fe 1X
N	Pectin	75%	Fe 2X
O	Pectin 80% Alginate 20%	50%	Ca 1X
P	Pectin 80% Alginate 20%	50%	Fe 1X
Q	Pectin 80% Alginate 20%	50%	Ca 2X
R	Pectin 80% Alginate 20%	50%	Fe 2X
S	Pectin	75%	Ca 1X
T	Pectin	75%	Ca 2X

Table 5. All the formulations (A-T).

The UV-Vis absorbance of the grape pomace extract at 560 nm was used to determine the loading efficiency of phenolic compounds within the polymeric matrix, and the results are reported in Table 3. The thermal properties of the beads were characterised using Thermogravimetric analysis (TGA) to evaluate the polymer integrity and the thermal stability of the encapsulated bioactive compounds, as well as to further confirm the loading efficiency. Finally, scanning electron microscopy (SEM) was used to analyse the morphology and surface feature of the hydrogel beads (Fig. 22).

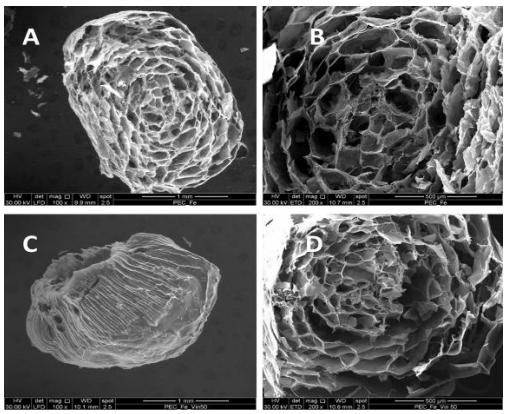

Fig. 22. SEM micrographs of hydrogel beads loaded with grape pomace extract. SEM images, only for example of Pectin-Fe1x beads **(A,B**) and Pectin-Fe1x- 50% of grape pomace extract Beads (**C,D**)

The analysis revealed that the incorporation of Fe^{2+} as a cross-linking ion, together with grape pomace extract rich in polyphenols, enhanced the thermal stability of the hydrogel beads. This formulation exhibited reduced mass loss and a delayed onset of degradation compared to non-loaded or Ca^{2+}-crosslinked systems. Moreover, the presence of Fe^{2+} and polyphenolic compounds promoted a higher char yield, likely due to the synergistic effect of metal–carboxylate interactions and the char-forming tendency of phenolic structures

To quantify the amount of grape pomace extract released from the hydrogel beads, an in vitro release assay was performed. The beads were placed on a filter within a beaker and covered with distilled water. The system was subjected to magnetic stirring for 3h at pH 7, simulating the condition to the intestinal tract. The released extract was subsequently collected from the aqueous phase and freeze-dried to enable quantitative analysis. The results, expressed as milligrams of released extract, are reported in Table 6.

SAMPLES	% OF LOADING EFFICACY	% OF RELEASED
A	88.9	18%
B	90.4	25%
C	89.6	45%
D	87.5	43%
E	90.2	42%
F	87.9	52%
G	88.2	34%
H	93.2	43%
I	95.4	34%
L	93.7	47%
M	95.4	56%
N	94.1	51%
O	91.8	56%
P	87.7	25%
Q	88.9	66%
R	90.4	31%
S	92.3	83%
T	94.2	100%

Table 6. Percentage of beads' loading efficacy and their released.

All hydrogel matrices exhibited high grape pomace (GP) loading efficiency ranging from 87 to 95%, primarily driven by a combination of ionic and non-covalent interactions between polyphenols and polysaccharide network. The release of GP was strongly depended on both the polymer composition and the type of crosslinking ion. Specifically, Ca^{2+}- alginate networks retained GP most effectively, due to the formation of compact "egg-box" structures, whereas Fe^{2+}-crosslinked systems demonstrated higher release rates, likely resulting from looser metal-polymer coordination. Pectin-based and pectin-rich blends exhibited the greatest GP release, consistent with their more flexible and less densely crosslinked network architectures.

Morphological analysis revealed that the incorporation of GP reduced macroporosity and improved structural uniformity, suggesting enhanced mechanical stability and a more controlled diffusion of the encapsulated compounds

5.2 Biological properties of beads-grape pomace releases

To evaluate the effects of grape pomace extract and its different hydrogel release formulations on mammalian cells, HaCaT human keratinocytes were subjected to a cell viability assay using the MTT method (Fig. 23). Cells were treated with increasing concentrations of extract 1, 10, 100 and 1000μg/mL**.** Lycorine, a well-characterized bioactive metabolite, was used as a positive control.

The results demonstrated that after 48h of treatment, the lower concentrations 1 and 10 μg/mL did not exert any cytotoxic effects on HaCaT cells. In contrast, higher concentrations (100 μg/mL) led to a measurable reduction in cell viability. The most pronounced effect was observed at 1000 μg/mL where a drastic decrease in cell viability was detected after both 48 and 72h of exposure. These findings indicate that the biological activity of the extract is concentration-dependent, with potential applications at sub-cytotoxic doses.

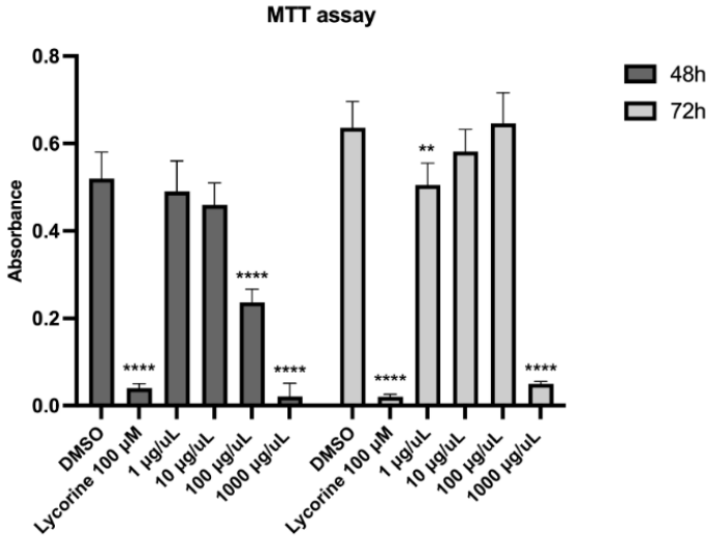

Fig. 23. MTT assay of HaCaT cells treated with grape pomace extracts. Cells were exposed to the indicated concentrations of the extracts for 48 and 72 hours. All samples contained 0.1% DMSO. Data represents the mean ± SD of six technical replicates for each experimental point, obtained from three independent biological experiments. Statistical analysis was performed using one-way ANOVA followed by Dunnett's multiple comparisons test (**$p < 0.01$, ****$p < 0.0001$).

To evaluate the potential antioxidant activity of the crude grape pomace extract, a DCFDA assay was performed in HaCaT cells. When cells were treated with sub-lethal concentrations of the extract (1, 10, and 100 µg/mL), a dose-dependent reduction in intracellular reactive oxygen species (ROS) levels was observed. Notably, treatment with 100 µg/mL of extract resulted in a decrease in ROS levels comparable to that achieved with the antioxidant control, Trolox (Fig. 24). These

results indicate that the extract exhibits significant antioxidant activity at concentrations that are non-cytotoxic to HaCaT cells.

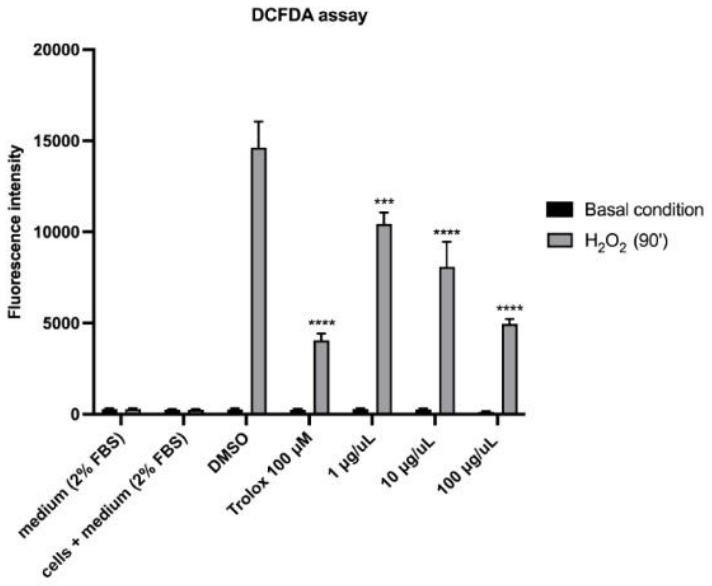

Fig. 24. DCFDA antioxidant assay. HaCaT cells were seeded and pretreated with the indicated amount of pomace organic extract for 4 h. Trolox 100µm was used as a positive control. The fluorescence intensity of DCFDA was measured under basal condition (NT) or samples following exposure to H_2O_2 (4 mM; 3%) for 1.5 h. Data represents the mean's six technical replicates per experimental point from three independent biological replicates. Statistical analysis was performed with two-way ANOVA, using Tukey's multiple comparison test. Levels of significance between points of expression are shown (p-value ***$p < 0.001$; ****$p < 0.0001$).

To assess the antioxidant properties of the compounds released from the hydrogel beads, a DCFDA assay was performed using the released fractions of the beads prepared with different formulations were first subjected to the *in-vitro* release procedure. The collected fractions were freeze-dried and subsequently dissolved in DMSO for cellular assays.

Consistent with the previous experiments using the crude extract alone, the highest concentration (1000 µg/mL) was excluded due to its cytotoxicity. The results in Figure 25 showed that none of the formulations tested had a significant effect on the release of antioxidant compounds.

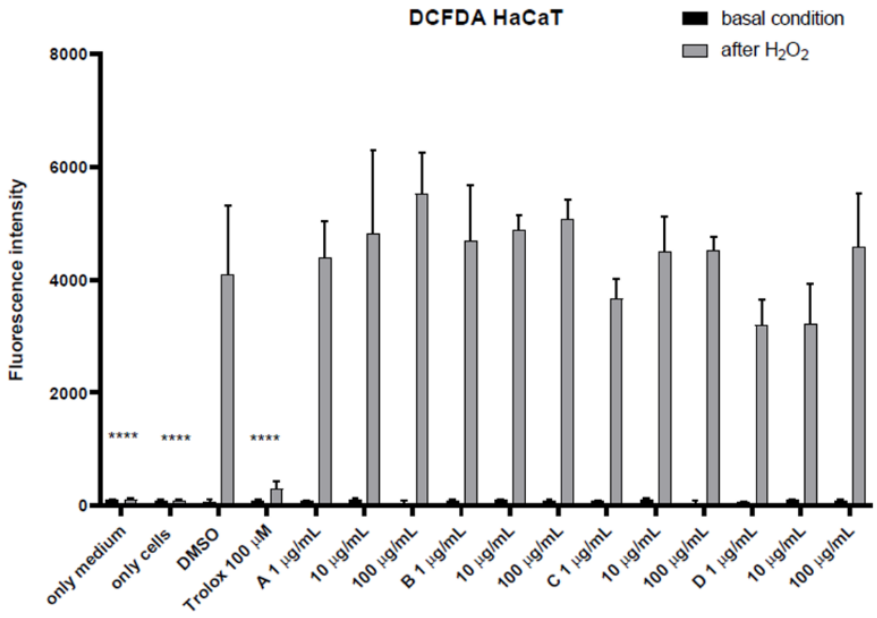

Fig. 25. Antioxidant activity of metabolites released from hydrogel beads, evaluated by DCFDA assay in HaCaT cells. Released samples from different hydrogel formulations were freeze-dried, dissolved in DMSO, and applied to HaCaT cells at sub-cytotoxic concentrations. ROS levels were measured after 48 hours of treatment. Data represents the mean ± SD of six technical replicates for each experimental point, obtained from three independent biological experiments. Statistical significance was determined using one-way ANOVA followed by Dunnett's multiple comparisons test ****$p < 0.0001$).

Finally, hydrogel beads from formulations E to T were evaluated for their antioxidant activity in HaCaT cells. The released compounds were collected, lyophilized, and subsequently dissolved in DMSO. An *in vitro* DCFDA assay was performed using a concentration range of 1–100 µg/mL of the released samples (Figure 26), to assess their ability to reduce intracellular ROS levels.

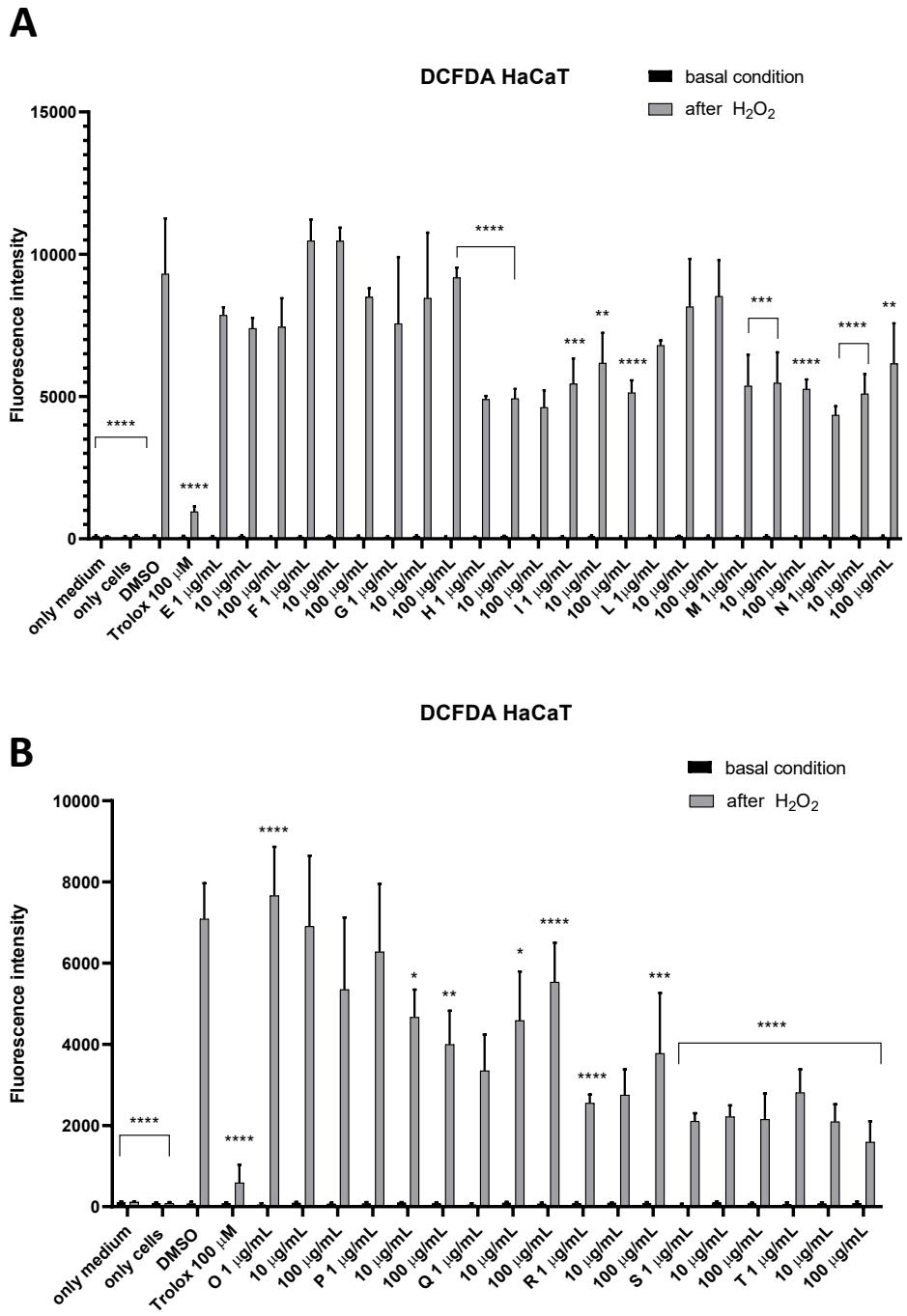

Fig. 26. DCFDA antioxidant assay. HaCaT cells were seeded and pre-treated with the indicated amount of metabolites released from beads (E-N, panel **A**) and (O-T, panel **B**). for 4 h Trolox (100μm) was used as a positive control. The fluorescence intensity of DCFDA was measured under basal conditions (NT) and after exposure to H_2O_2 (4 mM; 3%) for 1.5 h. Data are expressed as the mean's of six technical replicates for each experimental point obtained from three independent biological replicates. Statistical analysis was performed with two-way

ANOVA, followed by Tukey's multiple comparison test. Levels of statistical significance are indicated as follows: (p-value *< 0.01, ** < 0.05, ***p < 0.001; ****p < 0.0001).

As shown in Figure 26, panel A, all hydrogel formulations, except for E (alginate-Fe^{2+} 4% w/w by weight-pomace 75%), F (alginate-Fe^{2+} 8% w/w by weight-pomace 75%), released antioxidant metabolites, although with different efficacies. Remarkably, as depicted in panel B, all released exhibited significant antioxidant activity. Particularly noteworthy was formulation T (pectin Ca^{2+} 8% w/w, grape pomace 75%), which resulted in a ROS reduction of approximately 80%.

5.3 Discussion and Conclusion

Italy ranks among the world's leading wine producers, with the annual output reaching 43.9 million hectoliters in 2024. The country's diverse climatic and soil conditions enable the cultivation of numerous grape varieties with distinct organoleptic characteristics. Grape pomace, one of the most abundant by-products of winemaking, is a rich source of phenolic compounds with well-documented health-promoting effects, including antioxidant, anti-inflammatory, cardioprotective, and antitumor activities (Lopes et al., 2025).

With the aim of developing nutraceutical formulations, a extract enrich in antioxidant compounds from grape pomace were obtained using ethanol, selected for its environmental compatibility, safety, broad solubility, and reusability (Lee et al., 2024; Do et al., 2014). *In vitro* assays on HaCaT cells revealed that the extract was non-cytotoxic at concentrations up to 10 µg/mL after 48 h, whereas higher concentrations (1000 µg/mL) significantly reduced cell viability after 72 h. Moreover, the extract displayed potent antioxidant activity comparable to Trolox at 100 µg/mL.

The extract was subsequently encapsulated in edible hydrogel beads composed of alginate and pectin, crosslinked with Fe^{2+} or Ca^{2+} ions, to identify the most effective formulations for sustained release without chemical modification of the active compounds. These divalent cations were chosen due to their low toxicity, capacity to stabilize the polymeric network, and physiological relevance (Tie et al., 2024). Among the tested formulations, formulation T (pectin, 8% w/w Ca^{2+}crosslinked, 75% grape pomace) showed the highest antioxidant efficacy, reducing intracellular ROS level by approximately 77.5% at 100 µg/mL. This effect is likely attributable to the Ca^{2+}-crosslinked matrix which provides

a more open and flexible structure that facilitates metabolites diffusion and release. Increasing the grape pomace content from 50% to 75% further enhanced antioxidant performance, underscoring the importance of optimizing the pomace-to-pectin polymer ratio.

All hydrogel formulations exhibited high loading efficiency (87–95%), driven by ionic interactions between divalent cations and polysaccharides as well as non-covalent interactions between polyphenols and the polymeric matrix. Thermogravimetric analysis (TGA) revealed that Fe^{2+} crosslinking improved thermal stability by reducing mass loss, delaying degradation, and increasing char yield, likely due to synergistic metal–carboxylate and phenolic interactions. Scanning Electron Microscopy confirmed that grape pomace incorporation enhanced structural uniformity and mechanical integrity; Ca^{2+}- alginate beads formed compact “egg-box” structures capable of retaining metabolites efficiently, while Fe^{2+}-crosslinked and pectin-rich matrices displayed looser networks favoring controlled release.

In vitro release studies at pH 7 confirmed that matrix composition and crosslinking ion strongly influence the release profile: Ca^{2+}–alginate beads retained GP effectively, while Fe^{2+}-crosslinked and pectin-rich beads exhibited faster release. These findings correlate with SEM and TGA observations, demonstrating that polymer density, network flexibility, and metal–polymer coordination govern the release kinetics.

Overall, the combined analysis of encapsulation efficiency, thermal stability, morphology, and release behavior demonstrate that the careful selection of polymer composition and crosslinking ion is essential for optimizing the encapsulation and delivery of bioactive polyphenols. Pectin-rich, Ca^{2+}-crosslinked hydrogels provide a promising balance between structural integrity and efficient antioxidant release, supporting their potential application in functional food or nutraceutical formulations. Future research should focus on *in vivo* bioavailability and metabolic interactions of grape pomace polyphenols to fully elucidate their therapeutic and preventive potential.

CHAPTER VI

6.1 Materials and methods

6.1.1 Plants materials

Brassica rapa L.

One hundred seeds of *Brassica rapa* L. subsp. *rapa* were sown in two 0.5 L containers filled with Vigorplant© universal potting soil, composed of 21% Baltic peat (0–10 mm), 37% Irish peat (0–20 mm), 13% volcanic pumice (3–8 mm), and 29% superfine peat (0–3 mm), enriched with slow-release fertilizer. The seeds were grown in a controlled-environment chamber under the following conditions: photosynthetic photon flux density (PPFD) of 270 ± 10 µmol photons m^{-2} s^{-1}, day/night temperature of 25/15 °C, relative humidity of 50/70% (day/night), and a 12-hour photoperiod. Two light quality regimes were applied: broad-spectrum white (W) and red–blue (RB, 60:40) light, with emission peaks at 630 nm (red) and 460 nm (blue). Temperature and relative humidity were monitored using a digital thermo-hygrometer (HC520 Digital Thermo-Hygrometer, Cheerman, Shenzhen, China), while PPFD was measured with a quantum sensor (Li-Cor, Lincoln, NE, USA). Microgreens were grown for fifteen days and regularly irrigated to compensate for water loss due to evapotranspiration.

Preparation of methanolic extracts

Plant material collected at 15 days after sowing (DAS) was finely ground in liquid nitrogen using a mortar and pestle. Extracts were prepared by weighing 0.20 g of the powdered sample and solubilizing it in 2 mL of 80% methanol. After centrifugation at 11,000 rpm, the supernatants were stored at 4 °C until analysis.

Determination of Polyphenols and Flavonoids

Total polyphenol content was determined according to the method described by Sun et al. (1998). An aliquot of the methanolic extract was mixed with an equal volume (1:1, v/v) of 10% Folin–Ciocâlteu reagent and a fivefold volume (1:5, v/v) of 700 mM Na_2CO_3. The mixture was incubated in the dark for 2 h, and absorbance was measured at 765 nm using a UV–VIS spectrophotometer (Cary 100, Agilent Technologies,

Palo Alto, CA, USA). Total polyphenol content was calculated from a gallic acid standard curve and expressed as milligrams of gallic acid equivalents per gram of fresh weight (mg GAE g^{-1} FW). Flavonoid content was quantified following the protocols of Moulehi et al. (2017) and Dewanto et al. (2002). Briefly, an aliquot of the supernatant was mixed with 75 µL of 5% $NaNO_2$, followed by the addition of 150 µL of 10% $AlCl_3$ and 500 µL of 1 M NaOH. Distilled water was added to reach a final volume of 1.525 mL. The absorbance was measured at 510 nm using the same spectrophotometer model. Flavonoid concentration was calculated from a catechin standard curve and expressed as milligrams of catechin equivalents per gram of fresh weight (mg CE g^{-1} FW). Statistical analysis was performed on eight technical replicates using an unpaired *t*-test in GraphPad Prism software, version 8.0 (GraphPad, San Diego, CA, USA).

FRAP Assay

Antioxidant capacity was assessed using the ferric reducing antioxidant power (FRAP) assay, following the method described by George et al. (2004). Briefly, 0.25 g of powdered sample was extracted with 5 mL of a methanol/water solution (60:40, v/v). After incubation on ice for 1 h, the extracts were centrifuged at 14,000 rpm for 15 min at 4 °C. Subsequently, a 150 µL aliquot of the supernatant was added to the FRAP reagent, consisting of 2.5 mL of 300 mM acetate buffer (pH 3.6), 250 µL of 10 mM 2,4,6-tripyridyl-s-triazine (TPTZ), and 250 µL of 12 mM $FeCl_3$. The mixture was incubated in the dark for 1 h, and absorbance was measured at 593 nm using a UV–VIS spectrophotometer (Cary 100, Agilent Technologies, Palo Alto, CA, USA). Antioxidant capacity was calculated from a Trolox standard curve and expressed as micromoles of Trolox equivalents per gram of fresh weight (µmol TE g^{-1} FW). Statistical analysis was conducted on eight technical replicates using an unpaired *t*-test in GraphPad Prism software, version 8.0 (GraphPad, San Diego, CA, USA).

Staphylea Pinnata

The aerial parts of S. pinnata were collected in late August 2023 in a thermophilic mixed wood at an elevation of 600 m in the proximity of Luzzano, a village belonging to the municipality of Moiano (Benevento, Italy). The identification of the plant material was performed according to the Flora of Italy, comparing the collected material to reference vouchers (PI 010576,

https://erbario.unipi.it/it/erbario/view?id=1283285, accessed on 18 May 2024). The collection was carried out in a period far from flowering and fruiting, collecting the terminal part of the leafy twigs from about 30 individuals, spaced 5–10 m apart to reduce the risk of sampling clonal individuals. Distilled water was used to rinse the plant material and remove the dust particles. The plant was then dried for a few days in the air at room temperature and ground in a blender.

Chemical procedures

Solid-phase extraction (SPE) was carried out using SUPELCO Supelclean LC-18 SPE cartridges (10 g/60 mL; Merck, Darmstadt, Germany) on a SUPELCO Visiprep™ SPE Vacuum Manifold system (Merck, Darmstadt, Germany). Analytical and preparative thin-layer chromatography (TLC) was performed on silica gel plates (Kieselgel 60, F254; 0.25 and 0.5 mm, respectively) or on reverse-phase plates (Whatman KC18, F254; 0.20 mm) (Merck, Darmstadt, Germany). Compounds were visualized by exposure to UV light and/or iodine vapors, or by sequential spraying with 10% H_2SO_4 in methanol followed by 5% phosphomolybdic acid in ethanol, and subsequent heating at 110 °C for 10 min. All solvents were supplied by Sigma-Aldrich (Milan, Italy). ^{1}H nuclear magnetic resonance (NMR) spectra were recorded at 400 or 500 MHz on Bruker (Karlsruhe, Germany) or Varian (Palo Alto, CA, USA) spectrometers, respectively. Electrospray ionization (ESI) mass spectra and liquid chromatography–mass spectrometry (LC–MS) analyses were performed in negative ionization mode using an Agilent 6230B LC/MS TOF system coupled with an Agilent 1260 Infinity HPLC (Milan, Italy). Optical rotations were measured with a Jasco P-1010 digital polarimeter (Tokyo, Japan). The purity of the isolated compounds exceeded 98%, as determined by ^{1}H NMR and HPLC analyses.

Purification of pure metabolites

A total of 10 g of dried aerial parts of S. pinnata were minced with a blender and macerated under stirred conditions in a solution of methanol (MeOH)/H_2O 1:1, *v/v* (300 mL) for 3 days at room temperature. The resulting suspension was filtered, resulting in a hydroalcoholic crude extract. Two aliquots of this latter extract were further fractionated by performing a liquid–liquid extraction (LLE) and a solid-phase extraction (SPE). The first aliquot (100 mL) of the hydroalcoholic extract was subjected to stepwise extractions with n-hexane (3 × 100 mL), dichloromethane (CH_2Cl_2) (3 × 100 mL), and after

removing MeOH under reduced pressure, with ethyl acetate (EtOAc) (3 × 100 mL). Each extract was dried over anhydrous Na_2SO_4 and filtered, and the residual solvent was evaporated under reduced pressure, yielding 10.35 mg (*n*-hexane), 15.90 mg (CH_2Cl_2), and 36.87 mg (EtOAc) of organic extracts. The second aliquot (100 mL) of the hydroalcoholic extract was lyophilized after removing MeOH under reduced pressure. The extract obtained was suspended in 60 mL of distilled water and loaded onto an SPE column, which was previously conditioned with 60 mL of MeOH and equilibrated with 120 mL of distilled water. The purification yielded five fractions (A, B, C, D, and E) obtained via a stepwise elution with H_2O (60 mL), MeOH/H_2O 3:7, *v/v* (120 mL), MeOH/H_2O 7:3, *v/v* (120 mL), acetonitrile (CH_3CN) (120 mL), and CH_2Cl_2/MeOH 9:1, *v/v* (60 mL), respectively. Successively, the organic solvents were removed under reduced pressure, and the eventual residual water phases were lyophilized, yielding 570.59 mg (A), 310.94 mg (B), 132.01 mg (C), 4.36 mg (D), and 3.27 mg (E), respectively. The extracts and fractions obtained by applying the two procedures (LLE and SPE) were tested for biological activities, as reported below. Furthermore, the residue of SPE fraction C was purified using two subsequent steps of preparative TLC eluted with EtOAc/MeOH/H_2O(80:12:8, *v/v/v*) and TLC in reverse phase by eluting itwith MeOH/H_2O (6:4, *v/v*), affording isoquercetin (**1**, 3.78 mg), rutin (**2**, 7.50 mg), isorhamnetin glucoside (**3**, 4.78 mg), narcissoside (**4**, 2.69 mg), quercetin malonyl glucoside (**5**, 5.81 mg), and isorhamnetin malonyl glucoside (**6**, 3.62 mg) as amorphous solids. The extraction and purification process was repeated three times to accumulate the pure compounds for chemical and biological characterization. Isoquercetin (**1**): or quercetin 3-*O*-*β*-D-glucopyranoside, amorphous solid, $[\alpha]^{25}$ D −12.6 (*c* 0.1, MeOH) (He et al., 2017)] $[\alpha]^{25}$ D −10.7 (c 0.4, MeOH)); ^{1}H NMR data were in agreement with those previously reported by He et al. 2017; ESI MS (-): *m/z* 463 [M−H]−. Rutin (**2**): or quercetin 3-*O*-*β*-D-rutinoside, amorphous solid, $[\alpha]^{25}$ D −14.9 (c 0.1, MeOH) (Ly et al., 2006 $[\alpha]^{25}$ D −16.6 (c 0.1, MeOH)); ^{1}H NMR data were in agreement with those previously reported by Kazuma et al. 2003; ESI MS (-): *m/z* 609 [M-H]−. Isorhamnetin glucoside (**3**): or isorhamnetin-3-*O*-*β*-D-glucopyranoside, amorphous solid, $[\alpha]^{25}$ D −9.6 (c 0.1, MeOH) (He et al., 2017 $[\alpha]^{25}$ D −7.8 (c 0.2, MeOH)); ^{1}H NMR data were in agreement with those previously reported by He et al. 2017; ESI MS (-): *m/z* 477 [M-H]−. Narcissoside (**4**): or isorhamnetin-3-O-β-D-rutinoside, amorphous solid, $[\alpha]^{25}$ D −36.6 (c 0.1, MeOH) (Kim et al., 2011 $[\alpha]^{20}$ D −38.7 (c 0.3, MeOH)); ^{1}H NMR data were in agreement with those previously reported by Eskalieva et al. 2004; ESI MS (-): *m/z*

623 [M-H]−. Quercetin malonyl glucoside (**5**): or quercetin-3-O-(6″-*O*-malonyl)-*β*-*D*-glucopyranoside, amorphous solid, $[\alpha]^{25}$ D −14.6 (c 0.1, MeOH) (DuPont et al., 2000 $[\alpha]^{25}$ D −15.7 (c 0.1, MeOH)); ^{1}H NMR data were in agreement with those previously reported by Wald et al. 1989; ESI MS (-): *m/z* 549 [M-H]−. Isorhamnetin malonyl glucoside (**6**): or isorhamnetin-3-*O*-(6″-O-malonyl)-*β*-D-glucopyranoside, amorphous solid, $[\alpha]^{25}$ D −8.2 (c 0.1, MeOH) (Hasle Enerstvedt et al., 2017 $[\alpha]^{25}$ D −8.7 (c 0.1, MeOH)); ^{1}H NMR data were in agreement with those previously reported by Wald et al. 1989; ESI MS (-): *m/z* 563 [M-H]−.

***Lavanda angustifolia* Mill.**

All information relating to the preparation of plant material and extracts of Lavandula angustifolia Mill. is patented.

Grape pomace

Grape pomace obtained from the Mastroberardino winery was stored at –20 °C and subsequently lyophilized. A total of 100 g of dried pomace was ground in a blender and macerated with 500 mL of ethanol under continuous stirring for 24 h at room temperature to preserve the bioactive compounds present in the pomace. The suspension was then centrifuged at 7000 rpm for 30 min, and the solvent was removed under reduced pressure by rotary evaporation, yielding 5 g of organic extract. This extract was used for subsequent formulation studies.

6.1.2 Beads formulation

The obtained beads were collected, washed with Milli-Q water, and subsequently freeze-dried. Formulations based on grape pomace (GP) extract and biopolymers were prepared according to the following procedure. A 4% (w/v) polysaccharide solution was prepared by dissolving 400 mg of alginate, low-methoxyl (LM) pectin, or a mixture of the two in 10 mL of Milli-Q water. Different amounts of GP extract, corresponding to 50–75% (w/w) relative to the polysaccharide mass, were added to the polymer solution under magnetic stirring until complete homogenization was achieved. The resulting mixture was then added dropwise, under constant magnetic stirring, into an aqueous solution containing a divalent metal ion (Fe^{2+} or Ca^{2+}) used as a cross-linking agent to physically entrap the extract within the polysaccharide matrix. Cross-linking solutions were prepared in Milli-Q water using either $CaCl_2$ or $FeSO_4 \cdot 7H_2O$ at two concentrations: 4% (w/v) (1×) and

8% (w/v) (2×). Spherical beads were obtained, collected from the aqueous medium, washed with Milli-Q water, and finally freeze-dried.

Beads characterization

Thermogravimetric Analysis (TGA): Thermogravimetric analysis was performed using a Perkin-Elmer Pyris Diamond TGA/DTG analyzer equipped with a gas control station. Samples of 3–4 mg were placed in open ceramic crucibles and heated from 25 °C to 600 °C at a rate of 10 °C min^{-1} under a nitrogen flow of 30 mL min^{-1}. Loading Efficiency Determination: The UV–Vis spectra of the non-entrapped fraction of grape pomace extract, used to evaluate loading efficiency, were recorded using a Jasco V-570 double-beam spectrophotometer equipped with a single monochromator (Easton, Van Nuys, LA, USA). A calibration curve was prepared using extract solutions at five concentrations (0.5–2.5 mg mL^{-1}), measuring absorbance at 560 nm. Loading efficiency (LE, %) was calculated according to Equation (1):

$$LE(\%) = 100 - \left(\frac{M'_{\text{residual}}}{M_{\text{initial}}} \times 100\right)$$

where M'_{residual} is the mass of the non-entrapped extract (mg) quantified in the supernatant after encapsulation, and M_{initial} is the initial mass of extract used for encapsulation (mg). This equation expresses the percentage of extract successfully encapsulated within the biopolymer matrix, calculated as the difference between the total extract used and the unentrapped fraction.

Morphological Analysis (SEM): Morphological characterization of the beads was carried out using a scanning electron microscope (SEM, Quanta 200 FEG, FEI, Eindhoven, The Netherlands). Samples were coated with a homogeneous 18 ± 0.2 nm layer of Au/Pd alloy using a sputter coater (MED 020, Bal-Tec AG, Tucson, AZ, USA). Micrographs were obtained at room temperature under high-vacuum conditions.

Releases evaluation

The release behavior of the beads was assessed using a custom-designed vessel consisting of a small beaker covered with a saucer containing a 50-mesh glass filter. A total of 100 mg of the bead sample was placed on the saucer, while the beaker was filled with 11 mL of

distilled water (pH 7), corresponding to a volume sufficient to cover half of the saucer. The system was maintained under gentle magnetic stirring for 3 h at room temperature (RT). After incubation, the liquid fraction was collected, lyophilized, and the resulting residue was weighed gravimetrically. The percentage of extract released was calculated according to Equation (2):

$$\text{Release (\%)} = \left(\frac{M'_{\text{released}}}{M_{\text{initial}}}\right) \times 100$$

where M'_{released} is the mass of extract released into the liquid medium after 3 h (mg), and M_{initial} is the initial mass of extract encapsulated within the beads (mg). This equation expresses the proportion of bioactive compounds released from the beads into the aqueous medium, expressed as a percentage of the initially encapsulated content.

6.1.3 Cell culture and biological assays

Cell Lines and Culture Conditions

HeLa cells (ATCC CCL-2) were obtained from the American Type Culture Collection (Manassas, VA, USA). HaCaT cells, a spontaneously immortalized human keratinocyte line derived from adult skin, were purchased from Cell Lines Service (CLS GmbH, Eppelheim, Germany). Both HeLa and HaCaT cells were cultured in Dulbecco's Modified Eagle Medium (DMEM; Sigma-Aldrich, St. Louis, MO, USA) supplemented with 10% fetal bovine serum (FBS; Hyclone Laboratories, Logan, UT, USA), 1% penicillin–streptomycin, and 1% L-glutamine. Cells were maintained at 37 °C in a humidified atmosphere containing 5% CO_2. BJ-5ta human foreskin fibroblasts (hTERT-immortalized) were obtained from the CEINGE Biotecnologie Avanzate cell banking service (Naples, Italy). These cells were cultured in a medium consisting of Dulbecco's Modified Eagle Medium and Medium 199 (4:1, v/v), supplemented with 10% FBS, 4 mM L-glutamine, 4.5 g L^{-1} glucose, 1.5 g L^{-1} sodium bicarbonate, and 0.01 mg mL^{-1} hygromycin B. All cell lines were routinely tested for mycoplasma contamination using a Mycoplasma PCR Detection Kit (Abm, Richmond, BC, Canada).

Cell Viability Assay

Cell viability was evaluated using the MTT assay, which measures the reduction of 3-(4,5-dimethylthiazol-2-yl)-2,5-diphenyltetrazolium bromide (MTT) to formazan by mitochondrial succinate dehydrogenase (van Meerloo et al., 2011). Briefly, 4×10^3 cells were seeded into 96-well plates and treated. After treatment, cells were washed and incubated with MTT in PBS (0.5 mg mL^{-1}) for 3 h at 37 °C in a humidified atmosphere. The reaction was terminated by removing the supernatant, and the formazan crystals were dissolved in acidic isopropanol. Optical density was measured at 570 nm using a Synergy H4 microplate reader with Gen5 2.07 software (Thermo Fisher Scientific, Waltham, MA, USA). No undissolved formazan crystals were observed under these conditions. Cell viability was calculated by comparing the optical density of treated samples to that of untreated controls.

DCFDA assay

The antioxidant capacity was assessed using the DCF-DA assay. DCF-DA (2′,7′-dichlorofluorescein diacetate) is a non-fluorescent, cell-permeable compound that is hydrolyzed by intracellular esterases to DCF, which reacts with reactive oxygen species (ROS), particularly hydroxyl radicals (˙OH), forming the fluorescent molecule dichlorofluorescein (DCF; excitation: 485 nm, emission: 530 nm). Fluorescence was measured both in the absence of an oxidant stimulus and after induction of ROS production with H_2O_2. Trolox, a water-soluble analog of vitamin E, was used as a positive control. Briefly, 4×10^4 cells were treated. After 4 h, the medium was removed, and 4 mM (3%) H_2O_2 was added for 1.5 h to induce ROS production. Cells were then washed with PBS, and fresh medium containing 30 µM DCF-DA was added for 45 min. After incubation, DCF-DA was removed, cells were washed with PBS, and fluorescence was measured using a Synergy H4 microplate reader with Gen5 2.07 software (Thermo Fisher Scientific, Waltham, MA, USA). Fluorescence intensity of treated cells was compared to untreated controls. Values are reported as mean ± SD from six technical replicates. Biological triplicates were used, and statistical analysis was performed using GraphPad Prism software version 8.0.2 (GraphPad, San Diego, CA, USA).

Cell Growth curve

Cells were seeded at a density of 3 × 10^4 cells per well in 24-well plates. Every 24 h, cells were gently rinsed with 1× PBS, trypsinized, and counted. Cell viability was assessed using the trypan blue exclusion method to distinguish live and dead cells.

Wound healing assay

2 x 10^5 cells were seeded into each well of a 24-well plate. To simulate a wound, a scratch was made in the center of a confluent cell monolayer using a sterile 20 µL pipette tip when the cells reached approximately 90% confluence. Following scratching, the cells were washed twice with 1X PBS, and either fresh control medium or medium supplemented with treatment was added. Images were captured immediately after scratching (T0) and 24 hours post-treatment using a LEICA microscope. The wound area was quantified with ImageJ software (Version 1.54i) by comparing the remaining wound area of treated samples after 24 hours to their corresponding areas at T0. Each treatment was then analysed relative to the control.

Migration assay

Migration assays were conducted using 6.5 mm Transwell inserts with 8.0 µm pore-size polycarbonate membranes (Corning Incorporated, NY, USA). BJ5Ta fibroblasts and HaCaT cells were detached with trypsin-EDTA solution (Sigma Aldrich, USA). After washing with PBS, 1 × 10^5 cells were resuspended in serum-free DMEM containing stem, total, or distilled extracts at the same concentrations used for Western blot experiments and seeded into the upper chamber of the inserts. The lower chamber was filled with 600 µL of culture medium supplemented with 10% FBS. Cells were incubated at 37 °C for 24 hours. Following incubation, the membranes were stained with 0.1% Crystal Violet in 25% methanol. Non-migrated cells on the upper surface were removed with a cotton swab. The number of migrated cells was quantified by dissolving the stain in 1% SDS and measuring absorbance at 570 nm.

Western blot analysis

Whole-cell extracts (20 µg) were separated by sodium dodecyl sulfate–polyacrylamide gel electrophoresis (SDS-PAGE), transferred to membranes for Western blotting, and incubated overnight at 4 °C with primary antibodies against p21WAF, cyclin D1, (Cell Signaling Technology, Boston, MA, USA), and E-cadherin, GAPDH, NRF-2 (A-

10) and β-actin (Santa Cruz Biotechnology, Dallas, TX, USA), Mytho (AbCam-AB181987), IL6 (Elabscience AB-30095). Each experiment was performed in triplicate. Band intensities were quantified using Quantity One software (Version 2, Bio-Rad Laboratories, London, UK) and analyzed with GraphPad Prism 8.0.2 (GraphPad, San Diego, CA, USA).

Immunofluorescence Assay

HaCaT cells (3.0×10^4) were seeded on coverslips and treated for 24 h. After treatment, both control and treated cells were rinsed with PBS and fixed with 3.7% paraformaldehyde (PFA) for 10 min at room temperature. Cells were then washed three times with PBS and twice with 3% bovine serum albumin (BSA) solution to block nonspecific antibody binding.
Following blocking, cells were incubated for 1 h at room temperature with primary antibodies: anti-YB-1 (Abcam, #12148) and anti-γH2AX (Cell Signaling Technology, #9718S). Subsequently, cells were incubated with Alexa Fluor 488 donkey anti-rabbit and Alexa Fluor 594 donkey anti-mouse secondary antibodies (Thermo Fisher Scientific, USA) for 45 min in the dark. Nuclear staining was performed with DAPI (1:50,000; Sigma-Aldrich, USA) for 5 min, followed by rinsing in 0.01% Tween-PBS. Coverslips were mounted using Dako mounting medium (Agilent, USA) on glass slides.
Images were acquired using a Carl Zeiss LSM 700 confocal microscope equipped with a 40× oil immersion objective. The number of foci or fluorescence intensity per nucleus was quantified using Fiji (ImageJ) software, version 1.52, and statistical analysis was performed with GraphPad Prism 8.0.2 (GraphPad Software, San Diego, CA, USA).

DNA Extraction

HaCaT cells were seeded in 60 mm culture dishes at a density of 2.5×10^5 cells per dish. After 24 h, cells were treated with the distilled extract at a concentration of 50 μg/mL. Cells were collected at different time points (24 h, 48 h, and 5 days) following treatment. Genomic DNA was extracted using the FastPure Blood/Cell/Tissue/Bacteria DNA Isolation Mini Kit (Vazyme, China) according to the manufacturer's instructions.

Methylation analysis

Extracted DNA samples were treated with sodium bisulfite using the EZ DNA Methylation ™ Kit (Zymo Research, Irvine, CA, USA) as per manufacturer instructions. DNA methylation profiling was conducted using the Illumina Infinium MethylationEPIC v2.0 BeadChip Kit (Illumina™, San Diego, CA, USA), according to the manufacturer´s protocol. Approximately 500 ng of bisulfite-treated DNA samples were amplified, fragmented, precipitated, resuspended and load on BeadChips to allow hybridation. After incubation in the Illumina Hybridization Oven at 48 °C for 24 h, slides were washed to eliminate non-specifically hybridized and unhybridized DNA samples. Next, the process of labelling nucleotides to extend primers that have been hybridized to the sample was performed, and the primers are then stained. The detection of methylated cytosines was performed by scanning with the Illumina iScan™ system. The methylation microarray raw data (IDAT files) were analyzed in the R statistical environment using Bioconductor packages, which provide specialized tools for large-scale genomic data processing. Quality control and preprocessing steps were carried out with the minfi package. Differential methylation between study groups was then evaluated using the limma package. For each CpG site, methylation levels were expressed as β-values after normalization procedures to correct for color bias and background noise. In addition, quantile normalization was applied across all BeadChips. Only samples with a mean detection p-value below 0.01 were retained. The resulting β-values, ranging from 0 (unmethylated) to 1 (fully methylated), were further refined through a two-step filtering procedure: exclusion of SNP-associated probes and removal of unreliable measurements with detection p-values higher than 0.01. After filtering, the remaining CpGs were used in the downstream analyses.

Antimicrobial assay

The bactericidal and antibacterial activities of SPE fraction C and the pure compounds isoquercetin (1) and quercetin malonyl glucoside (5) were evaluated against two bacterial strains—*Staphylococcus aureus* ATCC®6538 and *Pseudomonas aeruginosa* ATCC®9027—and their fungicidal/antifungal activity was assessed against *Candida albicans* ATCC®14053.
Single cultures of each strain were grown under optimal conditions: *S. aureus* ATCC®6538 for 24–48 h at 37 °C (UNI EN ISO 6888-1:2021), *P. aeruginosa* ATCC®9027 for 24 h at 37 ± 1 °C (UNI EN ISO 13720:2010), and *C. albicans* ATCC®14053 for 48 h at 22 ± 1 °C (UNI

EN ISO 21527-1:2008). Bacterial inocula were cultured with constant shaking (200 rpm) in 30 mL of Tryptic Soy Broth (TSB; Thermo Fisher Scientific, USA), and yeast cultures were grown in 30 mL of Sabouraud Dextrose Broth (SAB; Thermo Fisher Scientific, USA) in sterile 50 mL tubes.
A spectrophotometer (Hach Lange DR6000, Hach, USA) was used to adjust the microbial concentration to 10^8 cells/mL, based on an optical density (OD) of 0.125 at 560 nm (bacteria) or 600 nm (yeast). The inocula were then serially diluted to reach a final concentration of 10^7 CFU/mL in 10 mL. Fraction C was tested at 150 µg/mL and 100 µg/mL, while isoquercetin (1) and quercetin malonyl glucoside (5) were evaluated at 100 µM, corresponding to the highest non-toxic concentration for the cells. The experimental procedure followed UNI EN 1276:2020, employing the time-kill test (Alrashidi et al., 2021) to determine bactericidal and fungicidal effects after a 30 min contact period. The test samples, diluted in 50 µL of dimethyl sulfoxide (DMSO; Sigma-Aldrich, USA), were added to 6-well plates containing 10 mL of 0.9% NaCl suspensions of bacteria or yeast at a microbial load of 10^6 CFU/mL, maintained under constant shaking at optimal growth temperatures (37 ± 1 °C for bacteria and 22 ± 1 °C for yeast). Negative controls consisted of inocula treated with 50 µL DMSO alone, while positive controls included 100 µg/mL chloramphenicol for bacteria and 100 µg/mL econazole for yeast. Aliquots were collected immediately after sample addition (t_0 min) and after 30 min (t_{30} min). Surviving cell counts were determined, and microbial reduction was calculated. Microbiological analyses were performed according to ISO guidelines for each microorganism, using selective agar media: Baird Parker Agar Base for *S. aureus* (Thermo Fisher Scientific, USA, ISO 6888-1:2021), Pseudomonas Agar Base for *P. aeruginosa* (Thermo Fisher Scientific, USA, UNI EN ISO 13720:2010), and Dichloran Rose Bengal Chloramphenicol Agar Base for *C. albicans* (Thermo Fisher Scientific, USA, UNI EN ISO 21527-1:2008). All experiments were conducted in independent triplicates, and results are presented as the mean values of the three replicates for each microorganism.

Statistical analysis

Statistical analyses were performed using GraphPad Prism version 8.1.2 (GraphPad Software; https://www.graphpad.com/scientific-software/prism/, accessed on 19 May 2024). Data are expressed as mean ± standard deviation (SD), and differences were considered statistically significant at $p < 0.05$. For antimicrobial assays, results are

presented as the mean of three replicates ± standard error (SE). Statistical analyses were conducted using XLSTAT 2014.5.03 (Addinsoft, 1995–2014, France). A one-way ANOVA was performed followed by Tukey's post hoc test, and comparisons between treated samples and negative controls were assessed using a two-sided Dunnett's test. Statistical significance was set at $p < 0.05$, and is indicated in figures as $p \leq 0.05$ and $p \leq 0.0001$.

Bibliography

Alrashidi, A.; Jafar, M.; Higgins, N.; Mulligan, C.; Varricchio, C.; Moseley, R.; Celiksoy, V.; Houston, D.M.J.; Heard, C.M. A time-kill assay study on the synergistic bactericidal activity of pomegranate rind extract and Zn (II) against methicillin-resistant Staphylococcus aureus (MRSA), Staphylococcus epidermidis, Escherichia coli, and Pseudomonas aeruginosa. Biomolecules 2021, 11, 1889.

Andreas G. Heiss Journal of Ethnological Studies, A fistfull of bladdernuts Vol 52 N2 2014

Arena, C., et al. "Suitability of Solanum lycopersicum L.'Microtom'for growth in Bioregenerative Life Support Systems: exploring the effect of high-LET ionising radiation on photosynthesis, leaf structure and fruit traits." *Plant Biology* 21.4 (2019): 615-626.

Babich, Olga, et al. "Modern trends in the in vitro production and use of callus, suspension cells and root cultures of medicinal plants." *Molecules* 25.24 (2020): 5805.

Badawy, Mohamed EI, et al. "A review of the modern principles and applications of solid-phase extraction techniques in chromatographic analysis." *Analytical Sciences* 38.12 (2022): 1457-1487.

Bartosz, Tylkowski, and Tsibranska Irene. "Polyphenols encapsulation–application of innovation technologies to improve stability of natural products." *Physical Sciences Reviews* 1.2 (2016): 20150005.

Bellezza, Ilaria, et al. "Nrf2-Keap1 signaling in oxidative and reductive stress." *Biochimica et Biophysica Acta (BBA)-Molecular Cell Research* 1865.5 (2018): 721-733.

Betlej, Izabela, et al. "Antimicrobial properties and assessment of the content of bioactive compounds Lavandula angustifolia Mill. cultivated in Southern Poland." *Molecules* 28.17 (2023): 6416.

Boncan, D.A.T.; Tsang, S.S.K.; Li, C.; Lee, I.H.T.; Lam, H.-M.; Chan, T.-F.; Hui, J.H.L. *Terpenes and Terpenoids in Plants: Interactions with Environment and Insects*. Int J of Mol Sci, 21, 7382. 2020.

Byrd, Allyson L., Yasmine Belkaid, and Julia A. Segre. "The human skin microbiome." *Nature Reviews Microbiology* 16.3 (2018): 143-155.

Cardia, Gabriel Fernando Esteves, et al. "Effect of lavender (Lavandula angustifolia) essential oil on acute inflammatory response." *Evidence-Based Complementary and Alternative Medicine* 2018.1 (2018): 1413940.

Costanzo, Giulia, et al. "Modulation of antioxidant compounds in fruits of Citrus reticulata Blanco using postharvest LED irradiation." *Biology* 12.7 (2023): 1029.

Davalli, Pierpaola, et al. "ROS, cell senescence, and novel molecular mechanisms in aging and age-related diseases." *Oxidative medicine and cellular longevity* 2016 (2016).

Dewanto, V.; Wu, X.; Adom, K.; Liu, R.H. Thermal processing enhances the nutritional value of tomatoes by increasing total antioxidant activity. J. Agric. Food Chem. 2002, 50, 3010–3014.

Dewick, P. M. (2002). *Medicinal natural products: a biosynthetic approach*. John Wiley & Sons.

Do, Quy Diem, et al. "Effect of extraction solvent on total phenol content, total flavonoid content, and antioxidant activity of Limnophila aromatica." *Journal of food and drug analysis* 22.3 (2014): 296-302.

Drašar, Pavel B. "Plant secondary metabolites used for the treatment of diseases and drug development." *Biomedicines* 10.3 (2022): 576.

DuPont, M.S.; Mondin, Z.; Williamson, G.; Price, K.R. Effect of variety, processing, and storage on the flavonoid glycoside content and composition of lettuce and endive. J. Agric. Food Chem. 2000, 48, 3957–3964.

Eskalieva, B.K.; Akhmed, A.; Burasheva, G.S.; Abilov, Z.A.; Akhmad, V.U. Biologically active compounds from Climacoptera. Chem. Nat. Compd. 2004, 40, 87–88

Eskalieva, B.K.; Akhmed, A.; Burasheva, G.S.; Abilov, Z.A.; Akhmad, V.U. Biologically active compounds from Climacoptera.Chem. Nat. Compd. 2004, 40, 87–88

Fasha, Fathima, and Neelamanie Yapa. "Development of an Antimicrobial Topical Skin Cream with Using Wood Apple (Limonia acidissima L.) Pulp Against Staphylococcus aureus, Pseudomonas aeruginosa and Candida albicans." *Turkish Journal of Agriculture-Food Science and Technology* 11.2 (2023): 292-295.

George, B.; Kaur, C.; Khurdiya, D.S.; Kapoor, H.C. Antioxidants in tomato (Lycopersium esculentum) as a function of genotype. Food Chem. 2004, 84, 45–51.

Gherardi, Giovanni. "Staphylococcus aureus infection: pathogenesis and antimicrobial resistance." *International journal of molecular sciences* 24.9 (2023): 8182.

Godinho, Patrícia IC, Raquel G. Soengas, and Vera LM Silva. "Therapeutic potential of glycosyl flavonoids as anti-coronaviral agents." *Pharmaceuticals* 14.6 (2021): 546.

Grgić, Josipa, et al. "Role of the encapsulation in bioavailability of phenolic compounds." *Antioxidants* 9.10 (2020): 923.

Guarino, Andrea Maria, et al. "YB-1 recruitment to stress granules in zebrafish cells reveals a differential adaptive response to stress." *Scientific reports* 9.1 (2019): 9059.

Hasle Enerstvedt, K.; Lundberg, A.; Jordheim, M. Characterization of polyphenolic content in the aquatic plants Ruppia cirrhosa and Ruppia maritima—A source of nutritional natural products. Molecules 2017, 23, 16.

He, Z.; Lian, W.; Liu, J.; Zheng, R.; Xu, H.; Du, G.; Liu, A. Isolation, structural characterization and neuraminidase inhibitory activities of polyphenolic constituents from Flos caryophylli. Phytochem. Lett. 2017, 19, 160–167.

https://erbario.unipi.it/it/erbario/view?id=1283285

Hu, Chuhuan, et al. "Ions-induced gelation of alginate: Mechanisms and applications." *International Journal of Biological Macromolecules* 177 (2021): 578-588.

Ikeuchi, Momoko, Keiko Sugimoto, and Akira Iwase. "Plant callus: mechanisms of induction and repression." *The plant cell* 25.9 (2013): 3159-3173.

ISO 13720:2010; Meat and Meat Products Enumeration of Presumptive Pseudomonas spp. International Organization for Standardization: Geneva, Switzerland, 2010. Available online: https://www.iso.org/standard/45099.html (accessed on 12 February 2024).

ISO 21527-1:2008; Microbiology of Food and Animal Feeding Stuffs. ISO 21527-1:2008; Microbiology of Food and Animal Feeding Stuffs. Horizontal Method for the Enumeration of Yeasts and Moulds. International Organization for Standardization: Geneva, Switzerland, 2008. Available online: https://www.iso.org/standard/38275.html (accessed on 12 February 2024).

ISO 6888-1:2021; Microbiology of the Food Chain−Horizontal Method for the Enumeration of Coagulase-Positive Staphylococci (Staphylococcus aureus and Other Species)−Part 1: Method Using Baird-Parker Agar Medium. International Organization for Standardization: Geneva, Switzerland, 2021. Available online: https://www.iso.org/standard/76672.html (accessed on 12 February 2024).

Jahangir, Muhammad, et al. "Health-affecting compounds in Brassicaceae." *Comprehensive Reviews in Food Science and Food Safety* 8.2 (2009): 31-43.

Kaur, Navneet, and Tawseef Ahmed. "Bioactive secondary metabolites of medicinal and aromatic plants and their disease-fighting properties." *Medicinal and aromatic plants: Healthcare and industrial applications*. Cham: Springer International Publishing, 2021. 113-142.

Kazuma, K.; Noda, N.; Suzuki, M. Malonylated flavonol glycosides from the petals of Clitoria ternatea. Phytochemistry 2003, 62, 229–237

Kim, J.S.; Kwon, Y.S.; Sa, Y.J.; Kim, M.J. Isolation and identification of sea buckthorn (Hippophae rhamnoides) phenolics with antioxidant activity and α-glucosidase inhibitory effect. J. Agric. Food Chem. 2011, 59, 138–144.

Lacikova L, Jancova M, Muselik J, Masterova I, Grancai D, Fickova M. *Antiproliferative, cytotoxic, antioxidant activity and polyphenols contents in leaves of four Staphylea L. species.* Molecules. Aug 28;14(9):3259-67. 2009.

Lee, Ji-Eun, et al. "The influence of solvent choice on the extraction of bioactive compounds from Asteraceae: A comparative review." *Foods* 13.19 (2024): 3151.

Lee, S.U.; Lee, J.H.; Choi, S.H.; Lee, J.S.; Kameyama, M.O.; Kozukue, N.; Friedman, M. Flavonoid content in fresh, home-processed, and light-exposed onions and in dehydrated commercial onion products. J. Agric. Food Chem. 2008, 56, 8541–8548

Lindsay, Allia K., and Deborah A. Hogan. "Candida albicans: molecular interactions with Pseudomonas aeruginosa and Staphylococcus aureus." *Fungal Biology Reviews* 28.4 (2014): 85-96.

Liu, Ji-Kai. "Natural products in cosmetics." *Natural Products and Bioprospecting* 12.1 (2022): 1-43.

Lopes, Janice da Conceição, et al. "Grape pomace: A review of its bioactive phenolic compounds, health benefits, and applications." *Molecules* 30.2 (2025): 362.

Lopes, José Pedro, and Michail S. Lionakis. "Pathogenesis and virulence of Candida albicans." *Virulence* 13.1 (2022): 89-121.

Lugrin Jérôme, Rosenblatt-VelinNathalie, Parapanov Roumen and Liaudet Lucas The role of oxidative stress during inflammatory processes. Biol Chem. 2014; 395 (2):203-230.

Ly, T.N.; Shimoyamada, M.; Yamauchi, R. Isolation and characterization of rosmarinic acid oligomers in Celastrus hindsii Benth leaves and their antioxidative activity. J. Agric. Food Chem. 2006, 54, 3786–3793

Mah, L. J., A. El-Osta, and T. C. Karagiannis. "γH2AX: a sensitive molecular marker of DNA damage and repair." *Leukemia* 24.4 (2010): 679-686.

Martins, Gabriel Rocha, et al. "A validated Folin-Ciocalteu method for total phenolics quantification of condensed tannin-rich açaí (Euterpe oleracea Mart.) seeds extract." *Journal of Food Science and Technology* 58.12 (2021): 4693-4702.

Mielko, Karolina Anna, et al. "Metabolomic studies of Pseudomonas aeruginosa." *World Journal of Microbiology and Biotechnology* 35.11 (2019): 178.

Moulehi, I.; Bourgou, S.; Ourghemmi, I.; Tounsi, M.S. Variety and ripening impact on phenolic composition and Antioxidant activity of mandarin (Citrus reticulate Blanco) and bitter orange (Citrus aurantium L.) seeds extracts. Ind. Crop. Prod. 2012, 39, 74–80.

Naczk, Marian, and Fereidoon Shahidi. "Extraction and analysis of phenolics in food." *Journal of chromatography A* 1054.1-2 (2004): 95-111.

Narayanankutty, Arunaksharan, Ademola C. Famurewa, and Eliza Oprea. "Natural bioactive compounds and human health." *Molecules* 29.14 (2024): 3372.

Ning, Bo-Tao, and Yong-Min Tang. "Establishment of the cell line, HeLa-CD14, transfected with the human CD14 gene." *Oncology letters* 3.4 (2012): 871-874.

O'Reilly, Michael A. "Redox activation of p21Cip1/WAF1/Sdi1: a multifunctional regulator of cell survival and death." *Antioxidants & redox signaling* 7.1-2 (2005): 108-118.

Pant, Poonam, Sudip Pandey, and Stefano Dall'Acqua. "The influence of environmental conditions on secondary metabolites in medicinal plants: A literature review." *Chemistry & Biodiversity* 18.11 (2021): e2100345.

Paul, Swastika, et al. "Phytochemical and health-beneficial progress of turnip (Brassica rapa)." *Journal of food science* 84.1 (2019): 19-30.

Perveen, Shagufta, and Areej Al-Taweel, eds. *Terpenes and terpenoids*. BoD–Books on Demand, 2018.

Roman-Benn, Analese, et al. "Pectin: An overview of sources, extraction and applications in food products, biomedical, pharmaceutical and environmental issues." *Food Chemistry Advances* 2 (2023): 100192.

Saqib, Md Nazmus, et al. "Hydrogel beads for designing future foods: Structures, mechanisms, applications, and challenges." *Food Hydrocolloids for Health* 2 (2022): 100073.

Savic, Velibor, et al. "Formation of dynamic γ-H2AX domains along broken DNA strands is distinctly regulated by ATM and MDC1 and dependent upon H2AX densities in chromatin." *Molecular cell* 34.3 (2009): 298-310.

Šircelj, H., Vidrih, R., Veberič, R., & Mikulic-Petkovsek, M. *Evaluation of bioactive constituents in European bladdernut (Staphylea pinnata L.) seed kernels*. Journal of Food Composition and Analysis, 78, 33-41. 2019.

Sohn, S. J., Kwon, Y. S., Kim, S. S., Chun, W. J., & Kim, C. M. *Chemical constituents of the leaves of Staphylea bumalda*. Natural Product Sciences, 10(4), 173-176. 2004.

Soufi, Hamid Reza, et al. "Manipulation of light spectrum is an effective tool to regulate biochemical traits and gene expression in lettuce under different replacement methods of nutrient solution." *Scientific Reports* 13.1 (2023): 8600.

Sun, B.; Richardo-da-Silva, J.M.; Sprenger, I. Critical factors of vanillin assay for catechins and proanthocyanidins. J. Agric. Food Chem. 1998, 46, 4267–4274.

Tie, Luna, Wei-xian Zhang, and Zilong Deng. "Ferrous ion-induced cellulose nanocrystals/alginate bio-based hydrogel for high efficiency tetracycline removal." *Separation and Purification Technology* 328 (2024): 125024.

Ullah, Asad, et al. "Important flavonoids and their role as a therapeutic agent." *Molecules* 25.22 (2020): 5243.

UNI EN 1276:2020; Chemical Disinfectants and Antiseptics-Quantitative Suspension Test for the Evaluation of Bactericidal Activity of Chemical Disinfectants and Antiseptics Used in Food, Industrial, Domestic and Institutional Areas-Test Method and Requirements (Phase 2, Step 1). European Standards: Bruxelles, Belgium, 2020. Available online: https://www.en-standard.eu/ (accessed on 12 February 2024).

Van Meerloo, J.; Kaspers, G.J.L.; Cloos, J. Cell sensitivity assays: The MTT assay. Methods Mol. Biol. 2011, 731, 237‑245.

Wald, B.; Wray, V.; Galensa, R.; Herrmann, K. Malonated flavonol glycosides and 3,5-dicaffeoylquinic acid from pears. Phytochemistry 1989, 28, 663–664.

Wong, Tin Wui, Gaia Colombo, and Fabio Sonvico. "Pectin matrix as oral drug delivery vehicle for colon cancer treatment." *Aaps PharmSciTech* 12.1 (2011): 201-214.Andreas G. Heiss Journal of Ethnological Studies, A fistfull of bladdernuts Vol 52 N2 2014

Appendix I

Experience in foreign laboratory

PhD Angel Diaz-Lagares

angel.diaz.lagares@sergas.es.

Epigenomics Unit, Cancer Epigenomics, Translational Medical Oncology Group (ONCOMET), Health Research Institute of Santiago de Compostela (IDIS), University Clinical Hospital of Santiago (CHUS/SERGAS), 15706, Santiago de Compostela, Spain.

- From 13.01.2025 to 11.07.2025

Appendix II

Scientific pubblications

- **Ida Paolillo,** Giulia Costanzo, Antonella Delicato, Filippo Villano, Carmen Arena and Viola Calabrò. *Light Quality Potentiates the Antioxidant Properties of Brassica rapa Microgreen Extracts against Oxidative Stress and DNA Damage in Human Cells.* Antioxidants, 2023 October
- **Ida Paolillo,** Giuseppina Roscigno, Michele Innangi, Jesús G. Zorrilla, Gianmarco Petraglia, Maria Teresa Russo, Federica Carraturo, Marco Guida, Alessandra Pollice, Alessio Cimmino, Marco Masi, and Viola Calabrò. *Health-Promoting Properties of Natural Flavonol Glycosides Isolated from Staphylea pinnata L.* International Journal of Molecular Sciences, 25(11), 5582. 2024 May.
- Giovanni Dal Poggetto, **Ida Paolillo**, Marco Masi, Geppino Falco, Valeria Lucci, Antonio Evidente, Viola Calabrò, Gabriella Santagata. *Valorization of winemaking process by-product for the production of polysaccharides encapsulated antioxidants as functional food*. Submitted Carbohydrate Polymers. 2025 November.

The manuscripts reporting the data obtained on Lavandula angustifolia and grape pomace edible beads are in preparation.

Congress and activities

- Poster session at **AGI 2023 Congress,** Cortona, Italy, *YB-1 oncoprotein as an oxidative stress sensor and DNA damage repair factor*
- Poster session and oral presentation at **FISV 2024 Congress,** Padua, Italy, *Characterization of beneficial properties of natural flavonol glycosides isolated from Staphylea pinnata L.*
- Poster session at **AGI 2025 Congress,** Bari, Italy, *From Antioxidant to Epigenetic Modulator: The Multifaceted Bioactivity of Lavandula angustifolia*
- **BIOINTEGRASAÚDE 2025 Congress,** Santiago de Compostela, Spain
- **SYMPOSIUM LIQUID BIOPSY 2025 Congress,** Santiago de Compostela, Spain

- **Ida Paolillo** "*Coscienza del benessere: lo stile di vita*" Futuro Remoto October 2024, Naples, Italy

antioxidants

MDPI

Article

Light Quality Potentiates the Antioxidant Properties of *Brassica rapa* Microgreen Extracts against Oxidative Stress and DNA Damage in Human Cells

Ida Paolillo [1,†], Giulia Costanzo [1,†], Antonella Delicato [1,†], Filippo Villano [1], Carmen Arena [1,2,*] and Viola Calabrò [1]

[1] Department of Biology, University of Naples Federico II, Via Cinthia, 80126 Napoli, Italy; ida.paolillo@unina.it (I.P.); giulia.costanzo2@unina.it (G.C.); antonella.delicato@unina.it (A.D.); fil.villano@studenti.unina.it (F.V.); vcalabro@unina.it (V.C.)

[2] NBFC—National Biodiversity Future Center, 90133 Palermo, Italy

* Correspondence: c.arena@unina.it; Tel.: +39-081679173

† These authors contributed equally to this work.

Abstract: Plants are an inexhaustible source of bioactive compounds beneficial for contrasting oxidative stress, leading to many degenerative pathologies. *Brassica rapa* L. subsp. *rapa* is well known for its nutraceutical properties among edible vegetable species. In our work, we aimed to explore an eco-friendly way to enhance the beneficial dietary phytochemicals in this vast world of crop-growing plants at selected light quality conditions. White broad-spectrum (W) and red–blue (RB) light regimes were used for growing brassica microgreens. The organic extracts were tested on keratinocytes upon oxidative stress to explore their capability to act as natural antioxidant cell protectors. Our results show that both W and RB extracts caused a notable reduction in reactive oxygen species (ROS) levels induced by H_2O_2. Interestingly, according to its higher contents of polyphenols and flavonoids, the RB was more efficient in reducing ROS amount and DNA damage than the W extract, particularly at the lowest concentration tested. However, at higher concentrations (up to 100 µg/mL), the antioxidant effect reached a plateau, and there was little added benefit. These findings confirm that RB light effectively increases the antioxidant compounds in *Brassica rapa* L. microgreens, thus contributing to their enhanced activity against oxidative-induced genotoxicity compared to microgreens grown under W light.

Keywords: antioxidants; phytochemicals; human cells; DNA damage; NRF2; p21WAF proteins

Citation: Paolillo, I.; Costanzo, G.; Delicato, A.; Villano, F.; Arena, C.; Calabrò, V. Light Quality Potentiates the Antioxidant Properties of *Brassica rapa* Microgreen Extracts against Oxidative Stress and DNA Damage in Human Cells. *Antioxidants* **2023**, *12*, 1895. https://doi.org/10.3390/antiox12101895

Academic Editor: Dimitrios Stagos

Received: 26 September 2023
Revised: 17 October 2023
Accepted: 19 October 2023
Published: 23 October 2023

1. Introduction

Consumption of foods rich in bioactive compounds has been associated with positive effects on human health, acting on inflammation and diseases such as cancer and diabetes, as supported by many preclinical and clinical studies [1,2]. Edible green vegetables, including herbal medicines, are well-established sources of phytochemicals [3] which are crucial components in promoting human health and longevity [4]. Bioactive compounds are often found in edible plant extracts and are known for their antioxidant and anti-inflammatory properties. Natural antioxidants can counteract tissue inflammation and oxidative stress, which are underlying factors in developing and progressing systemic diseases such as metabolic disorders, cardiovascular diseases, neurodegenerative diseases, and cancer [5]. Unlike synthetic antioxidants, natural compounds from edible plants play a vital role in protecting cells with minimal or no side effects [6]. Therefore, the demand for plant-based antioxidants in pharmaceuticals and nutraceuticals is continuously increasing. This trend reflects the growing interest in using plants as sources of phytochemicals to promote health and prevent or manage various health conditions.

Brassicaceae plants are vegetables consumed all over the world [7]. *Brassica* is a source of healthful compounds, i.e., polyphenols, vitamins, fiber, soluble sugars, glucosinolates minerals, and carotenoids [8]. More specifically, the health benefits of *Brassica* are related to its antioxidant capacity due to the presence of many phenolic compounds [9], phenolic acids, flavonoids, and isoflavonoids. The main phenolics in *Brassica* are hydroxycinnamic acids, i.e., caffeic, ferulic, protocatechuic and sinapic acids [10]. These health-promoting compounds are involved in numerous biological activities, such as cancer prevention [11], cardiovascular system protection, and inhibition of oxidative damage [12]. Considering the importance of therapeutic consumption of this family of vegetables, it represents an innovative scientific frontier to develop an eco-friendly strategy to increase the concentration of antioxidants, including flavonoids and phenolic compounds, in *Brassica* species destined for human consumption.

Light is one of the critical factors that can be modulated to influence the accumulation of these metabolites. Several studies showed that light quality significantly impacts on plant growth and chemical composition [13–17].

The modulation of the light spectrum through Light-Emitting Diode (LED) technology enables obtaining desired plant characteristics in plants, i.e., growth enhancement, changes in morphology, flavor and pigmentation, and the stimulation of specific bioactive molecule synthesis.

Therefore, monochromatic light or a mix of different wavelengths may be effectively used to affect plant material/extract with customized composition for various purposes such as medicinal, nutritional, and industrial applications [16].

Recent studies proved that red and blue regions of the light spectrum are the most effective in influencing plant growth and phytochemical composition [18–20]. The use of red–blue light (RB) and white full-spectrum light (W) has distinct effects on plants. It has been reported that RB and W treatments affected the synthesis of polyphenols, anthocyanins, and flavonoids in some fruits and vegetables [21,22].

More specifically, as described by [19], RB light regimes increased the concentration of some flavones, flavanols, anthocyanidins, and benzoic and cinnamic acids in citrus fruits compared to W regime. The more specific qualitative analysis of the phenolic profile in fruits showed that RB light boosted some phenolic substances such as sinensetin, linarin, caffeic, ferulic, and vanillic acids, known for their anti-inflammatory, antimicrobial, cardioprotective, anticancer, and antidiabetic properties. On the other hand, fruits stored under W light showed an increased concentration of other metabolites, i.e., flavonoids such as rutin, quercetin, and naringin, effective in treating neurodegenerative diseases, COVID-19, and metabolic syndrome, respectively.

However, even if combining red and blue light can yield impressive results, it is crucial to adjust the ratio of these light regimes appropriately as well as the light intensity [23]. Excessive blue light, indeed, may lead to a decrease in yield, showing the importance of finding the right balance between the two wavelengths [24,25]. The present work aims to investigate the possibility of enhancing the antioxidant compounds of *Brassica rapa* L. microgreens growing plants under RB light regime and test the corroborated extracts for their antioxidant potential on non-transformed human cells. More specifically, we have treated human immortalized keratinocytes with different concentrations of the brassica crude extracts from plants grown at RB and W light regimes to explore their activity against hydrogen peroxide-induced oxidative stress in human cells.

In our experiments, the cruciferous species *Brassica rapa* L. (Broccoli raab) and, more specifically, broccoli microgreens were used for preparing the crude extracts. *Brassica* microgreens are young plants already known as a fount of valuable bioactive compounds [26,27] showing rapid growth and adaptability to environmental factors [28].

2. Materials and Methods

2.1. Chemicals and Reagents

Folin and Ciocalteu's phenol reagent, sodium carbonate, aluminium chloride hexahydrate, sodium nitrite, sodium hydroxide, 2,4,6-tri(2-pyridyl)-s-triazine (TPTZ), iron (III) chloride hexahydrate and all standards (gallic acid, catechin, 6-hydroxy-2,5,7,8-tetramethylchroman-2-carboxylic acid, 97% (Trolox)) and Dymethil Sulfoxide (DMSO) were purchased from Sigma-Aldrich (St. Louis, MO, USA). All other chemicals used were of analytical grade. Dulbecco's Modified Eagle's Medium (DMEM, Sigma Chemical Co., St. Louis, MO, USA), FBS, Hyclone Laboratories, Inc. Logan, UT, USA, 3-(4,5-methylthiazol-2)-2,5-diphenyltetrazolium bromide (MTT, neoFroxx Einhausen Deutschland, Germany), Dimethyl Sulfoxide for cell culture, Applichem GmbH ITW Reagents, Glenview, IL, USA, 2′-7′ dichlorofluorescein diacetate (DCFDA, Sigma Chemical Co., St. Louis, MO, USA), Hydrogen peroxide solution 30%, Carlo Erba Reagents GmbH, Milan, Italy, Trolox, 6-Hydroxy-2,5,7,8-tetramethylchroman-2-carboxylic Acid (Sigma Chemical Co., St. Louis, MO, USA), PBS Dulbecco's Phosphate-Buffered Saline (Euroclone S.p.A, Milan, Italy), DAPIsolution (1:50,000) (Sigma Chemical Co., St. Louis, MO, USA), Dako mounting medium (Agilent, Santa Clara, CA, USA), anti-YB-1 (Abcam 12148, Cambridge, UK), anti-g-H2AX histone (Cell signaling 9718S, Danvers, MA, USA), Alexa Fluor 488 anti-rabbit donkey and Alexa Fluor 594 donkey (Thermo Fisher Scientific, Waltham, MA, USA), anti-β-actin (C4) and anti-NRF-2 (A-10) were from Santa Cruz Biotechnology (Dallas, TX, USA), while p21WAF were from Invitrogen (Thermo Fisher Scientific, Waltham, MA, USA).

2.2. Experimental Design and Plant Material

One hundred seeds of *Brassica rapa* L. subsp. *rapa* were sown in two 0.5 L boxes filled with Vigorplant© complete universal soil (21% Baltic peat 0–10 mm, 37% Irish peat 0–20 mm, slow-release fertilizer, 13% volcanic pumice 3–8 mm, 29% superfine peat 0–3 mm). The seeds were placed in a chamber at the following controlled condition: Photosynthetic Photon Flux Densities (PPFD) 270 ± 10 mmol(photon) m^{-2} s^{-1}, 25/15° day/night temperature, 50/70% day/night relative humidity, at 12 h photoperiod. The light quality regimes set in the chamber were: broad-spectrum white (W) and red–blue (RB: 60–40) with emission peaks of 630 and 460 nm for red and blue, respectively (Figure 1).

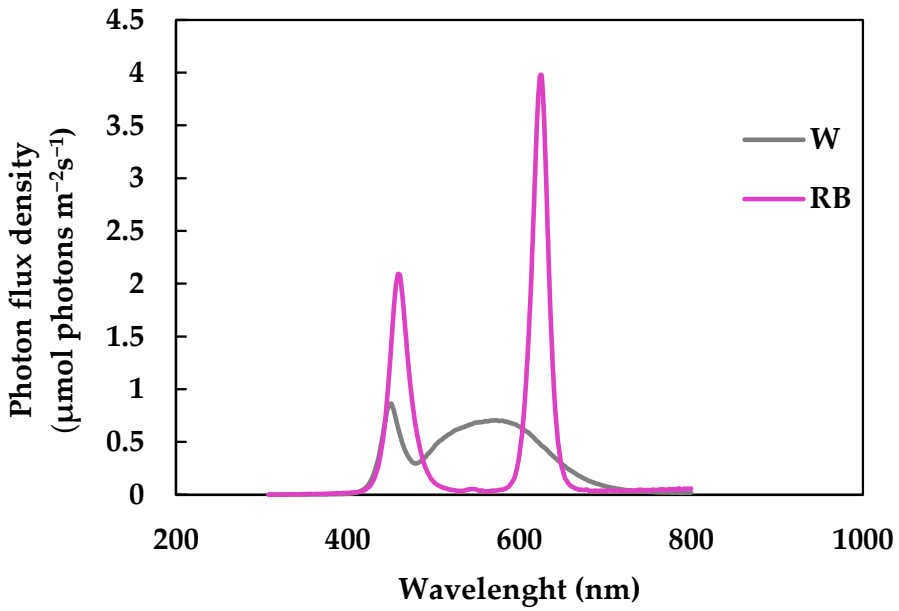

Figure 1. Light quality treatments applied to plants in chamber: white (W) and red-blue (RB), with a red emission peak at 630 nm, and a blue emission peak at 460 nm.

Temperature and RH% were recorded by a digital thermo-hygrometer (HC520 Digital Thermo-Hygrometer, Cheerman, Shenzhen, China) while PPFD was measured by a quantum sensor (Li-Cor, Lincoln, NB, USA). Microgreens were left in the chamber for fifteen days and regularly watered to reintegrate water lost by evapotranspiration.

2.3. Preparation of Methanolic Extracts

Plant material, collected at 15 DAS, was finely powered with liquid nitrogen by mortar and pestle. The extracts were prepared by weighing 0.20 g of sample, solubilized in 2 mL of 80% methanol. After centrifugation at 11.000 rpm samples were stored at 4 °C until analysis.

2.4. Polyphenols and Flavonoids Determination

Total polyphenols were evaluated as described by Sun et al. (1998) [29]. An aliquot of methanolic extract was mixed with 1:1 (*v*/*v*) 10% Foli—Ciocálteu and 1:5 (*v*/*v*) 700 mM Na_2CO_3 and the solution was stored in the dark for 2 h. The absorbance was detected by a spectrophotometer (UV-VIS Cary 100, Agilent Technologies, Palo Alto, CA, USA) at 765 nm. The total polyphenol content was calculated by means of a gallic acid standard curve and expressed as mg Gallic Acid Equivalents (GAE) g^{-1} FW.

Flavonoids were quantified accordig to Moulehi et al. (2017) and Dewanto et al. (2002) [30,31]. Briefly, an aliquot of supernatant was added to 75 µL of 5% $NaNO_2$ (sodium nitrite). After, 150 µL of 10% $AlCl_3$ (aluminum chloride) and 500 µL NaOH (1 M), distilled water was added to the mixture up to a final volume of 1.525 mL. The absorbance was quantified spectrophotometrically (spectrophotometer UV-VIS Cary 100, Agilent Technologies, Palo Alto, CA, USA) at 510 nm. Flavonoid concentration was estimated using a catechin standard curve as mg Catechin Equivalents per gram of fresh weight (mg CE g^{-1} FW). Statistical analysis was performed on 8 technical replicates by *t*-test, using GraphPad Prism8 software Prism software, version 8.0 (GraphPad, San Diego, CA, USA).

2.5. Antioxidant Activity Assay

The antioxidant capacity was evaluated by FRAP (Ferric Reducing Antioxidant Power) assay, as reported by George et al. (2004) [32]. Briefly, 0.25 g of powdered sample was extracted with 5 mL of methanol/water solution (60:40 *v*/*v*). After 1 h on ice, the extracts were centrifuged at 4 °C for 15 min at 14.000 rpm. After, an aliquot of 150 µL t was added to the FRAP reagents (2.5 mL of 300 mM acetate buffer pH 3.6, 250 µL of 10 mM triperidoltriazine (TPTZ), and 250 µL of 12 mM $FeCl_3$), and stored in the dark for 1 h. The absorbance was detected at 593 nm spectrophotometrally (UV-VIS Cary 100, Agilent Technologies, Palo Alto, CA, USA). The antioxidant capacity was calculated using a Trolox standard curve and expressed as µmol Trolox equivalents (µmol TE g^{-1} FW). Statistical analysis was performed on 8 technical replicates by *t*-test, using GraphPad Prism software, version 8.0 (GraphPad, San Diego, CA, USA).

2.6. Cell Culture, Reagents, and Preparation Samples

HaCaT keratinocytes were provided from the Service Cell Line (GmBH, Eppelheim, CLS, Germany). They have spontaneously immortalized from adult skin having mutant p53 (H179Y/R282W) and are still able to differentiate upon calcium treatment. HaCaT cells were cultured in Dulbecco's Modified Eagle's Medium (DMEM, Sigma Chemical Co, St. Louis, MO, USA) added with 10% fetal bovine serum (FBS, Hyclone Laboratories, Inc. Logan, UT, USA) in a humified atmosphere of 5% CO_2. at 37 °C cells were grown at 60–70% for subculturing and routinely evaluated for mycoplasma contamination. After W and RB methanolic extracts have been dried, at a temperature of 50 °C for 30′ in Rotavapor RII (BÜCHI Labortechnik AG ®, Flawil, Switzerland), and dry material was weighed. The extracts were solubilized in Dimethyl Sulfoxide (DMSO) was added to reach the concentration of 1000 µg/mL (stock solution).

From stock solution, serial dilutions were added to the HaCaT cell culture medium to obtain the final concentrations of 100 μg/mL, 10 μg/mL and 1 μg/mL.

The DMSO concentration in negative control and treated samples was maintained at 0.1% in both 3-(4,5-methylthiazol-2)-2,5-diphenyltetrazolium bromide (MTT) and Dichlorofluorescein diacetate (DCFDA) assays.

2.7. Cell Viability (MTT) Assay

The effect of *Brassica rapa* extracts on cell viability was assessed on HaCaT cells measuring the reduction of 3-(4,5-methylthiazol-2)-2,5-diphenyltetrazolium bromide (MTT) to blue/purplish formazan salts by the mitochondrial enzyme succinate dehydrogenase. The experiment was carried out according to [33].

We performed the cell count at 24 and 48 h. Every 24 h, cells were rinsed with 1× PBS, trypsinized, and counted by Scepter 2.0 Handheld Automated Cell Counter (Millipore, Burlington, MI, USA) as previously described [34]. Statistical analysis was performed on six technical replicates by one-way ANOVA, followed by Dunnett's multiple comparisons test using GraphPad Prism software, version 8.0 (GraphPad, San Diego, CA, USA).

2.8. Dichlorofluorescein Diacetate (DCFDA) Assay

The antioxidant activity of *Brassica rapa* extracts was measured in HaCaT cells by means of 2′-7′ dichlorofluorescein diacetate (DCFDA), which gives a fluorescent compound following oxidation by Reactive Oxigen Species (ROS). Cells were seeded at 2×10^4 in 96 wells. After 24 h, cells were washed with PBS and pretreated with the extracts at the indicated concentrations for 4 h. The medium was supplemented with 1 mM DCFDA for 45 min, then 1 mM (3%) H_2O_2 was added for 1.5 h. The measurement of ROS was obtained using a Sinergy H4 microplate reader (Gen5 2.07). The fluorescence emitted from the cells treated with DCFDA was compared to the cells in 0.1% DMSO as a negative control. Trolox, a Vitamin E analogous, was used as a positive control.

Statistical analysis was performed on six technical replicates by two-way ANOVA, followed by Tukey's multiple comparison test using GraphPad Prism software, version 8.0 (GraphPad, San Diego, CA, USA).

2.9. Immunofluorescence Microscopy on HaCaT Cells

The 3.0×10^4 HaCaT cells were seeded on coverslips and treated for 24 h. After, both control and treated cell groups were rinsed with × PBS and fixed in PFA 3.7% for 10 and 15′, respectively. Cells were 3-fold washed with PBS and twice with a 3% BSA solution to avoid unspecific binding of antibodies. After 1 h incubation at RT with primary antibodies, anti-YB-1 (Abcam 12148), and anti-γ-H2AX histone (Cell signaling 9718S), cells were incubated with, Alexa Fluor 488 anti-rabbit donkey and Alexa Fluor 594 donkey secondary antibodies (Thermo Fisher Scientific) for 45 min in darkness. Then, HaCaT cells were incubated for 5 min in a DAPI solution (1:50.000) (Sigma-Aldrich) and then in 0.01% Tween PBS. Coverslips were immersed in a Dako mounting medium (Agilent).

Samples were mounted on glass slides. The images were acquired using Carl Zeiss LSM 700 (40X oil immersion optical lens) microscopes. The number of foci or the quantized immunofluorescent signals in the nuclei was measured with Fiji (ImageJ) software version 1.52 analyzed by GraphPad Prism 8.0.2 software (GraphPad, San Diego, CA, USA).

2.10. Western Blot Analysis

Western blot was carried out following Di martino et al. (2016) and Vivo et al. (2015) [35,36]. Immunoblots were revealed by means of specific antibodies. Antibodies against β-actin (C4) and NRF-2 (A-10) were from Santa Cruz Biotechnology, while p21WAF were from Invitrogen (Thermo Fisher Scientific). Each experiment was run in triplicate. The signal intensities of bands were quantified by Image Lab analysis software (Version Number 6.1, Biorad Laboratories, London, UK) and quantified by GraphPad Prism 8.0.2 software (GraphPad, San Diego, CA, USA).

3. Results

3.1. Evaluation of the Antioxidant Capacity of B. rapa Microgreens Exposed to Different Light Regimes

To analyze the effect of different light regimes (red–blue light and broad-spectrum white light) on the concentration of bioactive compounds in *Brassica rapa* L. microgreens, we evaluated the total polyphenols, flavonoids, and antioxidant capacity of the extracts from the microgreens grown under these two light conditions. The results of the FRAP assay, shown in Table 1, indicate that the total soluble antioxidant capacity of the microgreen extracts was significantly higher ($p < 0.05$) in samples exposed to RB light compared to those grown under W light. This shows that the red–blue light treatment enhanced the antioxidant capacity of the microgreens. Additionally, the concentration of total polyphenols and flavonoids was also found to be higher in microgreens grown under RB light in comparison to those grown under W light confirming that the RB light treatment was effective in increasing the levels of these phytochemicals in *Brassica rapa* L.

Table 1. Antioxidant capacity, total polyphenols, and total flavonoids. measured in microgreens of *Brassica rapa* L. grown for 15 days under W light (full spectrum) and RB light (60% R:40% B) regimes. Data are the means ± standard error (n = 8). Different letters indicate significant differences between conditions ($p < 0.05$).

	W Light Regime	**RB Light Regime**
Antioxidant capacity (μmol TE g^{-1} FW)	9.46 ± 0.11 ^{b}	13.56 ± 0.16 ^{a}
Total polyphenols (mg GAE g^{-1} FW)	2.96 ± 0.07 ^{b}	4.45 ± 0.07 ^{a}
Total flavonoids (mg CE g^{-1} FW)	3.86 ± 0.06 ^{b}	4.40 ± 0.09 ^{a}

TE: Trolox equivalent; GAE: Gallic Acid Equivalent; CE: Catechin Equivalent.

3.2. Cytotoxicity of B. rapa Microgreens MeOH Extract on Human Cells

We analyzed the cytotoxic effect of W or RB methanol extracts obtained from *Brassica rapa* on human spontaneously immortalized HaCaT keratinocytes using the MTT assay. The number of viable cells was expressed as a percentage of negative control cells (DMSO 0.1%). A reduction in cell viability would show cytotoxic effects. The W or RB methanolic extracts were added to the cell culture medium at concentrations ranging from 1 to 1000 μg/mL. The cell cultures were incubated with the extracts for 24 and 48 h (Figure 2). After 24 h of incubation, the W extract at concentrations of 10 μg/mL and 100 μg/mL caused a reduction in HaCaT cell viability to 83% and 84%, respectively (Figure 2A). The cell viability was further reduced after 48 h of incubation (Figure 2B). Conversely, the RB extract at the lowest concentration used (1 μg/mL) caused a noticeable increase in cell viability (22–23%) at both 24 and 48 h of incubation (Figure 2). However, at the concentration of 1000 μg/mL, both extracts caused a dramatic reduction in cell viability like that detected by treating cells with 100 μM lycorine, used as a positive control of cytotoxicity. Based on the obtained results, we decided to perform further experiments using a concentration range from 1 to 100 μg/mL of both W and RB extract, and a 24 h incubation period.

3.3. Antioxidant Activity of B. rapa W and RB Extracts

Next, we evaluated the antioxidant activities of *Brassica rapa* microgreens extracts in human HaCaT keratinocytes using the 2′-7′ dichlorofluorescein diacetate (DCFDA) assay. This assay measures ROS level in cells. Reactive oxygen species were induced in the cells using 1 mM H_2O_2 (3%).

Cells pretreated or not for 4 h with sub-toxic concentrations of RB and W extracts (from 1 to 100 μg/mL) were exposed to H_2O_2. TROLOX, a water-soluble permeable vitamin E analog, was used as a positive control for its known antioxidant activity. The negative

control was treated with the vehicle alone (DMSO 0.1%) and was also used for diluting the extracts.

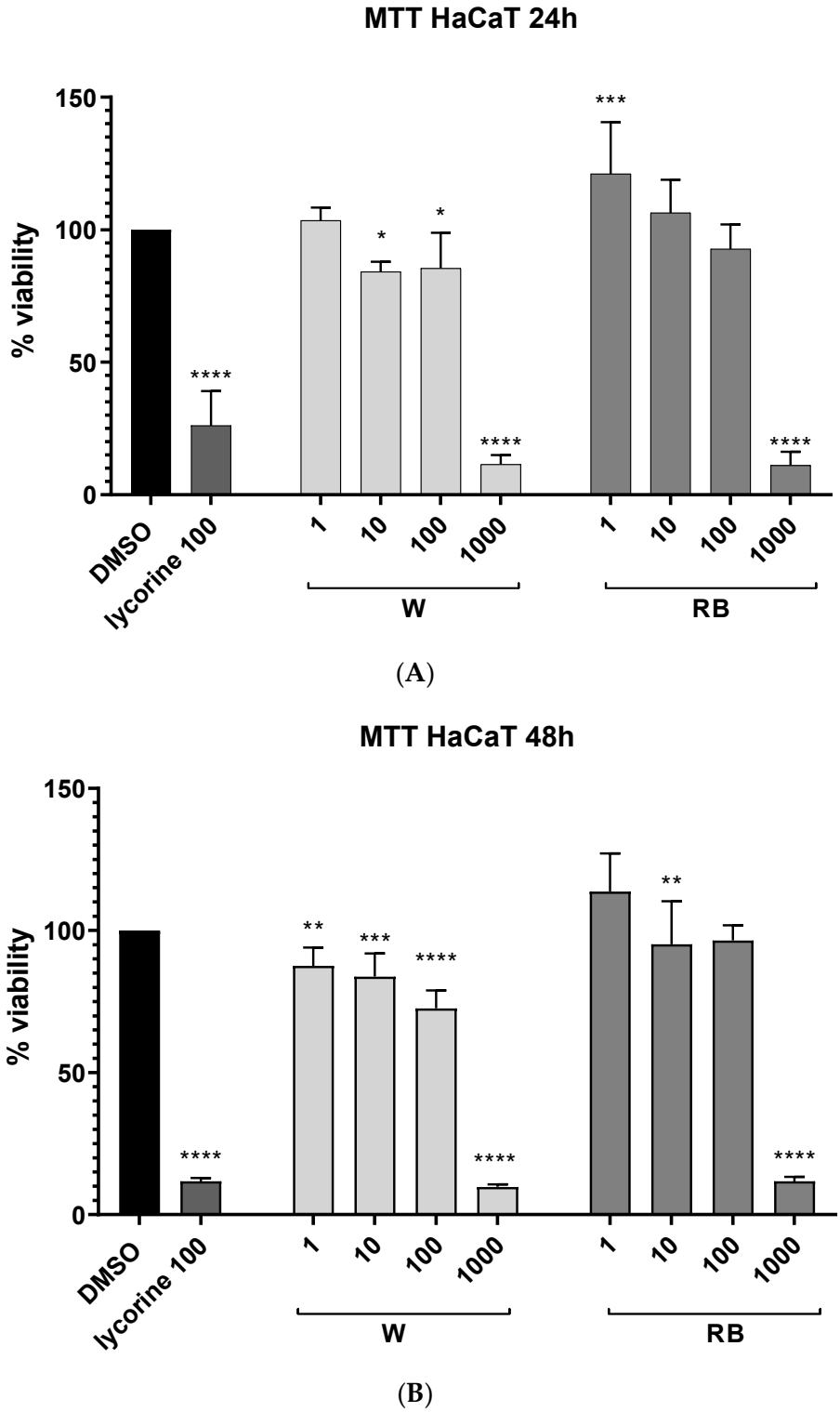

Figure 2. MTT viability test; on Y-axis the cell viability is showed in %. HaCaT cells were treated with the W (white light treatment) or RB (red–blue light treatment) organic extracts at the indicated concentrations for 24 h (**A**) and 48 h (**B**). Data are the means ± standard error (n = 6) of three independent biological replicates. Each mean was compared by one-way ANOVA, followed by Dunnett's multiple comparisons test (*p*-value * < 0.01, ** < 0.05, *** $p < 0.001$; **** $p < 0.0001$). DMSO: cells in 0.1% DMSO, negative control; lycorine: positive control.

The incubation of cells with increasing of the sole extract concentration did not significantly affect the basal level of intracellular ROS (Figure 3). However, pretreatment of cells with both W and RB extracts caused a notable reduction in ROS concentration induced by H_2O_2 (**** $p < 0.001$, *** $p < 0.01$). Interestingly, the RB extract proved higher efficiency in the quenching of ROS compared to the W extract, particularly at the lowest concentration applied (1 µg/mL) (Figure 3). These findings confirm that the microgreens grown under RB light conditions hold higher levels of antioxidant compounds that contribute to their enhanced antioxidant activity compared to microgreens grown under W light. However, at 10 µg/mL, the antioxidant effect reached a plateau and there was little added benefit in increasing the concentration of the extract up to 100 µg/mL) (Figure 3).

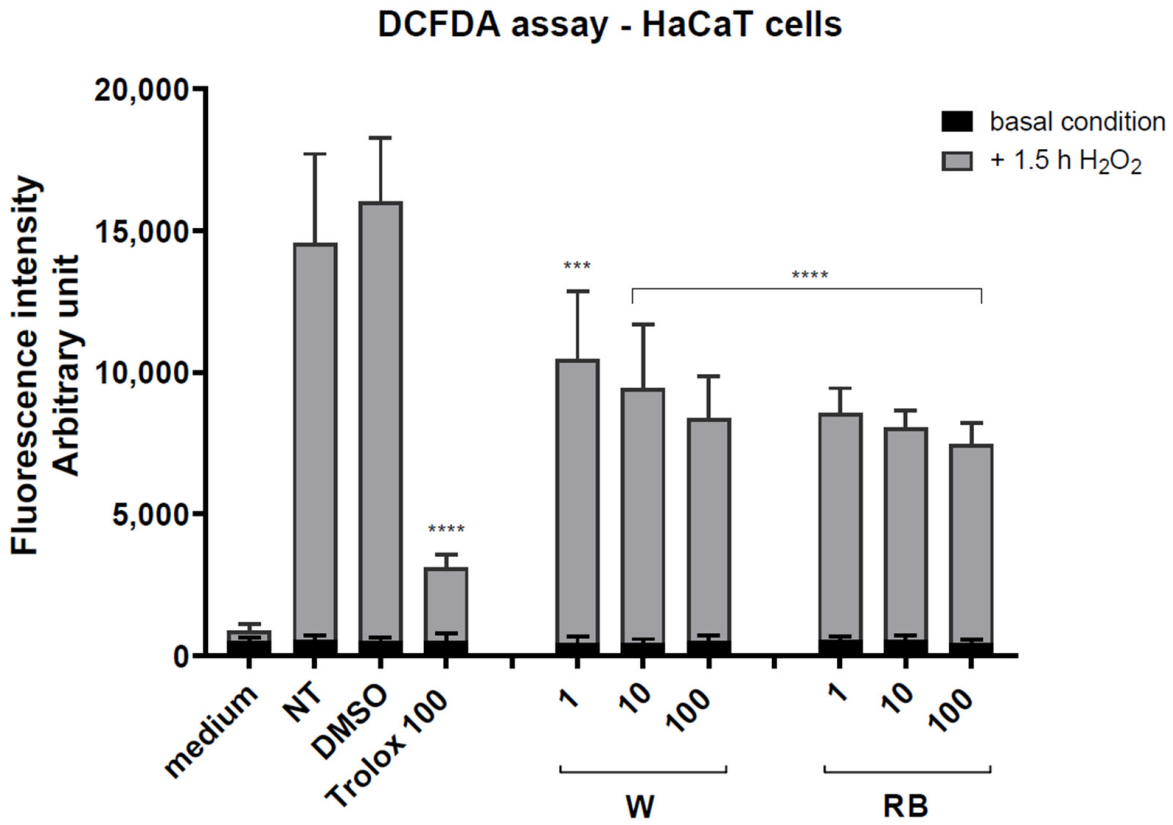

Figure 3. DCFDA antioxidant assay. HaCaT cells were seeded and pretreated with the indicated amount of W (white light treatment) or RB (red–blue light treatment) organic extract for 4 h. The DCFDA assay was performed on: medium (culture without cells used as background reference); NT (not-treated basal condition cells); DMSO (cells in 0.1% DMSO, negative control) and Trolox 100 µg/mL (positive control). All cell samples were treated with H_2O_2 (1 mM; 3%) for 1.5 h to induce ROS production. Data are the means ± standard error (n = 6) of three independent biological replicates. Statistical analysis was carried out by two-way ANOVA, followed by Tukey's multiple comparison test (**** $p < 0.001$, *** $p < 0.01$).

3.4. Effect of W and RB Crude Extracts on Stress Granules Formation and DNA Damage

The effect of the extracts on oxidative stress-induced stress granule (SG) formation and DNA damage were tested in HaCaT cells by confocal immunofluorescence using antibodies against YB-1 (the Y-box binding protein 1) and γH2AX.

We stimulated HaCaT cells, pretreated or not with W or RB microgreen extracts, with 300 µM H_2O_2 to induce oxidative stress and SGs assembly. As experimental controls, we used unstimulated cells and stimulated cells supplemented with the DMSO vehicle alone or with 100 µM Trolox as an antioxidant.

Hydrogen peroxide promoted the formation of YB-1 positive-SGs detectable as green spots in the cytoplasm and the assembly of γH2AX foci indicating the occurrence of DNA

damage (Figure 4A,B,E). As expected, in cells treated with the antioxidant Trolox, SGs were undetectable, YB-1 was uniformly distributed into the cytoplasm (Figure 4B), and γH2AX foci were reduced compared to the control (Figure 4B,E).

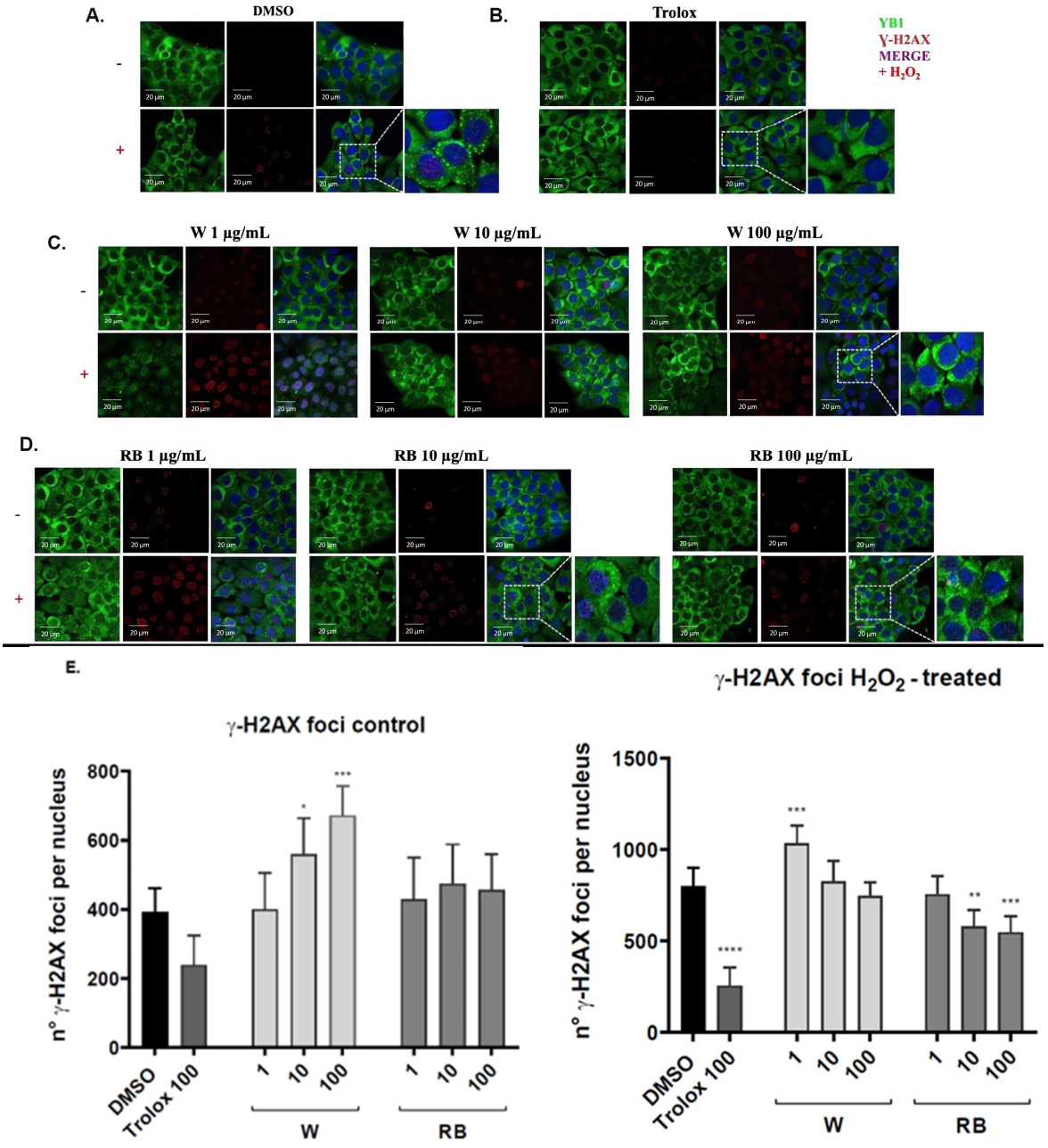

Figure 4. Confocal immunofluorescence to detect YB-1 subcellular localization and γ-H2AX foci in basal and oxidative stress conditions. (**A**–**D**) Confocal analysis of HaCaT cells treated with indicated concentrations of W (white light) and RB (red–blue light) extracts. Hydrogen peroxide was used to induce oxidative and/or genotoxic. Cells were stained with α-YB1 and α-γ-H2AX antibodies. Nuclei were stained with DAPI. (**E**) The quantitation of the foci number was performed by Fiji—ImageJ software version 1.52 and values were compared to the baseline/physiologic number of foci of the DMSO (cells in 0.1% DMSO, negative control) and Trolox 100 µg/mL (positive control). Data are the means ± standard error (n = 6) of three independent biological replicates. Statistical analysis was carried out by two-way ANOVA followed by Sidak's multiple comparison tests (*p*-value * < 0.01, ** < 0.05, *** $p < 0.001$; **** $p < 0.0001$).

In H_2O_2-unstimulated cells pretreated with the W or RB extract, SGs were undetectable. However, in cells treated with the W extract, the signal of γ-H2AX foci increased in a dose-dependent way, showing the occurrence of DNA damage. Conversely, in cells treated with the RB extract, the number of γ-H2AX foci was comparable to the control at all concentrations of RB extract used (Figure 4E, left panel). Upon oxidative stress, in W-treated cells, the number of γ-H2AX foci decreased in a dose-dependent way although it was higher compared to the control. Accordingly, YB-1 was completely nuclear at 1 μg/mL of W extract (Figure 4C,D) while it accumulated in the perinuclear region at 10 and 100 μg/mL of W extract. Conversely, in cells pretreated with 10 and 100 μg/mL of RB extract YB-1 was detected in SGs aggregates or distributed between the nucleus and cytoplasm while the number of γ-H2AX foci was significantly (* $p < 0.01$, ** $p < 0.05$, *** $p < 0.001$; **** $p < 0.0001$) reduced compared to the control thus indicating that the RB but not the W extract, was effective in protecting cells from oxidative stress-induced genotoxicity (Figure 4E).

To deepen the protective role of the RB extract, we test both RB and W extracts on NRF2 (NF-E2-related factor 2) transcription factor and the cell cycle regulator p21WAF protein under unstressed conditions or in cells subjected to oxidative stress. W We analyzed the expression level of NRF2 and p21WAF protein by Western blot in control and H_2O_2-stimulated cells pretreated or not with W or RB extracts.

Under unstressed conditions, pretreatment with low doses of W extract (1 and 10 μg/mL) upregulated NRF2 and p21WAF as a signal of activation of the cellular response to oxidative stress (Figure 5, upper panel). However, the highest concentration of W extract used (100 μg/mL) resulted in a dramatic decrease in NRF2 and p21WAF proteins (Figure 5, upper panel) thus suggesting that the toxic effect was prominent and negatively affected the pro-survival response of cells. This agreed with the data of the MTT assay indicating a reduced cell viability in this experimental condition (Figure 2). On the other hand, under basal conditions, RB extract did not affect NRF2 levels at all concentrations tested. The p21WAF protein was slightly induced only at the lowest concentration of RB, which shows a very mild activation of the oxidative stress response (Figure 5, upper panel). Following the oxidative stress, both W and RB extracts increased NRF2 protein levels (Figure 5, lower panel).

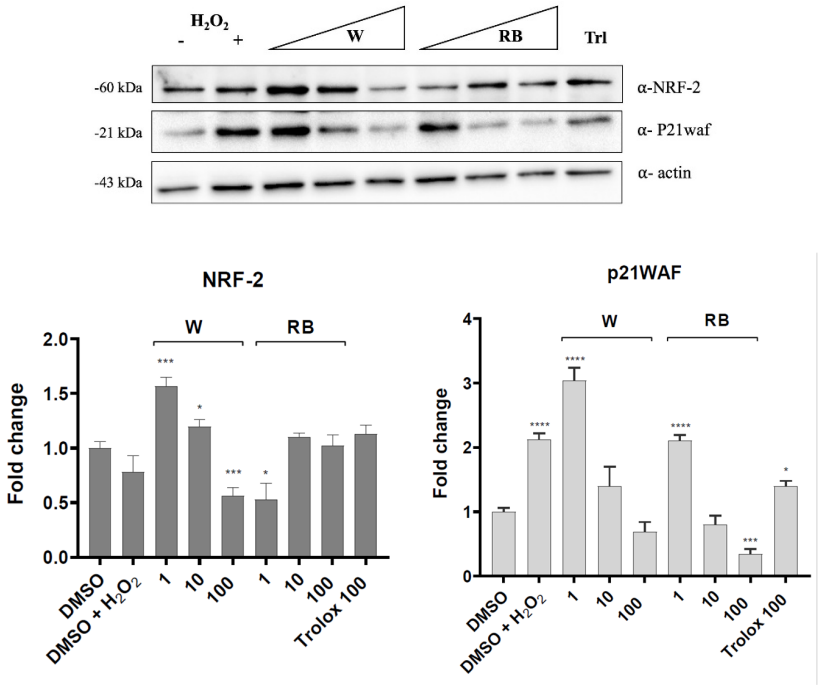

Figure 5. *Cont.*

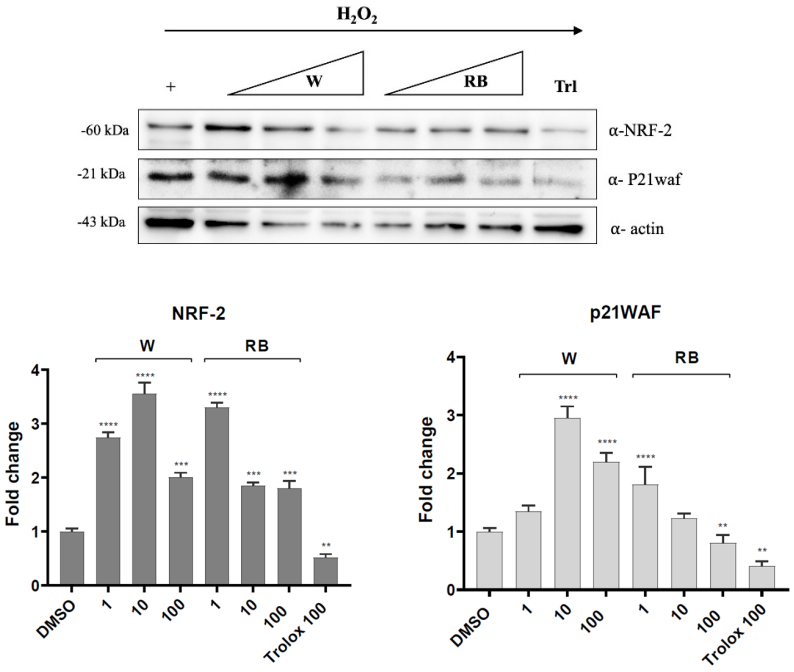

Figure 5. Western blot analysis of total extracts from HaCaT keratinocytes treated for 4 h with 1, 10 and 100 µg/mL of W (white light) and RB (red-blue light) extracts stimulated with H_2O_2 (**upper panel**) and without H_2O_2 (**lower panel**). DMSO (cells in 0.1% DMSO, negative control); DMSO + H_2O_2 (cells in 0.1% DMSO, negative control plus H_2O_2) and Trolox 100 µg/mL (positive control). Immunoblots were probed with NRF2 and p21WAF antibodies. β-actin was used as a loading control. The protein bands were quantified by ImageLab software version 4.1 (Bio-Rad, Hercules, CA, USA). Statistical analyses were carried out by two-way ANOVA followed by Sidak's or Dunnett's multiple comparison test (**** $p < 0.0001$, *** $p < 0.001$, ** $p < 0.01$, * $p < 0.05$).

4. Discussion

Microgreens are widely known as an excellent source of antioxidants and the choice of proper light treatment, during plant growth, especially enriched of red and blue wavelengths represents an efficient mean to regulate the synthesis of health-promoting molecules. Our study demonstrated that the *Brassica rapa* microgreens developed under W and RB light quality regimes exhibited a different modulation of phytochemicals.

Our data agree with previous studies on different crops.

In blueberry fruit, the exposure to LED blue light (470 nm) significantly potentiates the total phenolic concentration [37,38]. Similar results have been obtained for brassica exposed at blue (660 nm) wavelength [39,40]. Other studies demonstrated that RB light boosted the production of polyphenols, anthocyanins, and flavonoids in strawberry [41] onion [21], and raspberry fruits [42].

Our results showed that RB light quality regimes strongly influence the concentration of phenolic compounds (total polyphenols and flavonoids) and the antioxidant capacity of *Brassica rapa*, confirming that the manipulation of the light spectrum is a promising approach for the modulation of antioxidant properties in vegetables. Light quality treatments is perceived by plants through specific photoreceptors [42]. Specifically, phytochrome (red light) and cryptochrome (blue light), are involved in the accumulation of phytochemicals [39,40]. We assume that red and blue light may play a significant role in the activation of specific biosynthetic pathways, crucial for the synthesis of phenolics such as phenylalanine ammonia-lyase (PAL), chalcone synthase flavanone-3-hydroxylase and anthocyanidin synthase [19]. Consistent with other studies [43,44] our results also showed that phenolic substances strongly contribute to the antioxidant activity of brassica seedlings. Indeed, total antioxidant capacity (FRAP) increased in RB compared to W microgreens.

Oxidative stress represents one of the key conditions triggering the formation of stress granules (SG), non-membrane-bound cytoplasmic aggregates of RNA and proteins [45,46]. The formation of stress granules (SGs) is a cellular strategy to face injuries caused by stress and enhance cell survival [45]. The oxidative stress can cause severe DNA damages whose extent determines an arrest of the cellular cycle and DNA repair or the activation of the apoptotic pathways [47]. YB-1 is a well-known oxidative stress sensor and a component of SGs. Hydrogen peroxide promoted the formation of YB-1 positive-SGs.

The YB-1 protein in cytoplasmic aggregates indicates the formation of SGs, while its accumulation in the nuclear compartment indicates the occurrence of DNA damage which is confirmed by histone γH2AX foci [48].

Inizio modulo

Our data suggest that, compared to RB, W extracts may have a higher concentration of cytotoxic pro-oxidant metabolites, which impair the correct assembly of stress granules. Accordingly to our hypothesis, in basal conditions in W-treated cells, SGs were not detected while the dose-dependent increase in γ-H2AX was evidence of the occurrence of DNA damage. Testing the antioxidant power of the brassica W and RB extract on human cells, we found intriguing results. More specifically, under basal conditions, conversely to the RB, the W extract seems to activate the nuclear factor NRF2, which represents a crucial regulator of cellular resistance to oxidative stress.

Both NRF2 and p21WAF proteins are known to be upregulated in response to oxidative stress, in order to protect cells from oxidative damage. In mammals, the NRF2 transcription factor modulates the expression of reactive oxygen species (ROS) detoxification enzymes to preserve cellular homeostasis [49], while the p21WAF protein promotes cell survival in response to oxidative stress [50].

Moreover, NRF-2 factor plays a pivotal role in maintaining the balance of redox homeostasis within cells by controlling a wide range of antioxidant enzymes and proteins involved in detoxification, such as superoxide dismutase (SOD), glutathione peroxidase (GPx), and catalase. Furthermore the NRF-2 also induces the expression of enzymes, such as glutathione-S-transferase (GST) and NAD(P)H quinone oxidoreductase 1 (NQO1). These enzymes work together to neutralize ROS and toxic electrophilic compounds, protecting cells from oxidative damage and maintaining cellular redox balance [51].

Our data indicate that, compared to control, W and RB extracts increased NRF2 protein levels under oxidative stress, suggesting that both extracts are active in triggering a cellular response against oxidative stress. However, the two extracts sorted different effects on the p21WAF cell cycle regulator. More specifically, only the RB extract was efficient in reducing p21WAF levels, indicating in RB-treated cells signs of recovery from oxidative stress facilitating cell cycle progression. On the other hand, the W extract did not significantly reduce p21WAF levels suggesting that the W extract was less efficient in helping cells recover from stress.

Our study demonstrated that the two extracts exert different effects on cells under oxidative stress: the RB extract promotes cell recovery and proliferation, while the W extract is not useful in cell protection against free radicals. Further studies would be needed to understand the underlying mechanisms of these differential effects on p21WAF regulation.

Our data provide valuable insights into how extracts from plants grown in different light conditions may modulate cellular mechanisms related to stress granules and DNA damage. Understanding these aspects is crucial for assessing *B. rapa* microgreens' effect on cellular health and may contribute to the identification of potential benefits in managing oxidative stress-related conditions. Our study also suggests that low concentrations of extracts are more effective than higher ones in free radical scavenging.

We can assume, as reported in [19], that compounds contributing to the antioxidant activity of RB extracts include some phenolics, namely flavones, flavanols, anthocyanidins, benzoic and cinnamic acids, which at specific concentrations—in our case, 1 μg/mL—may contrast and/or mitigate the DNA damage and the oxidative-induced genotoxicity. Identify-

ing a method to boost such compounds in plant crude extract is worthy of attention because these molecules have powerful antioxidant, anti-inflammatory, and anti-cancer activity.

5. Conclusions

Our study demonstrated that the growth of *Brassica rapa* microgreens under light quality regimes white full spectra (W) and red, blue (RB) changes the concentrations of antioxidants in plant cells. In particular, the RB extract, according to its higher content of phenolic compounds and antioxidant activity, was more effective in reducing ROS levels and DNA damage compared to the W extract, particularly at the lowest applied concentration (1 μg/mL).

Our results also indicate that the effects obtained by RB extracts on human cells depend on the applied concentration, which has a critical role in determining beneficial or detrimental responses. This study may be relevant considering that controlling light spectrum is an eco-friendly, sustainable and safe approach to increase healthy compounds, because it does not require chemical or genetic manipulation. Plants richer in antioxidants may be used for the treatment of several diseases caused by oxidative stress with implications in the medical, nutraceutical, and biotechnological fields.

However, further investigation is required to fully understand the underlying mechanisms and to explore the broader applications of this approach. This could lead to further insights into the potential health benefits of microgreens and their optimal cultivation conditions.

Author Contributions: Conceptualization, C.A. and V.C.; methodology, C.A. and V.C.; software, I.P., G.C. and A.D.; validation, C.A. and V.C.; formal analysis, I.P., G.C. and A.D.; investigation, I.P., G.C., A.D. and F.V.; data curation, I.P., G.C., A.D. and C.A.; writing—original draft preparation, C.A. and V.C.; writing—review and editing, all the authors; visualization, I.P., G.C. and A.D.; supervision, C.A; funding acquisition, C.A. All authors have read and agreed to the published version of the manuscript.

Funding: This research received no external funding.

Institutional Review Board Statement: Not applicable.

Informed Consent Statement: Not applicable.

Data Availability Statement: Data are available from the corresponding author upon reasonable request.

Conflicts of Interest: The authors declare no conflict of interest.

References

1. Dhalaria, R.; Verma, R.; Kumar, D.; Puri, S.; Tapwal, A.; Kumar, V.; Nepovimova, E.; Kuca, K. Bioactive Compounds of Edible Fruits with Their Anti-Aging Properties: A Comprehensive Review to Prolong Human Life. *Antioxidants* **2020**, *9*, 1123. [CrossRef] [PubMed]
2. Teodoro, A.J. Bioactive Compounds of Food: Their Role in the Prevention and Treatment of Diseases. *Oxid Med. Cell. Longev.* **2019**, *2019*, 3765986. [CrossRef] [PubMed]
3. Thakur, A.; Singh, S.; Dulta, K.; Singh, N.; Ali, B.; Hafeez, A.; Vodnar, D.C.; Marc, R.A. Nutritional evaluation, phytochemical makeup, antibacterial and antioxidant properties of wild plants utilized as food by the Gaddis-a tribal tribe in the Western Himalayas. *Front. Agron.* **2022**, *4*, 1010309. [CrossRef]
4. Samtiya, M.; Aluko, R.E.; Dhewa, T.; Moreno-Rojas, J.M. Potential Health Benefits of Plant Food-Derived Bioactive Components: An overview. *Foods* **2021**, *10*, 839. [CrossRef] [PubMed]
5. Simunkova, M.; Alwasel, S.H.; Alhazza, I.M.; Jomova, K.; Kollar, V.; Rusko, M.; Valko, M. Management of oxidative stress and other pathologies in Alzheimer's disease. *Arch. Toxicol.* **2019**, *93*, 2491–2513. [CrossRef]
6. Lourenço, S.C.; Moldão-Martinsand, M.; Alves, V.D. Antioxidants of Natural Plant Origins: From Sourcesto Food Industry Applications. *Molecules* **2019**, *24*, 4132. [CrossRef]
7. Ferreres, F.; Sousa, C.; Valentão, P.; Seabra, R.M.; Pereira, J.A.; Andrade, P.B. Tronchuda cabbage (*Brassica oleracea* L. var. *costata* DC) seeds: Phytochemical characterization and antioxidant potential. *Food Chem.* **2007**, *101*, 549–558. [CrossRef]
8. Vallejo, F.; Tomás-Barberán, F.; García-Viguera, C. Health-Promoting Compounds in Broccoli as Influenced by Refrigerated Transport and Retail Sale Period. *J. Agric. Food Chem.* **2003**, *51*, 3029–3034. [CrossRef] [PubMed]
9. Jahangir, M.; Kim, H.K.; Choi, Y.H.; Verpoorte, R. Health-Affecting Compounds in Brassicaceae. *Compr. Rev. Food Sci. Food Saf.* **2009**, *8*, 31–43. [CrossRef]

10. Robbins, R.J.; Keck, A.S.; Banuelos, G.; Finley, J.W. Cultivation Conditions and Selenium Fertilization Alter the Phenolic Profile, Glucosinolate, and Sulforaphane Content of Broccoli. *J. Med. Food* **2005**, *8*, 204–214. [CrossRef] [PubMed]
11. Birt, D.F.; Hendrich, S.; Wang, W. Dietary agents in cancer prevention: Flavonoids and isoflavonoids. *Pharmacol Ther.* **2001**, *90*, 157–177. [CrossRef]
12. Satterfield, S.; Cutler, J.A.; Langford, H.G.; Applegate, W.B.; Borhani, N.O.; Brittain, E.; Cohen, J.D.; Kuller, L.H.; Lasser, N.L.; Oberman, A.; et al. Trials of hypertension prevention phase I design. *Ann. Epidemiol.* **1991**, *1*, 455–471. [CrossRef] [PubMed]
13. Liu, Y.Q.; Heying, E.; Tanumihardjo, S.A. History, Global Distribution, and Nutritional Importance of Citrus Fruits. *Compr. Rev. Food Sci. Food Saf.* **2012**, *11*, 530–545. [CrossRef]
14. Pagare, S.; Bhatia, M.; Tripathi, N.; Pagare, S.; Bansal, Y.K. Secondary metabolites of plants and their role: Overview. *Curr. Trends Biotechnol. Pharm.* **2015**, *9*, 294–305.
15. Izzo, L.G.; Arena, C.; De Micco, V.; Capozzi, F.; Aronne, G. Light quality shapes morpho-functional traits and pigment content of green and red leaf cultivars of *Atriplex hortensis*. *Sci. Hortic.* **2019**, *246*, 942–950. [CrossRef]
16. Hasan, M.M.; Bashir, T.; Ghosh, R.; Lee, S.K.; Bae, H. An overview of LEDs' effects on the production of bioactive compounds and crop quality. *Molecules* **2017**, *22*, 1420. [CrossRef]
17. Costanzo, G.; Vitale, E.; Iesce, M.R.; Naviglio, D.; Amoresano, A.; Fontanarosa, C.; Spinelli, M.; Ciaravolo, M.; Arena, C. Antioxidant Properties of Pulp, Peel and Seeds of Phlegrean Mandarin (*Citrus reticulata Blanco*) at Different Stages of Fruit Ripening. *Antioxidants* **2022**, *11*, 187. [CrossRef]
18. Lefsrud, M.G.; Kopsell, D.A.; Sams, C.E. Irradiance from distinct wavelength light-emitting diodes affect secondary metabolites in kale. *Hortic. Sci.* **2008**, *43*, 2243–2244. [CrossRef]
19. Costanzo, G.; Vitale, E.; Iesce, M.R.; Spinelli, M.; Fontanarosa, C.; Paradiso, R.; Amoresano, A.; Arena, C. Modulation of Antioxidant Compounds in Fruits of Citrus reticulata Blanco Using Postharvest LED Irradiation. *Biology* **2023**, *12*, 1029. [CrossRef]
20. Dutta Gupta, S. *Light Emitting Diodes for Agriculture: Smart Lighting. Light Emit*; Springer: Cham, Switzerland, 2017; Volume XIX, pp. 1–334.
21. Lee, S.U.; Lee, J.H.; Choi, S.H.; Lee, J.S.; Kameyama, M.O.; Kozukue, N.; Friedman, M. Flavonoid content in fresh, home-processed, and light-exposed onions and in dehydrated commercial onion products. *J. Agric. Food Chem.* **2008**, *56*, 8541–8548. [CrossRef]
22. Loi, M.; Villani, A.; Paciolla, F.; Mulè, G.; Paciolla, C. Challenges and Opportunities of Light-Emitting Diode (LED) as Key to Modulate Antioxidant Compounds in Plants. A Review. *Antioxidants* **2021**, *10*, 42. [CrossRef] [PubMed]
23. Paradiso, R.; Proietti, S. Light-Quality Manipulation to Control Plant Growth and Photomorphogenesis in Greenhouse Horticulture: The State of the Art and the Opportunities of Modern LED Systems. *J. Plant Growth Regul.* **2021**, *41*, 742–780. [CrossRef]
24. Darko, E.; Heydarizadeh, P.; Schoefs, B.; Sabzalian, M.R. Photosynthesis under artificial light: The shift in primary and secondary metabolism. *Philos. Trans. R. Soc. B Biol. Sci.* **2014**, *369*, 1471–2970. [CrossRef] [PubMed]
25. Dou, H.; Niu, G.; Gu, M.; Masabni, J. Effects of light quality on growth and phytonutrient accumulation of herbs under controlled environments. *Horticulturae* **2017**, *3*, 36. [CrossRef]
26. Haghi, A.; Azimi, H.; Rahimi, R. A Comprehensive Review on Pharmacotherapeutics of Three Phytochemicals, Curcumin, Quercetin, and Allicin, in the Treatment of Gastric Cancer. *J. Gastrointest. Cancer* **2017**, *48*, 314–320. [CrossRef]
27. Kyriacou, M.C.; Rouphael, Y.; Di Gioia, F.; Kyratzis, A.; Serio, F.; Renna, M.; De Pascale, S.; Santamaria, P. Micro-scale vegetable production and the rise of microgreens. *Trends Food Sci. Technol.* **2016**, *57*, 103–115. [CrossRef]
28. Świeca, M.; Dziki, D. Improvement in sprouted wheat flour functionality: Effect of time, temperature and elicitation. *Int. J. Food Sci. Technol.* **2015**, *50*, 2135–2142. [CrossRef]
29. Sun, B.; Richardo-da-Silva, J.M.; Sprenger, I. Critical factors of vanillin assay for catechins and proanthocyanidins. *J. Agric. Food Chem.* **1998**, *46*, 4267–4274. [CrossRef]
30. Moulehi, I.; Bourgou, S.; Ourghemmi, I.; Tounsi, M.S. Variety and ripening impact on phenolic composition and Antioxidant activity of mandarin (*Citrus reticulate Blanco*) and bitter orange (*Citrus aurantium* L.) seeds extracts. *Ind. Crop. Prod.* **2012**, *39*, 74–80. [CrossRef]
31. Dewanto, V.; Wu, X.; Adom, K.; Liu, R.H. Thermal processing enhances the nutritional value of tomatoes by increasing total antioxidant activity. *J. Agric. Food Chem.* **2002**, *50*, 3010–3014. [CrossRef]
32. George, B.; Kaur, C.; Khurdiya, D.S.; Kapoor, H.C. Antioxidants in tomato (*Lycopersium esculentum*) as a function of genotype. *Food Chem.* **2004**, *84*, 45–51. [CrossRef]
33. Sangermano, F.; Masi, M.; Vivo, M.; Ravindra, P.; Cimmino, A.; Pollice, A.; Evidente, A.; Calabrò, V. Higginsianins A and B, two fungal diterpenoid α-pyrones with cytotoxic activity against human cancer cells. *Toxicol In Vitro* **2019**, *61*, 104614. [CrossRef] [PubMed]
34. Fontana, R.; Guidone, D.; Sangermano, F.; Calabrò, V.; Pollice, A.; La Mantia, G.; Vivo, M. PKC Dependent p14ARF Phosphorylation on Threonine 8 Drives Cell Proliferation. *Sci. Rep.* **2018**, *8*, 7056. [CrossRef] [PubMed]
35. Di Martino, O.; Troiano, A.; Guarino, A.M.; Pollice, A.; Vivo, M.; La Mantia, G.; Calabrò, V. ΔNp63α controls YB-1 protein stability: Evidence on YB-1 as a new player in keratinocyte differentiation. *Genes Cells.* **2016**, *21*, 648–660. [CrossRef]
36. Vivo, M.; Matarese, M.; Sepe, M.; Di Martino, R.; Festa, L.; Calabrò, V.; La Mantia, G.; Pollice, A. MDM2-mediated degradation of p14ARF: A novel mechanism to control ARF levels in cancer cells. *PLoS ONE* **2015**, *10*, e0117252. [CrossRef]
37. Xu, F.; Cao, S.; Shi, L.; Chen, W.; Su, X.; Yang, Z. Blue light irradiation affects anthocyanin content and enzyme activities involved in postharvest strawberry fruit. *J. Agric. Food Chem.* **2014**, *62*, 4778–4783. [CrossRef]

38. Xu, F.; Shi, L.; Chen, W.; Cao, S.; Su, X.; Yang, Z. Scientia Horticulturae Effect of blue light treatment on fruit quality, antioxidant enzymes and radical-scavenging activity in strawberry fruit. *Sci. Hortic.* **2014**, *175*, 181–186. [CrossRef]
39. Zhan, L.; Hu, J.; Li, Y.; Pang, L. Combination of light exposure and low temperature in preserving quality and extending shelf-life of fresh-cut broccoli (*Brassica oleracea* L.). *Postharvest Biol. Technol.* **2012**, *72*, 76–81. [CrossRef]
40. Zhan, L.; Hu, J.; Li, Y.; Pang, L.; Fan, H. Browning inhibition and quality preservation of fresh-cut romaine lettuce exposed to high-intensity light. *Innov. Food Sci. Emerg. Technol.* **2012**, *14*, 70–76. [CrossRef]
41. Nassarawa, S.S.; Abdelshafy, A.M.; Xu, Y.; Luo, Z. Effect of Light-Emitting Diodes (LEDs) on the Quality of Fruits and Vegetables During Postharvest Period: A Review. *Food Bioprocess Technol.* **2021**, *14*, 388–414. [CrossRef]
42. Wang, S.Y.; Chen, C.T.; Wang, C.Y. The influence of light and maturity on fruit quality and flavonoid content of red raspberries. *Food Chem.* **2009**, *112*, 676–684. [CrossRef]
43. Silva, F.G.D.; O'Callagahan, Y.; O'Brien, N.M.; Netto, F.M. Antioxidant capacity of flaxseed products: The effect of in vitro digestion. *Plant Food Hum. Nutr.* **2013**, *68*, 24–30. [CrossRef] [PubMed]
44. Sarker, U.; Oba, S. Augmentation of leaf color parameters, pigments, vitamins, phenolic acids, flavonoids and antioxidant activity in selected Amaranthus tricolor under salinity stress. *Sci. Rep.* **2018**, *8*, 12349. [CrossRef] [PubMed]
45. Mahboubi, H.; Stochaj, U. Cytoplasmic stress granules: Dynamic modulators of cell signaling and disease. *Biochim. Biophys. Acta Mol. Basis. Dis* **2017**, *1863*, 884–895. [CrossRef]
46. Marcelo, A.; Koppenol, R.; de Almeida, L.P.; Matos, C.A.; Nóbrega, C. Stress granules, RNA-binding proteins, and polyglutamine diseases: Too much aggregation? *Cell Death Dis.* **2021**, *12*, 592. [CrossRef] [PubMed]
47. Barzilai, A.; Yamamoto, K.I. DNA damage responses to oxidative stress. *DNA Repair* **2004**, *3*, 1109–1115. [CrossRef]
48. Sharma, A.; Singh, K.; Almasan, A. Histone H2AX phosphorylation: A marker for DNA damage. *DNA Repair Protoc.* **2012**, *920*, 613–626.
49. Bellezza, I.; Giambanco, I.; Minelli, A.; Donato, R. Nrf2-Keap1 signaling in oxidative and reductive stress. *Biochim. Biophys. Acta Mol. Cell Res.* **2018**, *1865*, 721–733. [CrossRef]
50. O'Reilly, M.A. Redox activation of p21Cip1/WAF1/Sdi1: A multifunctional regulator of cell survival and death. *Antioxid. Redox Signal.* **2005**, *7*, 108–118. [CrossRef]
51. Espinosa-Diez, C.; Miguel, V.; Mennerich, D.; Kietzmann, T.; Sánchez-Pérez, P.; Cadenas, S.; Lamas, S. Antioxidant responses and cellular adjustments to oxidative stress. *Redox Biol.* **2015**, *6*, 183–197. [CrossRef]

International Journal of
Molecular Sciences

MDPI

Article

Health-Promoting Properties of Natural Flavonol Glycosides Isolated from *Staphylea pinnata* L.

Ida Paolillo [1], Giuseppina Roscigno [1], Michele Innangi [2], Jesús G. Zorrilla [3,4], Gianmarco Petraglia [3], Maria Teresa Russo [3], Federica Carraturo [1], Marco Guida [1], Alessandra Pollice [1], Alessio Cimmino [3], Marco Masi [3,*] and Viola Calabrò [1]

1 Department of Biology, Complesso Universitario Monte Sant'Angelo, University of Naples Federico II, Via Cintia 4, 80126 Naples, Italy; ida.paolillo@unina.it (I.P.); giuseppina.roscigno@unina.it (G.R.); federica.carraturo@unina.it (F.C.); marco.guida@unina.it (M.G.); apollice@unina.it (A.P.); vcalabro@unina.it (V.C.)
2 EnviXLab, Department of Biosciences and Territory, University of Molise, Contrada Fonte Lappone, 86090 Pesche, Italy; michele.innangi@unimol.it
3 Department of Chemical Sciences, Complesso Universitario Monte Sant'Angelo, University of Naples Federico II, Via Cintia 4, 80126 Napoli, Italy; jesus.zorrilla@uca.es (J.G.Z.); petraglia.gianmarco17@gmail.com (G.P.); mariateresa.russo2@unina.it (M.T.R.); alessio.cimmino@unina.it (A.C.)
4 Allelopathy Group, Department of Organic Chemistry, Facultad de Ciencias, Institute of Biomolecules (INBIO), University of Cadiz, C/Avenida República Saharaui, s/n, 11510 Puerto Real, Spain
* Correspondence: marco.masi@unina.it

Abstract: *Staphylea*, also called bladdernuts, is a genus of plants belonging to the family Staphyleaceae, widespread in tropical or temperate climates of America, Europe, and the Far East. *Staphylea* spp. produce bioactive metabolites with antioxidant properties, including polyphenols which have not been completely investigated for their phytotherapeutic potential, even though they have a long history of use for food. Here, we report the isolation of six flavonol glycosides from the hydroalcoholic extract of aerial parts of *Staphylea pinnata* L., collected in Italy, using a solid-phase extraction technique. They were identified using spectroscopic, spectrometric, and optical methods as three quercetin and three isorhamnetin glycosides. Among the flavonol glycosides isolated, isoquercetin and quercetin malonyl glucoside showed powerful antioxidant, antimicrobial, and wound healing promoting activity and thus are valuable as antiaging ingredients for cosmeceutical applications and for therapeutic applications in skin wound repair.

Keywords: *Staphylea*; flavonoids; flavonol glycosides; antioxidants; antimicrobial; antiaging ingredients

Citation: Paolillo, I.; Roscigno, G.; Innangi, M.; Zorrilla, J.G.; Petraglia, G.; Russo, M.T.; Carraturo, F.; Guida, M.; Pollice, A.; Cimmino, A.; et al. Health-Promoting Properties of Natural Flavonol Glycosides Isolated from *Staphylea pinnata* L. *Int. J. Mol. Sci.* **2024**, *25*, 5582. https://doi.org/10.3390/ijms25115582

Academic Editor: Francesco Caruso

Received: 14 April 2024
Revised: 15 May 2024
Accepted: 18 May 2024
Published: 21 May 2024

1. Introduction

The exploration of poorly investigated plants for their natural bioactive components can lead to the discovery of new compounds with potential therapeutic benefits for human health. One of the specific uses of natural bio-derived compounds concerns their antioxidant potential [1–3]. Antioxidants help neutralize the free radicals, reducing the potential for damage to cells and tissues. The skin, in particular, is the major interface between the human body and its environment. UV radiation is absorbed by skin molecules and generates reactive oxygen species (ROS), causing "oxidative damage" to cellular components like cell walls, lipid membranes, mitochondria, and DNA. Oxidative stress is a major contributor to premature skin aging. Furthermore, plant-derived compounds, along with naturally sourced ingredients, show promise in accelerating wound healing, especially when incorporated into the cosmetic formulation [4].

Staphylea pinnata L., also referred to as the European bladdernut, is the only extant species of the genus Staphylea native to Central-Eastern Europe (Figure 1).

Figure 1. *Staphylea pinnata* plant.

It belongs to the family Staphyleaceae and the order Crossomatales. The species has a distribution restricted to east-central Europe, ranging from France to Ukraine and extending eastward to the Transcaucasus region. The seeds are edible and are occasionally called the "false pistachio" because of their similarity in flavor to *Pistacia vera* L. The plant is fairly abundant in Italy, with a limited distribution. It grows at altitudes between 0 and 900 m in almost all regions of Italy except Valle d'Aosta, Liguria, Sardinia, and Sicily. This plant often inhabits calciphilous soils, commonly in moist woods. In the past, this species was utilized for wood-carving and other traditional purposes in Europe [5]. Native Americans used an infusion of *Staphylea trifolia* L. for its antirheumatic, dermatological, sedative, and gynecological properties [6]. The seeds gained popularity due to their aesthetically pleasing hue, shape, and long-lasting nature. The Celts utilized them to create diverse embellishments. Furthermore, the seeds of this plant are rich in fat and can serve as a valuable oil source. Previously, they were pulverized and used in animal feed since it was thought that they might promote robust health and extend the lifespan of livestock. Additionally, they were utilized as medicinal remedies for ailing youngsters, as they were thought to possess therapeutic properties, although, if taken in excessive amounts, they may induce vomiting [7].

Data from the literature on the chemical composition of the flowers and leaves have shown promising results, including notable cytotoxic and antibacterial properties [6,8–11]. *Staphylea* spp. produce bioactive metabolites with antioxidant properties, including polyphenols, but their nature remains undefined [6]. One study referred to the flavonoids isolated from *Staphylea bumalda* L. without, however, evaluating their bioactivity [12]. In 2019, a work was published regarding the bioactive components present in the seeds of *S. pinnata* [13], but to date, there is no detailed report regarding the chemical composition of the bioactive constituents present in the aerial parts of the plant.

Here, we report the isolation of six flavonol glycosides from the hydroalcoholic extracts of *S. pinnata*'s aerial parts collected in southern Italy. The six pure metabolites were tested for their antioxidant, antimicrobial, and wound healing-promoting activities in human keratinocytes in light of their application in the cosmeceutical industry.

2. Results

2.1. Extraction of S. pinnata's Aerial Parts

The dried aerial parts of *S. pinnata* were macerated using a hydroalcoholic solution (crude extract) and partially purified using two different methods, as detailed in Section 4. In particular, a liquid–liquid extraction (LLE) and a solid phase extraction (SPE) were carried out to obtain different organic extracts and fractions, as summarized in Figure 2.

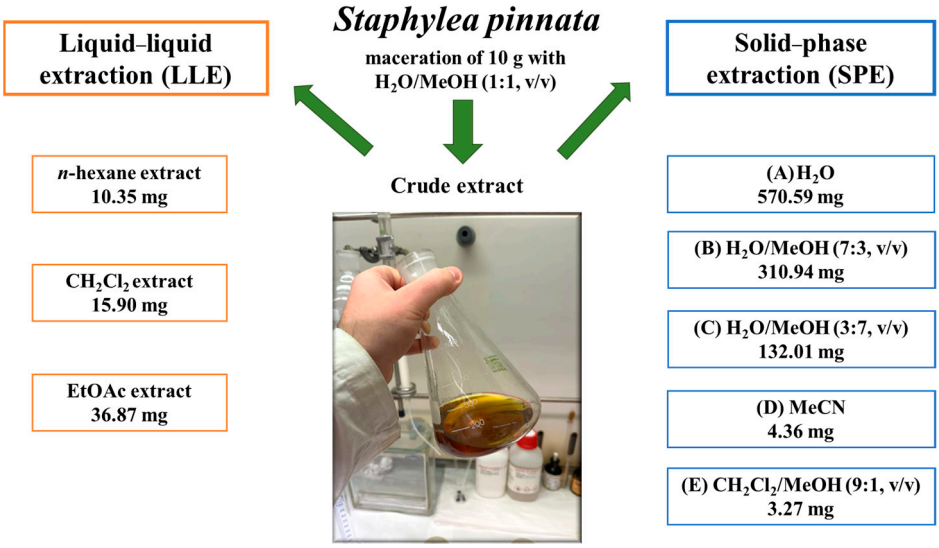

Figure 2. Extraction procedures applied to 10 g of the dried aerial parts of *S. pinnata*.

Briefly, three organic solvents with increasing polarity were employed for the LLE, while the SPE was carried out via stepwise elution with different solvent mixtures. The extraction yield of the SPE was higher than the LLE and the chromatographic profile of all the fractions obtained was compared using TLC on a silica gel and reverse phase. The results showed different metabolite contents in the various fractions obtained, and in particular, some major compounds were observed in both the EtOAc extract of the LLE and the C fraction of the SPE.

2.2. Cytotoxicity and Antioxidant Properties of S. pinnata's Crude Hydroalcoholic Extract and the LLE and SPE Fractions

The cytotoxicity and antioxidant activity of the crude hydroalcoholic extract and the LLE and SPE fractions obtained from *S. pinnata*'s aerial parts were evaluated as described in Section 4. Crude extract exhibited noticeable antioxidant activity on HeLa and HaCaT cells (Figure 3, B panels) alongside an almost complete absence of toxicity (Figure 3, A panels).

The cytotoxicities of the LLE fractions (*n*-hexane, CH_2Cl_2, and EtOAc organic extracts) were evaluated in HeLa and HaCaT cells at the indicated concentrations (Figure 4, A panels).

At 500 µg/mL, all three fractions were highly toxic to both cell lines. Moreover, the CH_2Cl_2 fraction caused significant toxicity at a concentration of 100 µg/mL in HeLa cells. (Figure 4, A upper panels). The antioxidant activity of the LLE fractions was evaluated by performing the DCFDA assays at concentrations showing minimal or no toxicity to the cells. As shown in Figure 4A's lower panels, all three fractions at the concentration of 100 µg/mL caused a 30% reduction of ROS in HaCaT cells, while in the HeLa cells, the *n*-hexane fraction was effective at 1 and 10 µg/mL, causing a 25% and 30% ROS reduction, respectively.

Considering the advantage in yield and sustainability of the SPE method, we focused on the fractions obtained using such a procedure. Therefore, SPE fractions A, B, and C were first tested for cytotoxicity. As shown in Figure 4, fraction A was not toxic, fraction B was toxic to HaCaT cells at 500 µg/mL (50% of the residual activity), while fraction C was toxic to HeLa and HaCaT cells at a concentration of 100 and 500 µg/mL, respectively. Given these

results, we evaluated the antioxidant activity of the SPE fractions at concentrations showing minimal or no toxicity to cells by performing DCFDA assays (Figure 4, B panels). In HeLa cells, none of the fractions showed effective antioxidant activity (Figure 4B, left panel). Remarkably, in HaCaT cells, fractions B and C exhibited significant antioxidant activity. Fraction C had the highest antioxidant power (a 50% reduction of ROS at 100 mg/mL), coupled with a substantial absence of toxicity (Figure 4B, right panel).

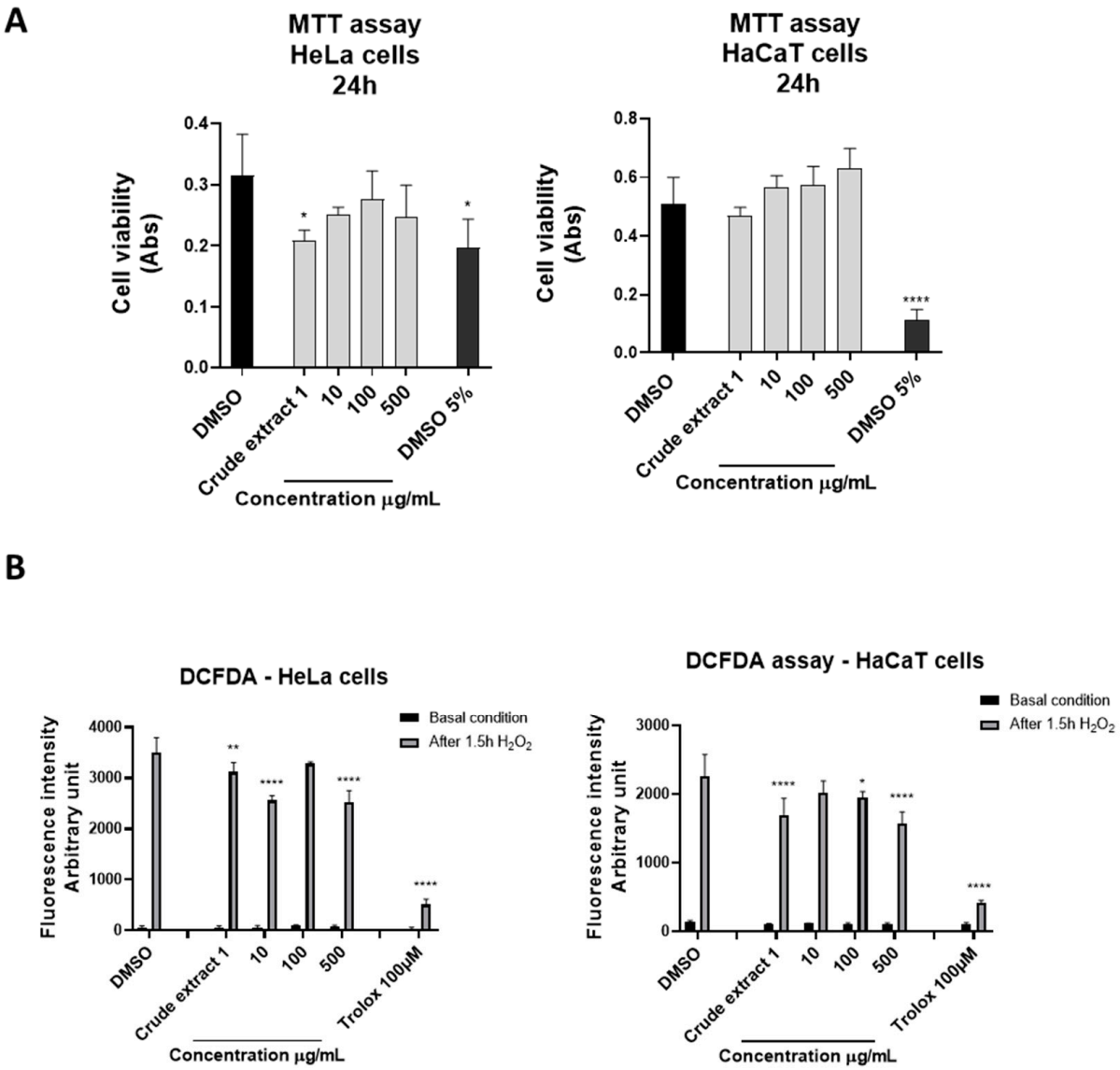

Figure 3. (**A**) MTT viability test. HeLa and HaCaT cells were incubated with the indicated amount of crude hydroalcoholic extract for 24 h. The values were the mean's six values for each experimental point of two independent biological replicates. Each mean was compared using a Dunnett's multiple comparisons test of a one-way ANOVA (*p*-value * $p < 0.01$, **** $p < 0.0001$). (**B**) DCFDA assay. HeLa and HaCaT cells were seeded and pre-treated for 4 h with 1, 10, 100, and 500 µg/mL of crude hydroalcoholic extract. H_2O_2 (4 mM; 3%) was added to the medium for 1.5 h. The fluorescence intensity of DCFDA was read after 45 min of incubation. Trolox was used as a positive control, and 0.5% DMSO, in which the metabolites were dissolved, was used as a negative control. The values are the mean's six values for each experimental point of two independent biological replicates. The statistical analysis was performed with a two-way ANOVA using Tukey's multiple comparison test. The levels of significance between the points of expression are indicated (**** $p < 0.001$, ** $p < 0.05$, * $p < 0.01$).

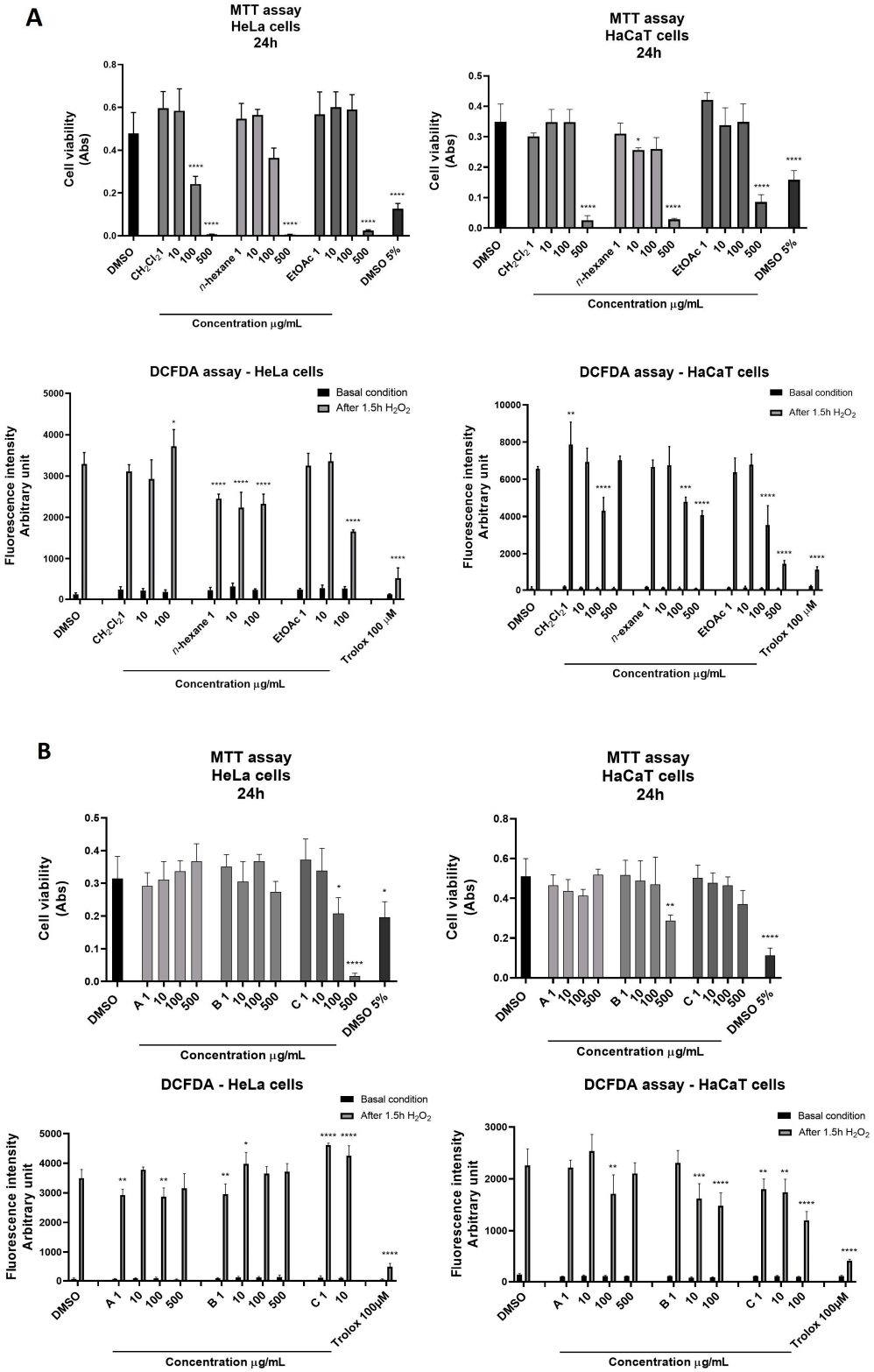

Figure 4. (**A**) MTT assays at 24 h of the CH_2Cl_2, *n*-hexane, and EtOAc fractions obtained through the LLE procedure on HeLa (left panel) and HaCaT cells (right panel) at concentrations of 1, 10, 100, and 500 µg/mL. Lycorine or 5% DMSO was used as a positive control. DCFDA assay of the CH_2Cl_2, *n*-hexane, and EtOAc fractions on HeLa (left panel) and HaCaT cells (right panel). Trolox was used as a positive control. (**B**) MTT viability test. HeLa and HaCaT cells were incubated with the indicated amount of the A, B, and C fractions obtained through the SPE technique for 24 h. The values were the mean's six values for each experimental point of two independent biological replicates. Each mean

was compared using a Dunnett's multiple comparisons test of a one-way ANOVA (p-value * $p < 0.01$, ** $p < 0.05$, *** $p < 0.001$; **** $p < 0.0001$). (**B**) panels, DCFDA assay. HeLa and HaCaT cells were seeded and pre-treated for 4 h with no toxic concentrations of the A, B, and C fractions obtained through the SPE technique. H_2O_2 (4 mM; 3%) was added to the medium for 1.5 h. The fluorescence intensity of DCFDA was read after 45 min of incubation. Trolox was used as a positive control, and DMSO, in which the metabolites were dissolved, was used as a negative control. The values are the mean's six values for each experimental point of two independent biological replicates. The statistical analysis was performed with a two-way ANOVA using Tukey's multiple comparison test. The levels of significance between the points of expression are indicated (**** $p < 0.001$, *** $p < 0.01$, ** $p < 0.05$, * $p < 0.01$).

2.3. Purification and Identification of Pure Metabolites from S. pinnata

The C fraction from the SPE was chromatographed as detailed in the Section 4 to afford six flavonol glycosides (Figure 5). Briefly, the residue of the SPE C fraction was purified using two steps of TLC on direct and reverse phases, yielding six pure compounds. By comparing their spectroscopic data (essentially the ^{1}H NMR, Figures S1–S6) with those reported in the literature, they were identified as isoquercetin (**1**) [14], rutin (**2**) [15], isorhamnetin glucoside (**3**) [14], narcissoside (**4**) [16], quercetin malonyl glucoside (**5**) [17], and isorhamnetin malonyl glucoside (**6**) [17]. Their identification was confirmed using the data obtained from the ESIMS spectra recorded in the negative mode (Figures S7–S12) that showed the deprotonated pseudomolecular ion [M-H]$^-$ peaks at m/z 463, 609, 477, 623, 549, and 563 (**1**–**6**). Finally, their configuration was confirmed by comparing the specific optical rotation data with those reported in the literature [14–17].

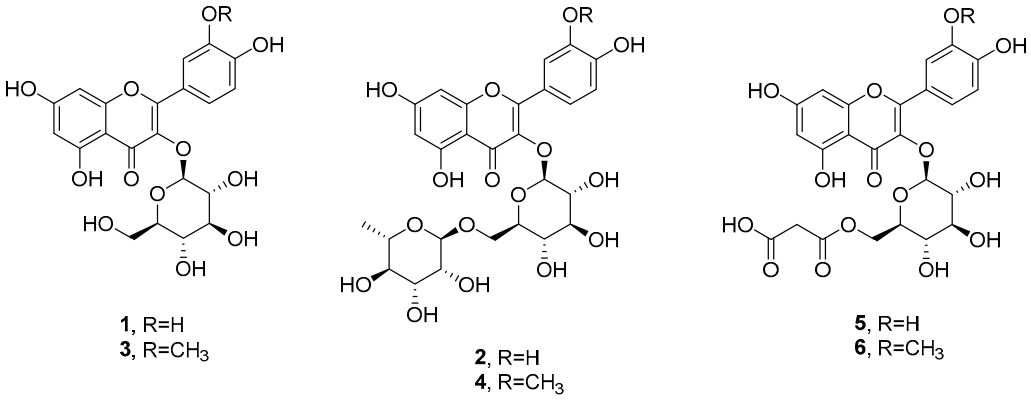

Figure 5. Chemical structures of the compounds isolated from *S. pinnata*: isoquercetin (**1**), rutin (**2**), isorhamnetin glucoside (**3**), narcissoside (**4**), quercetin malonyl glucoside (**5**), and isorhamnetin malonyl glucoside (**6**).

2.4. Cytotoxicity and Antioxidant Properties of the Pure Metabolites from S. pinnata

HaCaT cells are widely used as a model for studying the effect of natural compounds on keratinocyte proliferation and differentiation. Therefore, pure metabolites (**1**–**6**) obtained from fraction C of *S. pinnata* were tested for their effect on cell viability in HaCaT cells using the MTT assay. Each metabolite was tested at the range of concentration between 25 and 100 µM. As shown in Figure 6, A panel, the HaCaT cell viability was stimulated using treatments with the metabolites isoquercetin (**1**), rutin (**2**), isorhamnetin glucoside (**3**), and quercetin malonyl glucoside (**5**), although to a different extent.

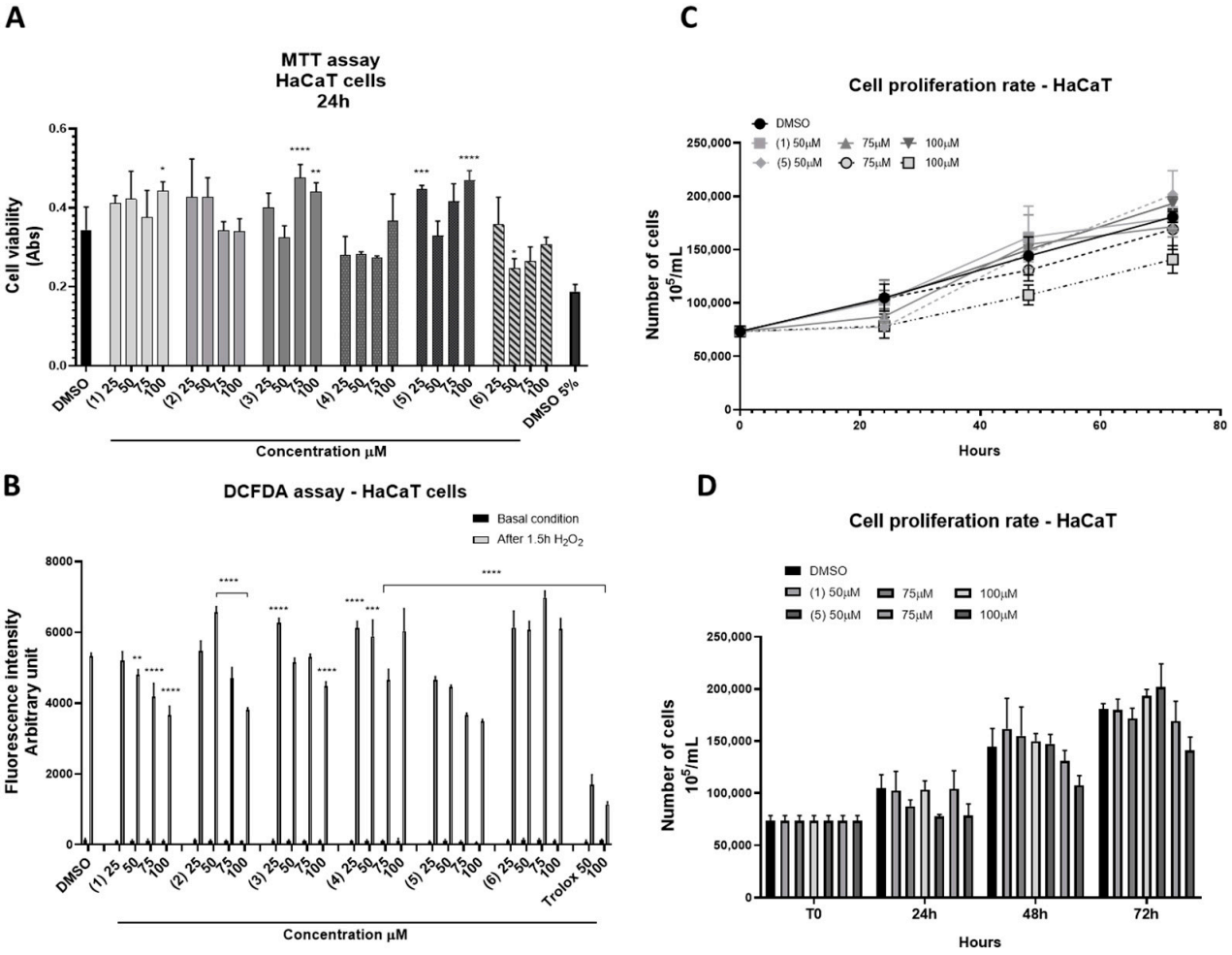

Figure 6. (**A**) MTT viability test. HaCaT cells were incubated with the indicated amount of pure metabolites (**1**–**6**) obtained from fraction C of *S. pinnata* for 24 h. The values were the mean's six values for each experimental point of two independent biological replicates. Each mean was compared using a Dunnett's multiple comparisons test of a one-way ANOVA (*p*-value * $p < 0.01$, ** $p < 0.05$, *** $p < 0.001$; **** $p < 0.0001$). (**B**) DCFDA assay. HaCaT cells were seeded and pre-treated for 4 h with no toxic concentrations of the pure metabolites (**1**–**6**) obtained from fraction C of *S. pinnata*. H_2O_2 (4 mM; 3%) was added to the medium for 1.5 h. The fluorescence intensity of DCFDA was read after 45 min of incubation. Trolox was used as a positive control, and DMSO, in which the metabolites were dissolved, was used as a negative control. The values are the mean's six values for each experimental point of two independent biological replicates. The statistical analysis was performed with a two-way ANOVA using Tukey's multiple comparison test. The levels of significance between the points of expression are indicated (**** $p < 0.001$, *** $p < 0.01$, ** $p < 0.05$). (**C**,**D**) Cell growth profile. HaCaT cells were seeded and treated with isoquercitin (**1**) and quercetin malonyl glucoside (**5**) at the indicated concentrations. The cells were counted with Scepter at T0, 24, 48, and 72 h of treatments, and the number was compared to the untreated cells. The results are the mean ± SEM of three independent biological experiments relative to the experimental control (DMSO). The statistical analysis was performed with a one-way ANOVA using Dunnett's multiple comparison test.

No significant effect on cell viability was observed by treating the cells with the metabolite narcissoide (**4**), while a 40% reduction in cell viability was observed by treating the cells with isoramnetin malonil glucoside (**6**) at the concentration of 50 mg/mL. The antioxidant activity of the pure metabolites (**1**–**6**) was evaluated using a DCFDA assay in the same range of concentration. As shown in Figure 6, B lower panel, among all the metabolites assayed, isoquercetin (**1**) and quercetin malonyl glucoside (**5**) exhibited

dose-dependent antioxidant power. Moreover, neither isoquercetin nor malonyl glucoside stimulated the rate of cell proliferation at the tested concentrations (Figure 6C,D).

2.5. In Vitro Wound Healing Assay

The in vitro wound healing activity of isoquercetin (**1**) and quercetin malonyl glucoside (**5**) was determined using a scratch assay, which is a model of a wound in which monolayer keratinocytes react to the disruption of contact between cells and are stimulated to proliferate and migrate, thus repairing the wound [18]. For this purpose, HaCaT cells were seeded in a 12-well plate and allowed to grow to 90% confluence. To mimic a wound, a linear scratch was created in the center of a confluent cell monolayer with a sterile 20 µL tip. The cells were washed and then incubated with fresh control medium or medium supplemented with isoquercetin (**1**) or quercetin malonyl glucoside (**5**) at 50 µM, 75 µM, and 100 µM to judge the rate of cell migration [19]. As shown in Figure 7A, both metabolites showed healing-promoting activity. In particular, quercetin malonyl glucoside (**5**) was the most effective by reducing the wound up to 25% after 24 h of incubation at the concentration of 50 mM. Interestingly, in HaCat keratinocytes treated with malonyl glucoside, we observed an increase in E-cadherin and p21WAF and a reduction in cyclin D1 protein expression (Figure 7B,C).

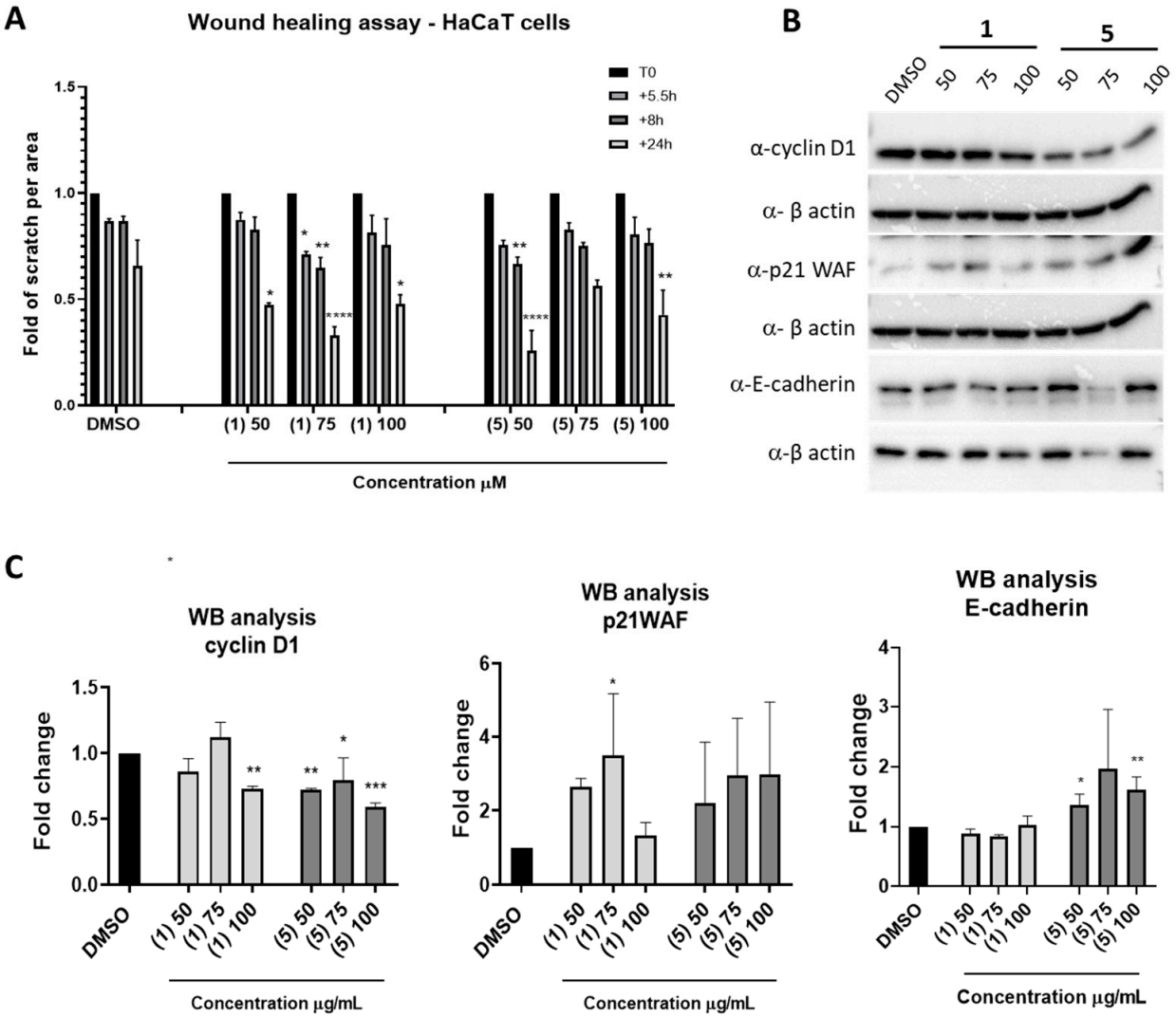

Figure 7. Wound healing assay. (**A**) The HaCaT cell monolayer was scratched in the center with a sterile tip and treated with isoquercetin (**1**) or quercetin malonyl glucoside (**5**) at 50 µM, 75 µM, and

100 µM. The statistical analysis was performed with a two-way ANOVA using Dunnett's multiple comparison test (*p*-value * $p < 0.01$, ** $p < 0.05$, **** $p < 0.0001$). The results are the mean ± SEM of three independent biological experiments relative to the experimental control (DMSO). (**B**) Representative image of the Western blot analysis of the extracts from HaCaT keratinocytes treated for 24 h with 50, 75, and 100 µg/mL of (**1**) and (**5**). DMSO (cells in 0.1% DMSO, negative control). The immunoblots were probed with p21WAF, cyclin D1, and E-cadherin antibodies. β-actin was used as a loading control. (**C**) The protein bands were quantified using ImageLab software version 4.1 (Bio-Rad, Hercules, CA, USA). The statistical analyses were carried out using an ordinary one-way ANOVA followed by Dunnett's multiple comparison test (*** $p < 0.001$, ** $p < 0.01$, * $p < 0.05$) and Student's *t*-test (** $p < 0.01$, * $p < 0.05$) for E-cadherin analysis. The results are the mean ± SEM of three independent biological experiments relative to the experimental control (DMSO).

2.6. Antimicrobial and Microbicidal Assays

The survival and die-off rates of *Staphylococcus aureus* ATCC®6538 (Table 1), *Pseudomonas aeruginosa* ATCC®9027 (Table 2), and *Candida albicans* ATCC®14053 (Table 3) were evaluated following contact with fraction C at 150 µg/mL and 100 µg/mL concentrations and isoquercetin (**1**) and quercetin malonyl glucoside (**5**) at 100 µM. The activity of fraction C (150 µg/mL) against *Staphylococcus aureus* ATCC®6538 evidenced a 96.97% die-off rate of the microbial load after 30 min of contact time. Fraction C (100 µg/mL) showed a 90.93% die-off rate. The activities of isoquercetin (**1**) and quercetin malonyl glucoside (**5**) (at a 100µM concentration) demonstrated low die-off rates against *S. aureus* ATCC®6538, ranging from 8 to 10% (Table 1).

Assays conducted to assess the effects of 150 µg/mL and 100 µg/mL of fraction C on *Pseudomonas aeruginosa* ATCC®9027 brought a reduction of 39.64% and 5.60% loads, respectively. Based on the data, the microbial loads of *P. aeruginosa* ATCC®9027 sensibly reduced following contact with isoquercetin (**1**) (85.77%) and quercetin malonyl glucoside (**5**) (72.88%) (Table 2).

The antifungal evaluation targeting *Candida albicans* ATCC®14053 highlighted a statistically significant (*p*-values < 0.05 and $p \leq 0.0001$, respectively) die-off efficacy of fraction C on the yeast, ranging from 21.02% (for the 150 µg/mL tested concentration) to 52.68% (for the 150 µg/mL tested concentration) (Table 3).

Table 1. Antibacterial/bactericidal susceptibility tests conducted on *Staphylococcus aureus* ATCC®6538 [10^6 CFU/mL] [1].

Sample	Die-Off Concentration (Mean ± SE) [CFU/mL]	Log CFU Reduction	Die-Off Rate [%]	*p*-Value
Negative control [50 µL DMSO]	1,750,000 ± 50	2×10^5	7.89	-
Positive control [100 µg/mL chloramphenicol]	5500 ± 15	2×10^6	99.71	≤0.0001
Fraction C [150 µg/mL]	57,525 ± 4	2×10^6	96.97	≤0.0001 **
Fraction C [100 µg/mL]	172,267 ± 15	2×10^6	90.93	≤0.0001 **
Isoquercetin (**1**) [100 µM]	1,708,000 ± 125	2×10^5	10.11	>0.05 *
Quercetin malonyl glucoside (**5**) [100 µM]	1,742,333 ± 89	2×10^5	8.30	>0.05 *

[1] Die-off concentration (3 replicates mean ± SE, expressed in CFU/mL = colony forming units/mL), log CFU reduction and die-off rate (percentage) of *S. aureus* ATCC®6538 following contact with fraction C at two different concentrations: isoquercetin (**1**) and quercetin malonyl glucoside (**5**) at 100 µM. Negative control = 50 µL of DMSO; positive control = 100 µg/mL chloramphenicol; * $p < 0.05$, ** $p \leq 0.0001$ compared to the negative control (a one-way ANOVA followed by Turkey's and Dunnett's post hoc tests).

Table 2. Antibacterial/bactericidal susceptibility tests conducted on *Pseudomonas aeruginosa* ATCC®9027 [10^6 CFU/mL] [1].

Sample	Die-Off Concentration (Mean ± SE) [CFU/mL]	Log CFU Reduction	Die-Off Rate [%]	*p*-Value
Negative control [50 µL DMSO]	1,636,667 ± 79	4×10^4	2.58	-
Positive control [100 µg/mL ehloramphenicol]	5083 ± 13	2×10^6	99.70	≤0.0001
Fraction C [150 µg/mL]	1,013,283 ± 101	7×10^5	39.69	≤0.0001 **
Fraction C [100 µg/mL]	1,586,000 ± 225	9×10^4	5.60	>0.05 *
Isoquercetin (**1**) [100 µM]	239,000 ± 107	1×10^6	85.77	≤0.0001 **
Quercetin malonyl glucoside (**5**) [100 µM]	455,700 ± 68	1×10^6	72.88	≤0.0001 **

[1] Die-off concentration (3 replicates mean ± SE, expressed in CFU/mL = colony forming units/mL), log CFU reduction and die-off rate (percentage) of *P. aeruginosa* ATCC®9027 following contact with fraction C at two different concentrations: isoquercetin (**1**) and quercetin malonyl glucoside (**5**) at 100 µM. Negative control = 50 µL of DMSO; positive control = 100 µg/mL chloramphenicol; * $p < 0.05$ ** $p \leq 0.0001$ compared to the negative control (a one-way ANOVA followed by Turkey's and Dunnett's post hoc tests).

Table 3. Antifungal/fungicidal susceptibility tests conducted on *Candida albicans* ATCC®14053 [10^6 CFU/mL] [1].

Sample	Die-Off Concentration (Mean ± SE) [CFU/mL]	Log CFU Reduction	Die-Off Rate [%]	*p*-Value
Negative control [50 µL DMSO]	1,400,000 ± 71	8×10^4	5.41	-
Positive control [100 µg/mL econazole]	46,913 ± 9	1×10^6	96.83	≤0.0001
Fraction C [150 µg/mL]	700,333 ± 72	8×10^5	52.68	≤0.0001 **
Fraction C [100 µg/mL]	1,168,867 ± 220	3×10^5	21.02	<0.05 *
Isoquercetin (**1**) [100 µM]	1,391,500 ± 122	9×10^4	5.98	>0.05 *
Quercetin malonyl glucoside (**5**) [100 µM]	1,359,667 ± 73	1×10^5	8.13	>0.05 *

[1] Die-off concentration (3 replicates mean ± SE, expressed in CFU/mL = colony forming units/mL), log CFU reduction and die-off rate (percentage) of *C. albicans* ATCC®14053 following contact with fraction C at two different concentrations: isoquercetin (**1**) and quercetin malonyl glucoside (**5**) at 100 µM. Negative control = 50 µL DMSO; positive control = 100 µg/mL chloramphenicol; * $p < 0.05$ ** $p \leq 0.0001$ compared to the negative control (a one-way ANOVA followed by Turkey's and Dunnett's post hoc tests).

The outcomes of the tests conducted with 100 µM isoquercetin (**1**) and quercetin malonyl glucoside (**5**) did not show statistically significant fungal load reductions. Thus, considering the obtained results and taking into account the assayed concentrations, it is possible to affirm that fraction C demonstrated a high die-off efficacy (a reduction from 91% to 97%) towards *S. aureus* ATCC®6538 and a milder effect on *C. albicans* ATCC®14053, while isoquercetin (**1**) and quercetin malonyl glucoside (**5**) showed a sensible bactericidal effect (a reduction from 73% to 86%) on *P. aeruginosa* ATCC®9027.

3. Discussion

The data from the literature indicate that *Staphylea* spp. extracts contain bioactive metabolites with potential applications in the cosmeceutical industry [6].

From the aerial parts of the hydroalcoholic extract of *Staphylea pinnata* L. collected in Italy, we isolated six pure compounds (compounds **1**–**6**) using SPE and chromatographic techniques. They were identified using spectroscopic, spectrometric, and optical methods. Compounds **1**, **2**, and **5** are quercetin glycosides, while compounds **3**, **4**, and **6** are isorhamnetin glycosides belonging to the flavonol group of flavonoids, a class of polyphenolic secondary metabolites found in plants [20]. These plant-specialized metabolites have important functions in plant growth and development [21] and show several biological activities [22,23].

The six pure metabolites were tested for their biological activity on human tumor-derived HeLa cells and immortalized HaCaT keratinocytes. In human immortalized keratinocytes, fractions B and C obtained using SPE showed remarkable antioxidant ac-

tivities. Such activities were not observed in tumor-derived HeLa cells. The variation in the antioxidant properties of plant extracts or their fractions across different cell types is not surprising and can be attributed to several factors. For instance, different cells have varying levels of oxidative stress and antioxidant defense mechanisms. Cells with different metabolic activities, receptors, activated signal pathways, and redox statuses may process and utilize antioxidants differently. This can affect the efficacy of plant extracts or partially purified fractions in exhibiting antioxidant properties. In particular, cancer-derived cells are usually characterized by constitutively activated antioxidant responses that promote their survival and can obscure the activity of antioxidant metabolites [24]. In HaCaT keratinocytes, fraction C turned out to be the most interesting as it had the highest antioxidant power coupled with a substantial absence of toxicity. Among the metabolites isolated from SPE fraction C, none of them were toxic to keratinocytes. Moreover, both isoquercetin (**1**) and quercetin malonyl glucoside (**5**) exhibited a significant capacity to reduce ROS levels induced by hydrogen peroxide, thus suggesting that quercetin glycosides, which are abundant in *S. pinnata*, show potential for being effective ingredients in cosmeceutical products designed to protect the skin from oxidative stress. The wound healing process was improved in keratinocytes treated with isoquercetin and quercetin malonyl glucoside, although our data indicated that quercetin malonyl glucoside was the most effective in wound repair. Wound repair requires keratinocyte proliferation and migration. However, the lack of enhanced cell proliferation in HaCaT treated with quercetin malonyl glucoside suggests that the improvement of the wound healing process may reflect an increase in cell migration rather than proliferation. This appears to be confirmed by the observed reduction in cyclin D1 and the increase in the p21WAF cell cycle inhibitor. On the other hand, the treatment of HaCaT with quercetin malonyl glucoside enhanced the expression level of E-cadherin, which facilitates the formation of adherent junctions between adjacent epithelial cells, thus promoting efficient wound closure [25].

The available bibliography highlighted sensitive antimicrobial and antifungal activities towards several bacteria and yeasts of either quercetin-derived substances or quercetin and malonyl glucoside-containing plant extracts. A study published in 2020 reported the potential synergistic activity of quercetin with antibiotics against multidrug-resistant clinical strains of *Pseudomonas aeruginosa*. Quercetin was indeed described as capable of targeting quorum sensing and demonstrated to be particularly active against biofilm-forming microorganisms. The research highlighted an $\geq$ 80% inhibition of *Pseudomonas aeruginosa* strains treated with blends of quercetin and selected antibiotic combinations [26]. Furthermore, quercetin exhibited antifungal activity against *Candida albicans* by means of the induction of yeast apoptosis through mitochondrial dysfunction following the accumulation of Mg^{2+} [27]. Tan et al. (2023) [28] confirmed the results of the present study, discovering that the minimum inhibitory concentration (MIC) and minimal fungicidal concentration (MFC) of quercetin for *C. albicans* were >128 µM and >512 µM, respectively [28]: a quercetin concentration lower than 128 µM, such as 100 µM, was not capable of inhibiting *C. albicans* [28]. With regards to quercetin malonyl glucoside, Abdalla et al. (2022) [29] reported the extraction of a substance from red lettuce: the extract showed antibacterial activity against *Pseudomonas aeruginosa* [29]. Quercetin malonyl glucoside was additionally described as holding an effective antibacterial activity towards *Staphylococcus aureus*, *S. epidermidis*, *S. faecalis*, and *S. pyogenes* [30]. Sensitive antibacterial activity was additionally described by Mugo and Njenga (2020) [31] for essential oil from an *Ixora scheffleri* subspecies, *keniensis*, from which the MS spectrum also detected the presence of malonyl glucoside quercetin: the extracts showed antimicrobial properties against human pathogen strains, such as *S. aureus*, *B. subtilis*, *E. coli*, *P. aeruginosa*, and *C. albicans* [31].

4. Materials and Methods

4.1. Plant Material

The aerial parts of *S. pinnata* were collected in late August 2023 in a thermophilic mixed wood at an elevation of 600 m in the proximity of Luzzano, a village belonging to

the municipality of Moiano (Benevento, Italy). The identification of the plant material was performed according to the Flora of Italy, comparing the collected material to reference vouchers (PI 010576, https://erbario.unipi.it/it/erbario/view?id=1283285, accessed on 18 May 2024). The collection was carried out in a period far from flowering and fruiting, collecting the terminal part of the leafy twigs from about 30 individuals, spaced 5–10 m apart to reduce the risk of sampling clonal individuals. Distilled water was used to rinse the plant material and remove the dust particles. The plant was then dried for a few days in the air at room temperature and ground in a blender.

4.2. General Experimental Procedures

The solid phase extraction (SPE) was performed using SUPELCO Supelclean LC-18 SPE 10 g/60 mL cartridges (Merck, Darmstadt, Germany) on a SUPELCO Visiprep™ SPE Vacuum Manifold system (Merck, Darmstadt, Germany). Analytical and preparative thin-layer chromatography (TLC) was performed on silica gel plates (Kieselgel 60, F_{254}, 0.25 and 0.5 mm, respectively) or reverse phase (Whatman, KC18, F_{254}, 0.20 mm) (Merck, Darmstadt, Germany) plates, and the compounds were visualized via exposure to UV light and/or iodine vapors and/or by spraying first with 10% H_2SO_4 in MeOH, and then with 5% phosphomolybdic acid in EtOH, followed by heating at 110 °C for 10 min. All the solvents employed were supplied by Sigma-Aldrich (Milan, Italy). ^{1}H nuclear magnetic resonance (NMR) spectra were recorded at 400 or 500 MHz on Bruker (Karlsruhe, Germany) or Varian (Palo Alto, CA, USA) spectrometers, respectively. Electrospray ionization (ESI) mass spectra and liquid chromatography (LC/MS) analyses were performed using the LC/MS TOF system AGILENT 6230B, HPLC 1260 Infinity (Milan, Italy) in the negative modality. Optical rotations were measured on a Jasco (Tokyo, Japan) P-1010 digital polarimeter. The purity of the purified compounds was >98%, as ascertained via ^{1}H NMR and HPLC analyses.

4.3. Extraction and Purification of the Metabolites

A total of 10 g of dried aerial parts of *S. pinnata* were minced with a blender and macerated under stirred conditions in a solution of methanol (MeOH)/H_2O 1:1, *v*/*v* (300 mL) for 3 days at room temperature. The resulting suspension was filtered, resulting in a hydroalcoholic crude extract. Two aliquots of this latter extract were further fractionated by performing a liquid–liquid extraction (LLE) and a solid-phase extraction (SPE).

The first aliquot (100 mL) of the hydroalcoholic extract was subjected to stepwise extractions with *n*-hexane (3 × 100 mL), dichloromethane (CH_2Cl_2) (3 × 100 mL), and after removing MeOH under reduced pressure, with ethyl acetate (EtOAc) (3 × 100 mL). Each extract was dried over anhydrous Na_2SO_4 and filtered, and the residual solvent was evaporated under reduced pressure, yielding 10.35 mg (*n*-hexane), 15.90 mg (CH_2Cl_2), and 36.87 mg (EtOAc) of organic extracts.

The second aliquot (100 mL) of the hydroalcoholic extract was lyophilized after removing MeOH under reduced pressure. The extract obtained was suspended in 60 mL of distilled water and loaded onto an SPE column, which was previously conditioned with 60 mL of MeOH and equilibrated with 120 mL of distilled water. The purification yielded five fractions (A, B, C, D, and E) obtained via a stepwise elution with H_2O (60 mL), MeOH/H_2O 3:7, *v*/*v* (120 mL), MeOH/H_2O 7:3, *v*/*v* (120 mL), acetonitrile (CH_3CN) (120 mL), and CH_2Cl_2/MeOH 9:1, *v*/*v* (60 mL), respectively. Successively, the organic solvents were removed under reduced pressure, and the eventual residual water phases were lyophilized, yielding 570.59 mg (A), 310.94 mg (B), 132.01 mg (C), 4.36 mg (D), and 3.27 mg (E), respectively.

The extracts and fractions obtained by applying the two procedures (LLE and SPE) were tested for biological activities, as reported below. Furthermore, the residue of SPE fraction C was purified using two subsequent steps of preparative TLC eluted with EtOAc/MeOH/H_2O (80:12:8, *v*/*v*/*v*) and TLC in reverse phase by eluting it with MeOH/H_2O (6:4, *v*/*v*), affording isoquercetin (**1**, 3.78 mg), rutin (**2**, 7.50 mg), isorhamnetin glucoside (**3**, 4.78 mg), narcissoside (**4**, 2.69 mg), quercetin malonyl glucoside (**5**, 5.81 mg), and isorham-

netin malonyl glucoside (**6**, 3.62 mg) as amorphous solids. The extraction and purification process was repeated three times to accumulate the pure compounds for chemical and biological characterization.

Isoquercetin (**1**): or quercetin 3-*O*-β-D-glucopyranoside, amorphous solid, $[\alpha]^{25}_{D}$ −12.6 (*c* 0.1, MeOH) (ref. [14] $[\alpha]^{25}_{D}$ −10.7 (*c* 0.4, MeOH)); ^{1}H NMR data were in agreement with those previously reported by He et al. 2017 [14]; ESI MS (-): *m*/*z* 463 $[M-H]^{-}$.

Rutin (**2**): or quercetin 3-*O*-β-D-rutinoside, amorphous solid, $[\alpha]^{25}_{D}$ −14.9 (*c* 0.1, MeOH) (ref. [32] $[\alpha]^{25}_{D}$ −16.6 (*c* 0.1, MeOH)); ^{1}H NMR data were in agreement with those previously reported by Kazuma et al. 2003 [15]; ESI MS (-): *m*/*z* 609 $[M-H]^{-}$.

Isorhamnetin glucoside (**3**): or isorhamnetin-3-*O*-β-D-glucopyranoside, amorphous solid, $[\alpha]^{25}_{D}$ −9.6 (*c* 0.1, MeOH) (ref. [14] $[\alpha]^{25}_{D}$ −7.8 (*c* 0.2, MeOH)); ^{1}H NMR data were in agreement with those previously reported by He et al. 2017 [14]; ESI MS (-): *m*/*z* 477 $[M-H]^{-}$.

Narcissoside (**4**): or isorhamnetin-3-*O*-β-D-rutinoside, amorphous solid, $[\alpha]^{25}_{D}$ −36.6 (*c* 0.1, MeOH) (ref. [33] $[\alpha]^{20}_{D}$ −38.7 (*c* 0.3, MeOH)); ^{1}H NMR data were in agreement with those previously reported by Eskalieva et al. 2004 [16]; ESI MS (-): *m*/*z* 623 $[M-H]^{-}$.

Quercetin malonyl glucoside (**5**): or quercetin-3-*O*-(6″-*O*-malonyl)-β-D-glucopyranoside, amorphous solid, $[\alpha]^{25}_{D}$ −14.6 (*c* 0.1, MeOH) (ref. [34] $[\alpha]^{25}_{D}$ −15.7 (*c* 0.1, MeOH)); ^{1}H NMR data were in agreement with those previously reported by Wald et al. 1989 [17]; ESI MS (-): *m*/*z* 549 $[M-H]^{-}$.

Isorhamnetin malonyl glucoside (**6**): or isorhamnetin-3-*O*-(6″-*O*-malonyl)-β-D-glucopyranoside, amorphous solid, $[\alpha]^{25}_{D}$ −8.2 (*c* 0.1, MeOH) (ref. [35] $[\alpha]^{25}_{D}$ −8.7 (*c* 0.1, MeOH)); ^{1}H NMR data were in agreement with those previously reported by Wald et al. 1989 [17]; ESI MS (-): *m*/*z* 563 $[M-H]^{-}$.

4.4. Cell Culture and Reagents

HeLa cells were obtained from the American Type Culture Collection (ATCC CCL-2) and cultured in DMEM supplemented with 10% FBS. HaCaT, spontaneously immortalized keratinocytes from adult skin, were purchased from Service Cell Line (GmBH, Eppelheim, CLS, Germany). The cells (10–14 passages) were cultured in Dulbecco's Modified Eagle's Medium (DMEM, Sigma Chemical Co, St. Louis, MO, USA) supplemented with 10% fetal bovine serum (FBS, Hyclone Laboratories, Inc. Logan, UT, USA) at 37 °C in a humified atmosphere of 5% CO_2 and routinely tested for mycoplasma contamination.

4.5. Western Blot Analysis

Whole-cell extracts (20 µg) were separated using sodium dodecyl sulfate-polyacrylamide gel electrophoresis (SDS-PAGE), subjected to a Western blot, and incubated overnight at 4 °C with antibodies against p21WAF, cyclin D1 from Cell Signaling Technologies (Boston, MA, USA), and e-cadherin and β-actin from Santa Cruz Biotechnology (Dallas, TX, USA). Each experiment was run in triplicates. The signal intensities of the bands were quantified using Quantity One analysis software (Version Number 2, Biorad Laboratories, London, UK) and analyzed using GraphPad Prism 8.0.2 software (GraphPad, San Diego, CA, USA).

4.6. DCFDA Assay

The antioxidant activities of the total hydroalcoholic extracts, fractions, and pure metabolites from *S. pinnata* L. leaves were measured using 2′−7′dichlorofluorescein diacetate (DCFDA), a non-fluorescent compound permeable to the cell membrane, which can be rapidly oxidized by reactive oxygen species (ROS), producing a fluorescent compound, as previously described [36]. In brief, 2×10^4 cells were treated with increasing doses of extract, fractions, or purified metabolites as indicated. The medium was removed after 4 h, and 4 mM (3%) H_2O_2 was added for 1.5 h. The cells were washed with PBS, and a fresh medium with DCFDA (30 mM) was added for 45 min; then, DCFDA was removed by washing in 1X PBS, and the cells were harvested. The measurement of the ROS was obtained using the Sinergy H4 microplate reader Gen5 2.07 (Thermofisher, Waltham, MA,

USA). The fluorescence emitted from the cells treated with DCFDA was compared to the untreated cells. Trolox was used as a positive control. The values shown in the plot are the mean ± SD of sixfold determinations. The means and the standard deviations were calculated as biological triplicates using GraphPad Prism 8.0.2 software (GraphPad, San Diego, CA, USA).

4.7. Cell Viability Assay

The cell viability was evaluated by measuring the reduction in 3-(4,5-dimethylthiazol-2) 2,5-diphenyltetrazolium bromide (MTT) to formazan by the mitochondrial enzyme succinate dehydrogenase [37]. Briefly, a day before, 1×10^4 cells were seeded on 96-well plates and treated with increasing concentrations of total extract or metabolites for 24 h. MTT (0.5 mg/mL) in PBS was then added to the wells and incubated for 3 h at 37 °C in a humidified atmosphere. The reaction was stopped by the removal of the supernatant followed by dissolving the formazan product in acidic isopropanol, and the optical density was measured with a Sinergy H4 microplate reader Gen5 2.07 (Thermofisher, Waltham, MA, USA) using a 570 nm filter. Under these experimental conditions, no undissolved formazan crystals were observed. The cell viability was assessed by comparing the optical density of the treated samples compared to the controls.

4.8. Cell Growth Profile

A total of 3.1×10^3 HaCaT cells were seeded in a 12-well plate; the cells were serum-starved for 24 h; after starvation, isoquercetin (**1**) and quercetin malonyl glucoside (**5**) were added at different concentrations. Every 24 h, the cells were gently rinsed with 1× PBS, trypsinized, and counted. The count was confirmed via Scepter 2.0 analysis (Millipore, Burlington, MI, USA), as previously described [38].

4.9. Wound Healing Assay

A wound healing assay was performed by seeding 9×10^4 HaCaT cells in a 12-well plate. We allowed them to grow to 90% confluence. To mimic a wound, a scratch was created in the center of a confluent cell monolayer with a sterile 20 µL tip. After scratching, the cells were washed twice with 1X PBS, and fresh control medium or medium supplemented with isoquercetin (**1**) or quercetin malonyl glucoside (**5**) at 50 µM, 75 µM, and 100 µM was added.

Images were obtained immediately after the scratch (t0) at 5.5, 8, and 24 h after treatment using a LEICA microscope. The wound area was analyzed using ImageJ software (Version 1.54i) by comparing the residual area of the treated samples to the control.

4.10. Antimicrobial Assays

The bactericidal/antibacterial activities of SPE fraction C and the pure compounds isoquercetin (**1**) and quercetin malonyl glucoside (**5**) were evaluated on two target microorganisms: *Staphylococcus aureus* ATCC®6538 and *Pseudomonas aeruginosa* ATCC®9027. The fungicidal/antifungal activity was assessed towards *Candida albicans* ATCC®14053. Single cultures of the three strains were grown according to the microorganism requirements: *S. aureus* ATCC®6538 for 24–48 h at 37 °C (UNI EN ISO 6888-1:2021) [39], *P. aeruginosa* ATCC®9027 for 24 h at 37 ± 1 °C (UNI EN ISO 13720:2010) [40], and *C. albicans* ATCC®14053 for 48 h at 22 ± 1 °C (UNI EN ISO 21527-1:2008) [41]. Microorganism inocula were kept in constant shaking conditions at 200 rpm in 30 mL of Tryptic Soy Broth (TSB, Thermo Fisher Scientific, USA) for the bacteria and 30 mL of Sabouraud Dextrose Broth (SAB, Thermo Fisher Scientific, USA) for the yeast in 50 mL total-volume sterile tubes. To obtain an equal 10^8 cell/mL concentration of both microorganisms, a spectrophotometer (Hach Lange DR6000, Hach, USA) was used to measure the absorbance at 560 nm (bacteria) and 600 nm (yeast): an optical density (OD) of 0.125 was used as an indicator of 10^8 cell/mL concentration. The inocula were serially diluted to reach the target concentration of 10^7 CFU/mL in 10 mL. Fraction C's activity was tested at two concentrations: 150 µg/mL and 100 µg/mL.

Assays with isoquercetin (**1**) and quercetin malonyl glucoside (**5**) were performed by selecting a 100 µM concentration, resulting in the lowest concentration that did not show toxicity to the cells.

The experimental protocol was set up according to UNI EN 1276:2020 [42], employing the time-kill test [43] for determining the bactericidal or fungicidal effect of the samples under analysis, with a 30-minute time of contact. The selected concentrations of the three samples, diluted in 50 µL of dimethyl sulfoxide (DMSO, Sigma-Aldrich, USA), were added to 6-well plates aimed at testing 0.9% NaCl suspensions of 10 mL of bacteria or yeast at a microbial load of 10^6 CFU/mL, maintained in constant shaking and at the optimal temperature (37 ± 1 °C for the bacteria, 22 ± 1 °C for the yeast) for a 30 min contact time. Negative controls were prepared with the sole bacterial or yeast inocula with 50 µL of DMSO without the addition of the test substances. The addition of the bacteria suspension of 100 µg/mL chloramphenicol and the yeast inoculum of 100 µg/mL econazole served as the positive controls. Shortly after the inoculation (t_{0min}) of the test substances and after 30 min (t_{30min}), aliquots were sampled, the activities were determined, verifying the numbers of surviving bacteria in each sample, and the reduction was calculated. The microbiological analyses were conducted following the ISO guidelines specific to each indicated microorganism, employing selective and specific agarized culture media for *S. aureus* (Baird Parker Agar Base, Thermo Fisher Scientific, USA, ISO 6888-1:2021), *P. aeruginosa* (Pseudomonas Agar Base, Thermo Fisher Scientific, USA, UNI EN ISO 13720:2010), and *C. albicans* (Dichloran Rose Bengal Chloramphenicol Agar Base, Thermo Fisher Scientific, USA, UNI EN ISO 21527-1:2008). The samples were analyzed in independent triplicates to validate the results. The reported results refer to the mean values of the three tests executed for each microorganism.

4.11. Statistical Analysis

The statistical analyses were carried out using GraphPad Prism version 8.1.2 (https://www.graphpad.com/scientific-software/prism/, accessed on 19 May 2024). The data were represented as the mean and standard deviation, and were analyzed for statistical significance using an ordinary one-way analysis of variance (ANOVA) and multiple comparisons and Student's *t*-test. For all tests, $p < 0.05$ was considered to indicate a statistically significant difference.

For the antimicrobial assays, the data were presented as the three replicates of the mean ± standard error (SE). XLSTAT 2014.5.03 (Addinsoft 1995–2014, France) was used for the statistical analysis: a one-way ANOVA was performed with post-test Tukey correction, and the comparisons of the samples with the negative controls were conducted by selecting the two-sided Dunnett's test: a *p*-value < 0.05 was considered statistically significant, and in the graphical plots, was denoted as * $p \leq 0.05$ and ** $p \leq 0.0001$.

5. Conclusions

Our study demonstrated that among the flavonol glycosides isolated from the hydroalcoholic extract of the aerial parts of *Staphylea pinnata* L., isoquercetin and quercetin malonyl glucoside had powerful antioxidant, antimicrobial, and wound healing-promoting activities in human keratinocytes. Therefore, they are of clinical relevance in skin repair and are promising antiaging chemicals for the cosmeceutical industry.

Supplementary Materials: The following supporting information can be downloaded at: https://www.mdpi.com/article/10.3390/ijms25115582/s1.

Author Contributions: Conceptualization, V.C. and M.M.; formal analysis, I.P., G.R., J.G.Z., G.P., M.T.R. and F.C.; investigation, I.P., J.G.Z., G.P., M.T.R. and F.C.; data curation, V.C., M.M. and I.P.; writing—original draft preparation, V.C. and M.M.; writing—review and editing, M.I., F.C., M.G., A.P. and A.C.; supervision, V.C.; project administration, V.C. and M.M. All authors have read and agreed to the published version of the manuscript.

Funding: This research received no external funding.

Institutional Review Board Statement: Not applicable.

Informed Consent Statement: Not applicable.

Data Availability Statement: The data that support the findings of this study are available from the corresponding author upon reasonable request.

Acknowledgments: This research was carried out within the Agritech National Research Center and received funding from the European Union Next-Generation EU (Piano Nazionale di Ripresa e Resilienza (PNRR)—Missione 4 Componente 2, Investimento 1.4—D.D. 1032 17/06/2022, CN00000022). J.G.Z. thanks the University of Cadiz for the postdoctoral support with the Margarita Salas fellowship (2021-067/PN/MSRECUAL/CD), funded by the Next Generation EU program of the European Union.

Conflicts of Interest: The authors declare no conflicts of interest.

References

1. Mukherjee, P.K.; Maity, N.; Nema, N.K.; Sarkar, B.K. Bioactive compounds from natural resources against skin aging. *Phytomedicine* **2011**, *19*, 64–73. [CrossRef] [PubMed]
2. Hernandez, D.F.; Cervantes, E.L.; Luna-Vital, D.A. Food-derived bioactive compounds with anti-aging potential for nutricosmetic and cosmeceutical products. *Crit. Rev. Food Sci. Nutr.* **2021**, *61*, 3740–3755. [CrossRef]
3. Bjørklund, G.; Shanaida, M.; Lysiuk, R.; Butnariu, M.; Peana, M.; Sarac, I.; Strus, O.; Smetanina, K.; Chirumbolo, S. Natural compounds and products from an anti-aging perspective. *Molecules* **2022**, *27*, 7084. [CrossRef] [PubMed]
4. Kepekçi, R.A.; İlçe, B.Y.; Kanmazalp, S.D. Plant-derived biomaterials for wound healing. *Stud. Nat. Prod. Chem.* **2021**, *70*, 227–264.
5. Madeja, J.; Harmata, K.; Kołaczek, P.; Karpińska-Kołaczek, M.; Piątek, K.; Naks, P. Bracken (Pteridium aquilinum (L.) Kuhn), mistletoe (Viscum album (L.)) and bladder-nut (Staphylea pinnata (L.))-mysterious plants with unusual applications. Cultural and ethnobotanical studies. *Cult. Ethnobot. Stud. Plants Cult. Seeds Cult. Herit. Eur.* **2009**, 207–214.
6. Lacikova, L.; Jancova, M.; Muselik, J.; Masterova, I.; Grancai, D.; Fickova, M. Antiproliferative, cytotoxic, antioxidant activity and polyphenols contents in leaves of four *Staphylea* L. species. *Molecules* **2009**, *14*, 3259–3267. [CrossRef] [PubMed]
7. Gostyńska, M. Zwyczaje i obrzędy ludowe w Polsce związane z kłokoczką południową (*Staphylea pinnata* L.). *Rocz. Dendrol.* **1962**, *16*, 113–120.
8. Jantova, S.; Nagy, M.; Ružeková, L.; Grancai, D. Cytotoxic effects of plant extracts from the families Fabaceae, Oleaceae, Philadelphaceae, Rosaceae and Staphyleaceae. *Phytother. Res.* **2001**, *15*, 22–25. [CrossRef] [PubMed]
9. Lacikova, L.; Muselik, J.; Masterova, I.; Grancai, D. Antioxidant activity and total phenols in different extracts of four *Staphylea* L. species. *Molecules* **2007**, *12*, 98–102. [CrossRef]
10. Laciková, L.; Švajdlenka, E.; Mašterová, I.; Grančai, D. Isolation and identification of flower oil components from four *Staphylea* L. species. *Chem. Pap.* **2007**, *61*, 512–514. [CrossRef]
11. Lacikova, L.; Pferschy-Wenzig, E.M.; Masterova, I.; Grancai, D.; Bauer, R. Antiinflammatory potential and fatty acid content of lipophilic leaf extracts of four *Staphylea* L. species. *Nat. Prod. Commun.* **2009**, *4*, 1934578X0900400420. [CrossRef]
12. Sohn, S.J.; Kwon, Y.S.; Kim, S.S.; Chun, W.J.; Kim, C.M. Chemical constituents of the leaves of *Staphylea bumalda*. *Nat. Prod. Sci.* **2004**, *10*, 173–176.
13. Šircelj, H.; Vidrih, R.; Veberič, R.; Mikulic-Petkovsek, M. Evaluation of bioactive constituents in European bladdernut (*Staphylea pinnata* L.) seed kernels. *J. Food Compos. Anal.* **2019**, *78*, 33–41. [CrossRef]
14. He, Z.; Lian, W.; Liu, J.; Zheng, R.; Xu, H.; Du, G.; Liu, A. Isolation, structural characterization and neuraminidase inhibitory activities of polyphenolic constituents from *Flos caryophylli*. *Phytochem. Lett.* **2017**, *19*, 160–167. [CrossRef]
15. Kazuma, K.; Noda, N.; Suzuki, M. Malonylated flavonol glycosides from the petals of *Clitoria ternatea*. *Phytochemistry* **2003**, *62*, 229–237. [CrossRef] [PubMed]
16. Eskalieva, B.K.; Akhmed, A.; Burasheva, G.S.; Abilov, Z.A.; Akhmad, V.U. Biologically active compounds from *Climacoptera*. *Chem. Nat. Compd.* **2004**, *40*, 87–88. [CrossRef]
17. Wald, B.; Wray, V.; Galensa, R.; Herrmann, K. Malonated flavonol glycosides and 3,5-dicaffeoylquinic acid from pears. *Phytochemistry* **1989**, *28*, 663–664. [CrossRef]
18. Liang, C.C.; Park, A.Y.; Guan, J.L. In vitro scratch assay: A convenient and inexpensive method for analysis of cell migration in vitro. *Nat. Protoc.* **2007**, *2*, 329–333. [CrossRef] [PubMed]
19. Sarkhail, P.; Navidpour, L.; Rahimifard, M.; Hosseini, N.M.; Souri, E. Bioassay-guided fractionation and identification of wound healing active compound from *Pistacia vera* L. hull extract. *J. Ethnopharmacol.* **2020**, *248*, 112335. [CrossRef]
20. Dewick, P.M. *Medicinal Natural Products*, 3rd ed.; John Wiley and Sons Ltd.: Chicester, UK, 2009.
21. Daryanavard, H.; Postiglione, A.E.; Mühlemann, J.K.; Muday, G.K. Flavonols modulate plant development, signaling, and stress responses. *Curr. Opin. Plant Biol.* **2023**, *72*, 102350. [CrossRef]
22. Barreca, D.; Trombetta, D.; Smeriglio, A.; Mandalari, G.; Romeo, O.; Felice, M.R.; Gattuso, G.; Nabavi, S.M. Food flavonols: Nutraceuticals with complex health benefits and functionalities. *Trends Food Sci. Technol.* **2021**, *117*, 194–204. [CrossRef]

23. Jucá, M.M.; Cysne Filho, F.M.S.; de Almeida, J.C.; Mesquita, D.D.S.; Barriga, J.R.M.; Dias, K.C.F.; Barbosa, T.M.; Vasconcelos, L.C.; Leal, L.K.A.M.; Ribeiro, J.E.; et al. Flavonoids: Biological activities and therapeutic potential. *Nat. Prod. Res.* **2020**, *34*, 692–705. [CrossRef] [PubMed]
24. Oberley, L.W.; Oberley, T.D.; Buettner, G.R. Cell division in normal and transformed cells: The possible role of superoxide and hydrogen peroxide. *Med. Hypotheses* **1981**, *7*, 21–42. [CrossRef] [PubMed]
25. Tunggal, J.A.; Helfrich, I.; Schmitz, A.; Schwarz, H.; Günzel, D.; Fromm, M.; Kemler, R.; Krieg, T.; Niessen, C.M. E-cadherin is essential for in vivo epidermal barrier function by regulating tight junctions. *EMBO J.* **2005**, *24*, 1146–1156. [CrossRef] [PubMed]
26. Vipin, C.; Saptami, K.; Fida, F.; Mujeeburahiman, M.; Rao, S.S.; Athmika; Arun, A.B.; Rekha, P.D. Potential synergistic activity of quercetin with antibiotics against multidrug-resistant clinical strains of *Pseudomonas aeruginosa*. *PLoS ONE* **2020**, *15*, e0241304. [CrossRef] [PubMed]
27. Kwun, M.S.; Lee, D.G. Quercetin-induced yeast apoptosis through mitochondrial dysfunction under the accumulation of magnesium in *Candida albicans*. *Fungal Biol.* **2020**, *124*, 83–90. [CrossRef] [PubMed]
28. Tan, Y.; Lin, Q.; Yao, J.; Zhang, G.; Peng, X.; Tian, J. In vitro outcomes of quercetin on *Candida albicans* planktonic and biofilm cells and in vivo effects on vulvovaginal candidiasis. Evidences of its mechanisms of action. *Phytomedicine* **2023**, *114*, 154800. [CrossRef] [PubMed]
29. Abdalla, M.A.; Famuyide, I.; Wooding, M.; McGaw, L.J.; Mühling, K.H. Secondary metabolite profile and pharmacological opportunities of lettuce plants following selenium and sulfur enhancement. *Pharmaceutics* **2022**, *14*, 2267. [CrossRef] [PubMed]
30. Pagano, C.; Perioli, L.; Baiocchi, C.; Bartoccini, A.; Beccari, T.; Blasi, F.; Calarco, P.; Ceccarini, M.R.; Cossignani, L.; di Michele, A.; et al. Preparation and characterization of polymeric microparticles loaded with *Moringa oleifera* leaf extract for exuding wound treatment. *Int. J. Pharm.* **2020**, *587*, 119700. [CrossRef]
31. Mugo, S.M.; Njenga, P.K. Chemical composition, antioxidant potential and antimicrobial activities of *Ixora scheffleri* subspecies *keniensis* essential oil. *J. Med. Plant Econ. Dev.* **2020**, *4*, a58.
32. Ly, T.N.; Shimoyamada, M.; Yamauchi, R. Isolation and characterization of rosmarinic acid oligomers in *Celastrus hindsii* Benth leaves and their antioxidative activity. *J. Agric. Food Chem.* **2006**, *54*, 3786–3793. [CrossRef]
33. Kim, J.S.; Kwon, Y.S.; Sa, Y.J.; Kim, M.J. Isolation and identification of sea buckthorn (*Hippophae rhamnoides*) phenolics with antioxidant activity and α-glucosidase inhibitory effect. *J. Agric. Food Chem.* **2011**, *59*, 138–144. [CrossRef]
34. DuPont, M.S.; Mondin, Z.; Williamson, G.; Price, K.R. Effect of variety, processing, and storage on the flavonoid glycoside content and composition of lettuce and endive. *J. Agric. Food Chem.* **2000**, *48*, 3957–3964. [CrossRef]
35. Hasle Enerstvedt, K.; Lundberg, A.; Jordheim, M. Characterization of polyphenolic content in the aquatic plants *Ruppia cirrhosa* and *Ruppia maritima*—A source of nutritional natural products. *Molecules* **2017**, *23*, 16. [CrossRef] [PubMed]
36. Xiao, D.; Powolny, A.A.; Singh, S.V. Benzyl isothiocyanate targets mitochondrial respiratory chain to trigger reactive oxygen species-dependent apoptosis in human breast cancer cells. *J. Biol. Chem.* **2008**, *283*, 30151–30163. [CrossRef]
37. Van Meerloo, J.; Kaspers, G.J.L.; Cloos, J. Cell sensitivity assays: The MTT assay. *Methods Mol. Biol.* **2011**, *731*, 237–245.
38. Fontana, R.; Guidone, D.; Sangermano, F.; Calabrò, V.; Pollice, A.; La Mantia, G.; Vivo, M. PKC dependent p14ARF phosphorylation on threonine 8 drives cell proliferation. *Sci. Rep.* **2018**, *8*, 7056. [CrossRef]
39. *ISO 6888-1:2021*; Microbiology of the Food Chain—Horizontal Method for the Enumeration of Coagulase-Positive Staphylococci (Staphylococcus aureus and Other Species)—Part 1: Method Using Baird-Parker Agar Medium. International Organization for Standardization: Geneva, Switzerland, 2021. Available online: https://www.iso.org/standard/76672.html (accessed on 12 February 2024).
40. *ISO 13720:2010*; Meat and Meat Products Enumeration of Presumptive Pseudomonas spp. International Organization for Standardization: Geneva, Switzerland, 2010. Available online: https://www.iso.org/standard/45099.html (accessed on 12 February 2024).
41. ISO 21527-1:2008; Microbiology of Food and Animal Feeding Stuffs. *ISO 21527-1:2008*; Microbiology of Food and Animal Feeding Stuffs. Horizontal Method for the Enumeration of Yeasts and Moulds. International Organization for Standardization: Geneva, Switzerland, 2008. Available online: https://www.iso.org/standard/38275.html (accessed on 12 February 2024).
42. *UNI EN 1276:2020*; Chemical Disinfectants and Antiseptics-Quantitative Suspension Test for the Evaluation of Bactericidal Activity of Chemical Disinfectants and Antiseptics Used in Food, Industrial, Domestic and Institutional Areas-Test Method and Requirements (Phase 2, Step 1). European Standards: Bruxelles, Belgium, 2020. Available online: https://www.en-standard.eu/ (accessed on 12 February 2024).
43. Alrashidi, A.; Jafar, M.; Higgins, N.; Mulligan, C.; Varricchio, C.; Moseley, R.; Celiksoy, V.; Houston, D.M.J.; Heard, C.M. A time-kill assay study on the synergistic bactericidal activity of pomegranate rind extract and Zn (II) against methicillin-resistant *Staphylococcus aureus* (MRSA), *Staphylococcus epidermidis*, *Escherichia coli*, and *Pseudomonas aeruginosa*. *Biomolecules* **2021**, *11*, 1889. [CrossRef]